PROCESSING AND CHARACTERIZATION OF HIGH DENSITY TUNGSTEN-NICKEL-IRON ALLOYS

A THESIS SUBMITTED TO
THE GRADUATE SCHOOL OF NATURAL AND APPLIED SCIENCES
OF
MIDDLE EAST TECHNICAL UNIVERSITY

BY

NECMETTİN KAAN ÇALIŞKAN

IN PARTIAL FULFILLMENT OF THE REQUIREMENTS
FOR
THE DEGREE OF DOCTOR OF PHILOSOPHY
IN
METALLURGICAL AND MATERIALS ENGINEERING

JULY 2013

Approval of the thesis:

PROCESSING AND CHARACTERIZATION OF HIGH DENSITY TUNGSTEN-NICKEL-IRON ALLOYS

Submitted by **NECMETTİN KAAN ÇALIŞKAN** in partial fulfillment of the requirements for the degree of **Doctor of Philosophy in Metallurgical and Materials Engineering, Middle East Technical University** by,

Prof. Dr. Canan ÖZGEN ----------
Dean, Graduate School of **Natural and Applied Sciences**

Prof. Dr. Hakan GÜR¸ ----------
Head of Department, **Metallurgical and Materials Engineering**

Prof. Dr. A. Şakir BOR ----------
Supervisor, **Metallurgical and Materials Engineering Dept., METU**

Assoc. Prof. Dr. Nuri DURLU ----------
Co-supervisor, **Mechanical Engineering Department, TOBB ETU**

Examining Committee Members:

Prof. Dr. Kadri AYDINOL ----------
Metallurgical and Materials Engineering Department, METU

Prof. Dr. Şakir BOR ----------
Metallurgical and Materials Engineering Department, METU

Assoc. Prof. Dr. Arcan DERİCİOĞLU ----------
Metallurgical and Materials Engineering Department, METU

Assoc. Prof. Dr. Caner DURUCAN ----------
Metallurgical and Materials Engineering Department, METU

Assist. Prof Dr. Ziya ESEN ----------
Materials Science and Engineering Department, ÇU

Date: ----------

I hereby declare that all information in this document has been obtained and presented in accordance with academic rules and ethical conduct. I also declare that, as required by these rules and conduct, I have fully cited and referenced all material and results that are not original to this work.

Name, Last Name : Necmettin Kaan Çalışkan

Signature :

ABSTRACT

PROCESSING AND CHARACTERIZATION OF HIGH DENSITY TUNGSTEN-NICKEL-IRON ALLOYS

Çalışkan, Necmettin Kaan
Ph.D., Department of Metallurgical and Materials Engineering
Supervisor : Prof. Dr. A. Şakir Bor
Co-supervisor : Assoc. Prof. Dr. Nuri Durlu

July 2013, 98 pages

In the present study, processing of W-Ni-Fe alloys by liquid phase sintering technique has been investigated. Effect of sintering atmospheres (hydrogen and vacuum), tungsten content altering from 90 to 97 wt.%, Ni/Fe ratio varied from 2 to 4 and post sintering treatments (heat treatment and swaging) on the microstructure and mechanical properties of W-Ni-Fe alloys have been analyzed. Liquid phase sintered alloys were characterized by mechanical tests, electron microscopy and XRD studies, thermal analyses and quantitative metallographic methods.

An optimum sintering cycle was investigated and applied to the W-Ni-Fe alloys. It has been observed that reduction under hydrogen led to superior mechanical properties due to better wetting of the surface oxide layer free tungsten particles by the binder phase. After characterization studies, it was found that ductility degrades significantly with the increase in contiguity upon an increase in tungsten content which also induces the transformation of dominant fracture mechanism from transgranular to intergranular fracture. Moreover, liquidus temperatures and tungsten solubility of the binder phase were found to increase with an increase in the Ni/Fe ratio which resulted in higher volume fraction of binder phase and better mechanical properties. It was also found that subsequent heat treatment also results in increase in volume fraction of the binder phase and reduction in contiguity which lead to better ductility. Tensile strength and hardness of the alloys increased after deformation due to higher dislocation density which but this also leads to an increase in the matrix failure as well as number of transgranular failure.

Keywords: Liquid Phase Sintering, W-Ni-Fe alloys, Mechanical Properties, Deformation. Ni/Fe Ratio, Contiguity.

ÖZ

YÜKSEK YOĞUNLUKLU TUNGSTEN-NİKEL-DEMİR ALAŞIMLARININ ÜRETİMİ VE KARAKTERİZASYONU

Çalışkan, Necmettin Kaan
Doktora., Metalurji ve Malzeme Mühendisliği Bölümü
Tez Yöneticisi : Prof. Dr. A. Şakir Bor
Ortak Tez Yöneticisi : Doç. Dr. Nuri Durlu

Temmuz 2013, 98 sayfa

Bu çalışmada, W-Ni-Fe alaşımlarının sıvı fazlı sinterleme işlemi ile üretilmesi incelenmiştir. Bu çalışma ile sinterleme atmosferlerinin (hidrojen ve vakum), ağırlıkça %90 ila %97 arasında değişen tungsten miktarının, 2 ila 4 değerleri arasında değişen nikel/demir oranının ve sinterleme sonrası işlemlerin (ısıl işlem ve dövme) W-Ni-Fe alaşımlarının mikroyapı ve mekanik özellikleri üzerindeki etkisi araştırılmıştır. Sıvı fazlı sinterlenmiş numuneler mekanik testlerle, elektron mikroskobu ve XRD çalışmaları ile, ısıl analizlerle ve kantitatif metalografik methotlar ile karakterize edilmiştir.

En uygun sinterleme döngüsü araştırılmış ve W-Ni-Fe alaşımlarına uygulanmıştır. Hidrojen altında indirgenmenin bağlayıcı fazın yüzey oksitsiz tungsten tanelerini daha iyi ıslatmasına bağlı olarak daha yüksek mekanik özellikler sağladığı sonucu elde edilmiştir. Karakterizasyon çalışmaları sonrasında, bitişiklik değerinin tungsten miktarına bağlı olarak artmasının sünekliği önemli ölçüde azalttığı ve ana kırılma mekanizmasının tane içi kırılmadan taneler arası kırılmaya geçişini sağladığı görülmüştür. Ayrıca, bağlayıcı fazın erime sıcaklığının ve tungsten çözünürlüğünün nikel/demir oranının artışına bağlı olarak arttığı görülmüştür. Tungsten çözünürlüğündeki bu artışın, hem bağlayıcı fazın hacim oranının yükselmesine hem de daha iyi mekanik özellikler elde edilmesini sağlamıştır. Sinterleme sonrası ısıl işlemin bitişiklik değerinin düşürmesi ve bağlayıcı fazın hacim oranını artırmasını sağladığı ve bunun sonucu olarak sünekliğin arttığı görülmüştür. Alaşımların deformasyon sonrası çekme mukavemetinin ve sertlik değerlerinin içyapıda ki dislokasyon yoğunluğunun artışına bağlı olarak arttığı fakat bu artışın aynı zamanda kırılma yüzeyindeki bağlayıcı faz kırılma ve tane içi kırılma miktarının artışına sebep olduğu gözlemlenmiştir.

Anahtar Kelimeler: Sıvı Fazlı Sinterleme, W-Ni-Fe Alaşımları, Mekanik Özellikler, Deformasyon, Ni/Fe Oranı, Bitişiklik.

To My Precious Family…

ACKNOWLEDGMENTS

It would not have been possible to write this doctoral thesis without the help and support of the kind and unique people around me, to only some of whom it is possible to give particular mention here.

I wish to express my deepest gratitude to my supervisor Prof. Dr. A. Şakir Bor and co-supervisor Assoc. Dr. Nuri Durlu for their firm guidance, helpful suggestions, prompt feedbacks, endless patience advice, criticism, encouragements and close collaboration throughout the research. This dissertation could not have been completed without their support.

I am also grateful to my colleagues and friends, Önder Soyer, Dr. Elif Öztürk, Kürşat Karail, Dr. M. Kaan Pehlivanoğlu, İlker Atik, Onur Dinçer and Hakan Der for their never ending support, encouragement and help throughout the entire period of the study.

The technical assistance of Fatih Koca, Mustafa Aktaş, Vedat İleri and Levent Kutlucan are gratefully acknowledged.

I would like to express my sincere gratitude to Serkan Yılmaz and Emin Erkan Aşık from Middle East Technical University for their assistance in the Scanning Electron Microscopy work.

I am most grateful to Önder Şahin for his assistance in the mechanical characterization work.

I would like to acknowledge the financial and technical support of the TÜBİTAK SAGE and its staff since the start of this doctoral thesis in 2006.

Finally, I would like to thank my beautiful wife Selin for her personal support, great patience and understanding my absence during my studies instead of spending time with her. My parents, Hatice Çalışkan, Cumali Çalışkan and my sister, Nazende Çalışkan, have given me their unequalled and precious support throughout this study, as always.

TABLE OF CONTENTS

ABSTRACT ..... **v**

ÖZ ..... **vi**

ACKNOWLEDGMENTS ..... **viii**

TABLE OF CONTENTS ..... **ix**

CHAPTERS

1. INTRODUCTION **1**

2. THEORETICAL FRAMEWORK **5**

2.1 Tungsten and Tungsten Based Alloys 5

2.2 Processing of High Density Tungsten Based Alloys 6

2.2.1 Mixing and Compaction 7

2.2.2 Liquid Phase Sintering 8

2.3 Microstructural Description of High Density Tungsten Heavy Alloys 11

2.3.1 Volume Fraction of Phases 11

2.3.2 Contiguity of Solid Tungsten Particles 12

2.3.3 Particle Size of Solid Tungsten Particles 15

2.4 Mechanical Properties of Tungsten Based Alloys 20

2.4.1 Effect of Sintering Conditions 22

2.4.2 Effect of Composition 25

2.4.3 Effect of Alloying Elements 32

2.4.4 Effect of Post Sintering Operations 32

2.4.4.1 Heat Treatment and Aging Behavior 32

2.4.4.2 Deformation 35

2.5 Fracture Behaviour of High Density Tungsten Based Alloys 37

3. EXPERIMENTAL PROCEDURE **41**

3.1 Alloy Preparation 41

3.1.1 Raw Materials Used in the Study 41

3.1.2 Alloy Systems Investigated 42

3.1.3 Mixing and Isostatic Compaction of Powder Components of W-Ni-Fe Alloys 42

3.1.4 Sintering and Heat Treatment Studies of W-Ni-Fe Alloys 43

3.1.5 Cold Deformation 44
3.2 Structural Characterization 44
3.2.1 Density Measurements 44
3.2.2 Microstructural Characterization 45
3.2.2.1 Microstructural Examination 45
3.2.2.1.1 Quantitative Metallographic Examinations 45
3.2.2.1.1.1 Contiguity Measurements 45
3.2.2.1.1.2 Volume Percent of Binder Matrix Phase Analysis 46
3.2.2.1.1.3 Average Particle Size Analysis 47
4. RESULTS AND DISCUSSION 51
4.1 Effect of Sintering Conditions on the Properties of Tungsten Heavy Alloys 51
4.2 Effect of Composition on the Properties of Tungsten Heavy Alloys 54
4.2.1 Tungsten Content 54
4.2.2 Binder Phase Composition 64
4.3 Effect of Post Sintering Operations on the Properties of Tungsten Heavy Alloys 72
4.3.1 Heat Treatment 72
4.3.2 Deformation 80
5. CONCLUSIONS 85
REFERENCES 87
CURRICULUM VITAE 97

CHAPTER 1

INTRODUCTION

Tungsten has been used in our daily life for more than 100 years in the form of different products from filament in a light bulb to counterweight in an aircraft. Tungsten has been an attractive and interesting metal for designers, engineers and scientists because of its unique physical properties such as high density, high elastic modulus and high melting point. However, due to the difficulties in processing and properties such as low ductility at the room temperature and poor weldability of pure tungsten, researchers studied extensively to find a way in order to produce tungsten alloys and make use most of unique tungsten properties in an easier and more feasible way. Therefore, tungsten and tungsten based alloys have been produced by the powder metallurgy processing routes since the beginning of 1930's.

Price et. al. [1] were first to find a way of producing tungsten based alloys at temperatures relatively low compared to pure tungsten melting point by mixing tungsten with nickel and copper. This processing technique was characterized by a liquid phase forming at a specified stage of the applied heat treatment cycle and was named as liquid phase sintering process. After this invention, studies were concentrated on the mechanical properties of these alloys. Further studies led to development of the tungsten based alloys with nickel and iron which have better mechanical properties compared to nickel and copper based tungsten alloys. Studies about improving the mechanical properties of these alloys are still going on.

Due to their high density, these alloys are also called as tungsten heavy alloys in the powder metallurgy literature. In addition to the property of high density, these alloys provide high ultimate tensile strength, yield strength and ductility. Due to this spectacular combination of physical and mechanical properties, these alloys are used in both civil and military applications such as electrical contact materials, radiation shields, counter weights, vibration damping devices and kinetic energy penetrators. Tungsten based alloys are also considered as dual-use, i.e. civil and military use, materials.

In order to improve the mechanical properties of these alloys, processing effects and physical metallurgy of these alloys during liquid phase processing should be well understood. Additionally, liquid phase sintered microstructure might be correlated to mechanical properties over a theoretical basis in order to predict the mechanical properties by utilizing a microstructural characterization. Therefore, considerable work and studies have been done on the microstructural characteristics and mechanical properties since mid-1950.

In the production of tungsten based alloys, residual porosity greater than 0.5% greatly decreases the mechanical properties such as toughness and ductility. Therefore, main goal is to reduce the porosity content in the microstructure in order to obtain superior and reproducible mechanical properties. Porosity might be resulted from the incomplete reduction of the metal powders which leads to incomplete wetting of liquid phase and low

cohesion interface strength, trapped gas due to hydrogen reduction reaction or inert gases utilization instead of hydrogen in pressureless sintering and shrinkage cracks due to rapid solidification of liquid phase. Therefore, in the present study, optimization of sintering cycle shall be performed in terms of complete oxide reduction of metal powders, low cooling rates from the liquid phase forming temperatures to prevent shrinkage cracks, sintering atmosphere change from hydrogen to argon in order to induce the degassing and remove the hydrogen embrittlement effects.

Microstructural properties of these alloys dictate the mechanical properties. Therefore, microstructural description of these alloys is very important to control and improve the mechanical properties. Tungsten heavy alloys are composed of tungsten varying from 80 to 98 weight percent and ductile binder matrix phase (Ni rich phase) containing generally nickel, copper, iron or cobalt which holds tungsten particles together. Microstructures of these alloys are characterized by some microstructural properties. These properties are volume fraction of both phases (tungsten particles and/or binder matrix phase), contiguity of tungsten particles and average tungsten particle size.

Volume fraction of the phases, contiguity of tungsten particles (the measure of the solid-solid particle contacts) and average tungsten particle size are easily affected by the raw materials used, processing conditions, post sintering operations including the thermo-mechanical treatments such as deformation and aging.

Ductility is a mechanical property which is very sensitive to the microstructural parameters. For instance, it is strongly dependent on the amount of W-W interfaces because these interfaces are considered as the weakest parts in the microstructure. These weakest parts behave as crack initiation areas in the microstructure.

During the liquid phase sintering process, coarsening of tungsten particles are also observed due to the solubility differences of the tungsten particles having different sizes in the binder matrix phase. Average particle size of tungsten might affect the yield strength and crack propagation such as transgranular or intergranular failure under tensile loading.

The mechanical properties of tungsten based alloys are mainly dominated by the strength of the interface between the tungsten particles and binder matrix phase. Tungsten solubility is the main concern for the mechanical properties since tungsten based alloys are chemically bonded composites. Tungsten solubility is mainly affected by the Ni/Fe ratio and sintering temperature. However, in order to prevent the intermetallic formation on the cooling step of sintering cycle, nickel to iron ratio is generally fixed to the ratio of 2.33.

Purity of the starting elemental powders may also affect the ductility and toughness of high density tungsten based alloys due to the segregation of the impurities such as carbon, phosphorus and sulfur to the boundaries in the microstructure.

Water quenching after heat treatment under vacuum or inert gases is also generally conducted to prevent the segregation at the interphase boundaries, homogenization of microstructure, removal of hydrogen and prevent the intermetallic formation in the microstructure.

In order to increase the mechanical properties of tungsten based alloys which will be used especially for the impact applications, thermomechanical studies including deformation and subsequent heat treatment, such as swaging, hydrostatic extrusion and rapid hot extrusion have been also used. Strength of the alloys were increased by work hardening which also affects the microstructural features such as tungsten particle shape/size, contiguity and fracture properties of tungsten based alloys.

Crack propagation and crack path selection under tensile loading are directly related to a minimum fracture energy path or weakest path in the microstructure. For the case of brittle tungsten based alloys having lower mechanical properties, mainly tungsten-matrix interfacial separation or failure can be observed on the fracture surfaces. For the case of ductile tungsten based alloys having higher mechanical properties, little tungsten-binder matrix phase separation is observed but mostly tungsten cleavage and ductile failure of the binder matrix phase is observed on the fracture surfaces. Crack propagation at the fracture surface might be impeded by the binder matrix phase if the tungsten-binder matrix phase interface strength is strong enough which is mainly affected by the tungsten solubility.

The main objective of this PhD study is to investigate the effect of tungsten content and binder composition on microstructural and mechanical properties of selected tungsten based alloys. Liquid phase sintering processing method was utilized for the processing of these alloys with different tungsten contents having Ni/Fe ratio varied from 2 to 4. Quantitative microstructural characterization and mechanical characterization were conducted for the analysis of the selected alloys. Other objectives of this study are to investigate the effect of post sintering operations such as heat treatment and deformation on the microstructural and mechanical properties of the selected liquid phase sintered alloys and the optimization of the processing conditions in terms of sintering atmosphere according to the mechanical characterization studies.

In the present study, literature review about tungsten based alloys including liquid phase sintering theory, processing conditions, microstructural parameters and effect of post sintering operations including heat treatment and deformation were presented in Chapter Two. The experimental procedure employed for processing tungsten based alloys and mechanical/microstructural characterization methods including the empirical formulas used were presented in Chapter Three. The optimization of sintering conditions, the effects of composition including tungsten content and Ni/Fe ratio, effect of heat treatment, effect of deformation and results of the characterization techniques were discussed in Chapter Four. Finally, Chapter Five was about a summary of the conclusions derived from this PhD study.

CHAPTER 2

THEORETICAL FRAMEWORK

2.1 Tungsten and Tungsten Based Alloys

Tin miners in Germany were the first people to discover the tungsten compound in the sixteenth century. The miners gave the mineral the German name Wolfrahm, meaning "wolf froth". In 1755, Swedish chemist Axel Frederik Cronstedt (1722-1765) realized that it was unidentified element and called this mineral as tungsten having meaning as "heavystone" in Swedish [2]. The largest known tungsten reserves in earth are in China, Canada, Russia and North America [3].

More than 200 years after the tungsten was discovered, the first and effective use for tungsten came into the existence at the start of the twentieth century. An U.S. chemist William D. Coolidge invented a way of making tungsten wire having ductile properties [2] in 1909. He applied for a patent which describes the way of the powder metallurgical production of his product as a ductile tungsten wire. This work induced the large scale powder metallurgy of tungsten and tungsten based alloys and his patent is still valid [3]. After this invention, production of tungsten and tungsten alloys become relatively easier and tungsten and its alloys found many application areas in our daily life.

About 65% of tungsten and its alloys consumption is as tungsten carbide and tungsten carbide alloys which are used mainly for cutting and wear applications in the industry. Tungsten and its alloys in a wire form are used mostly for lighting, electronic devices such as electron microscope filaments, and thermocouples. Another application area and main interest of this study is the military applications of tungsten and tungsten based alloys. These applications are kinetic energy penetrators and fragments in warheads in which high density and mechanical properties are strongly required [4]. In the powder metallurgy literature, these alloys are known as tungsten based alloys or high density tungsten based alloys. In this study, tungsten heavy alloys will be mentioned as high density tungsten based alloys or tungsten based alloys.

Price *et al.* [1] were the first to introduce the new processing procedures of high density tungsten based alloys. They worked with tungsten based alloys containing nickel and copper. It was noted in their study that alloys with high tungsten content can be sintered to almost full density at the temperatures relatively well below the melting point of tungsten. Although W-Ni-Cu alloys are still used for some applications such as for non-magnetic applications, their mechanical properties were unsatisfactory compared to other high density tungsten based alloys especially for W-Ni-Fe alloys which are described in the following sections.

After the invention of the W-Ni-Cu alloys, W-Ni-Fe alloys were discovered and these new type of tungsten based alloys exhibited better mechanical properties in terms of ductility and ultimate strength as compared to W-Ni-Cu alloys [5].

Ni-Cu based or Ni-Fe based tungsten heavy alloys have similar microstructures composed of two main distinct phases; round like tungsten particles and binder matrix phase consisting of alloying elements (Ni, Cu or Fe) with dissolved tungsten. Typical microstructure is given in Figure 1 [6]. As seen in Figure 1, tungsten is the main or principal phase of the microstructure and ranges from 90 to 98 wt% resulting in high density between 17 and 18.5 g/cm^3. Nickel, iron and copper form the binder matrix phase holding the tungsten particles together in the microstructure. Body centered cubic (bcc) tungsten particles are nearly pure and binder matrix phase has a face centered cubic (fcc) structure and contains around 20 wt% tungsten in the solid solution [2].

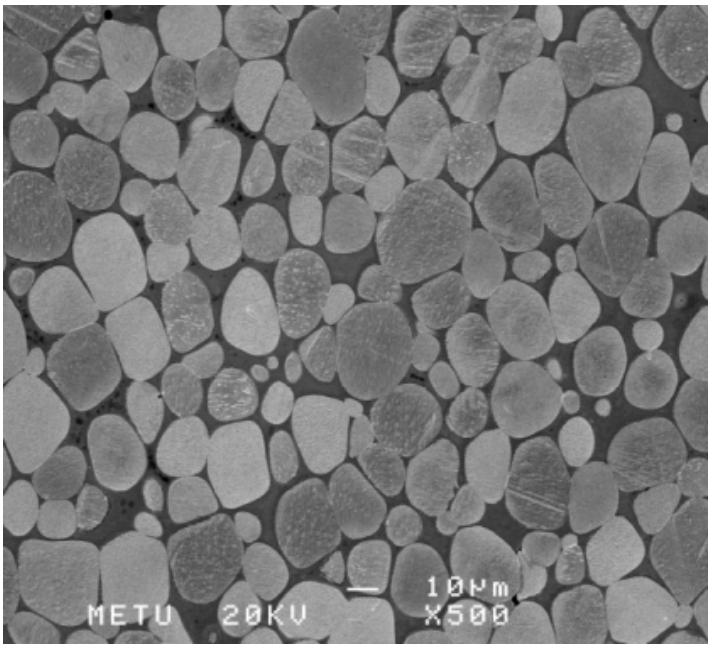

Figure 1. Typical microstructure of powder metallurgy processed tungsten based alloys, tungsten particles are surrounded by the binder matrix phase containing nickel, copper and tungsten [6].

2.2 Processing of High Density Tungsten Based Alloys

High density tungsten based alloys are processed by a conventional route of powder metallurgical technique including mixing, compaction and sintering processes. Each of the steps is very important to get the uniform microstructure as well as stable mechanical properties of the products. Two main steps; Pre-sintering step including mixing/compaction and liquid phase sintering steps will be discussed in the following sections.

2.2.1 Mixing and Compaction

Dry mixing without any lubrication is good enough to achieve a uniform mixture of elemental powders while mixing of tungsten based alloys. Therefore, any mixing or pulverising equipment such as turbula mixer, attritor or ball mill may be used for mixing of the high density tungsten based alloys. However, during the compaction step selection of the pressing equipment receives much more attention. There are considerable differences between the pressing of mixed alloy powder by using hydraulic/mechanical press or by using isostatic press.

In the process of single or double action pressing technique, density gradients occur in the green compact as a result of die wall friction or similar effects. The highest density in the green compact occurs next to the upper punch face as given in Figure 2.

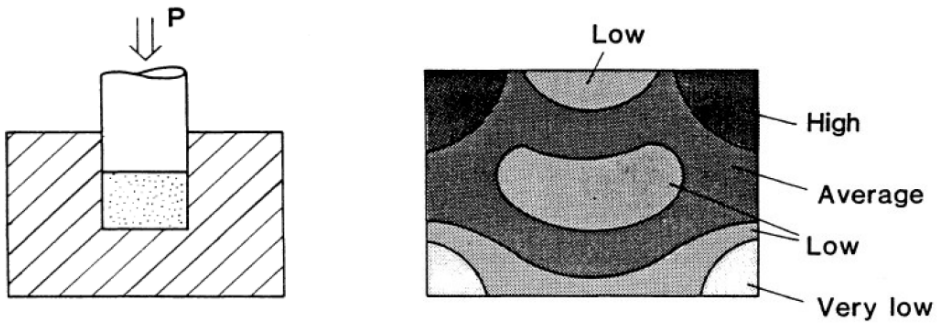

Figure 2. Non-uniform density distribution occurred in a rigid die while using hydraulic/mechanical press [7].

The height to diameter ratio of the compact affects the densification character of the green compact. As the height to diameter ratio increases, density gradients in a compact will increase and this results in a decrease in the overall compact density leading to low mechanical properties [8]. Density gradients occurred during the compaction steps may be reduced significantly by using isostatic press in which pressure is applied to the mixed alloy powder isostatically by media in the pressure vessel. However, the main disadvantage of isostatic pressing of the alloy powders is that dimensional control is not tight as in the hydraulic pressing because of using flexible polymeric mold. After shaping by using any route of shaping or compaction, tungsten alloy powders have enough green strength for the subsequent processes. Therefore, there is no need for the polymeric additives during isostatic pressing. Typical and reasonable compaction pressures for tungsten based alloys are in the range of 200-400 MPa. Owing to liquid phase during the sintering process, applying excessive pressures is meaningless in order to achieve the high density after sintering process [6].

After the mixing and shaping steps of the alloy powders, green compacts are sintered. Sintering can be defined as bonding of compacted powders when heated to temperatures in excess of approximately half of the absolute melting temperature of the constituents [9]. If a liquid phase occurs during the sintering process, this sintering process is called as liquid phase sintering (LPS) in the literature.

LPS is a widely used sintering process for the manufacturing of both ceramic and metallic alloys [10]. There are two main forms of liquid phase sintering. If a liquid phase exists throughout the high-temperature portion of the sintering cycle occurred by using alloyed powder mixture, this liquid phase is called as persistent liquid. If a liquid phase disappears during the sintering cycle due to dissolution into the solid or formation of a new phase, this liquid phase is called as transient liquid phase [11]

2.2.2 Liquid Phase Sintering

Due to having a liquid phase formed by the additive elements as Ni, Cu, Fe or Co diffusion during the process is very fast. The liquid phase provides for faster atomic diffusion than solid state sintering processes. The kinetics of LPS is controlled by various parameters such as wetting, segregation, solubility, and diffusivity [10]. Typical microstructural changes which occur during LPS is given in Figure 3.

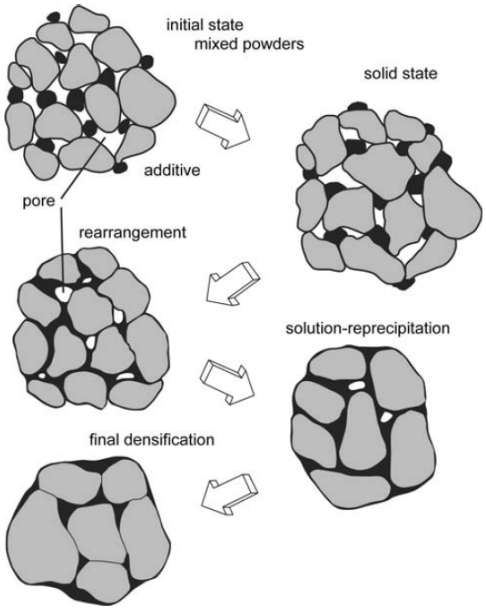

Figure 3. A schematic of the microstructural changes occurred during LPS [11].

At the beginning, solid state sintering occurs between the elemental powders. After a melt forms and spreads through the particles, rearrangement of the solid particles occur and rapid densification occurs due to capillary force applied by the wetting liquid on the solid particles.

As densification by rearrangement of tungsten particles slows, solubility and diffusivity effects become dominant factors in the solution–reprecipitation stage. The differences in curvature dependent solubility result in the concentration gradient in the liquid between the solid particles of different sizes. Owing to this solubility difference, material is transported from the small solid particles to large particles by the liquid. The result of this process is the significant densification and the coarsening of the solid particles which are tungsten particles in this study [10]. The last stage of LPS is referred to as final densification in solid state. Densification is slow and rearrangement is not possible in this stage because of the solid structure of the solid particles. However, coarsening of the solid particles keeps going and subsequent very little densification as compared to the densification occurred in the previous stages is achieved. However, residual pores may enlarge if they contain the entrapped gas such as argon or any similar gases which results in the compact swelling in the microstructure. Therefore, mechanical properties of liquid phase sintered materials are reduced by long sintering cycles and thus, short sintering times are generally preferred [9-11].

During the stages of the liquid phase sintering process especially in the rearrangement and the solution re-precipitation steps, solid and liquid solubility in each other determines the final microstructure of the alloy. Liquid phase occurred in the process should wet the solid particles in order to penetrate between the solid particles and dissolve the sinter bonds formed previously which provides particles rearrangement in the microstructure. Additionally, mass transport between the solid particles occurs owing to the solid solubility in the liquid might induce particle coarsening and densification in the microstructure [11].

In order to estimate the compatibility of any system for the liquid phase sintering process, binary and ternary phase diagrams of the system (W-Ni-Fe alloy system was selected for this study) shall be analyzed in detail in terms of the solubility. An ideal case for the densification in persistent liquid phase sintering process in terms of the relative solubility is given in Figure 4. According to this diagram, densification requires the high solid solubility in liquid and low liquid solubility in solid in persistent liquid phase sintering processes.

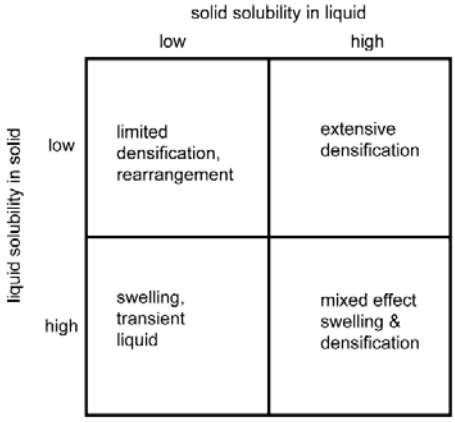

Figure 4. A schematic guide to the behavior expected based on the relative solubility of the two phases [11].

Binary phase diagrams of W-Ni and W-Fe are given in Figure 5. According to the binary phase diagram of W-Ni, with up to 40 wt.% tungsten solubility in the Ni rich primary solution can be achieved whereas nickel has negligible solubility in tungsten. Similar solubility trends are also observed in the binary W-Fe phase diagram. It can be concluded that W-Ni and W-Fe systems are appropriate for the liquid phase sintering processes if the main phase is selected as tungsten.

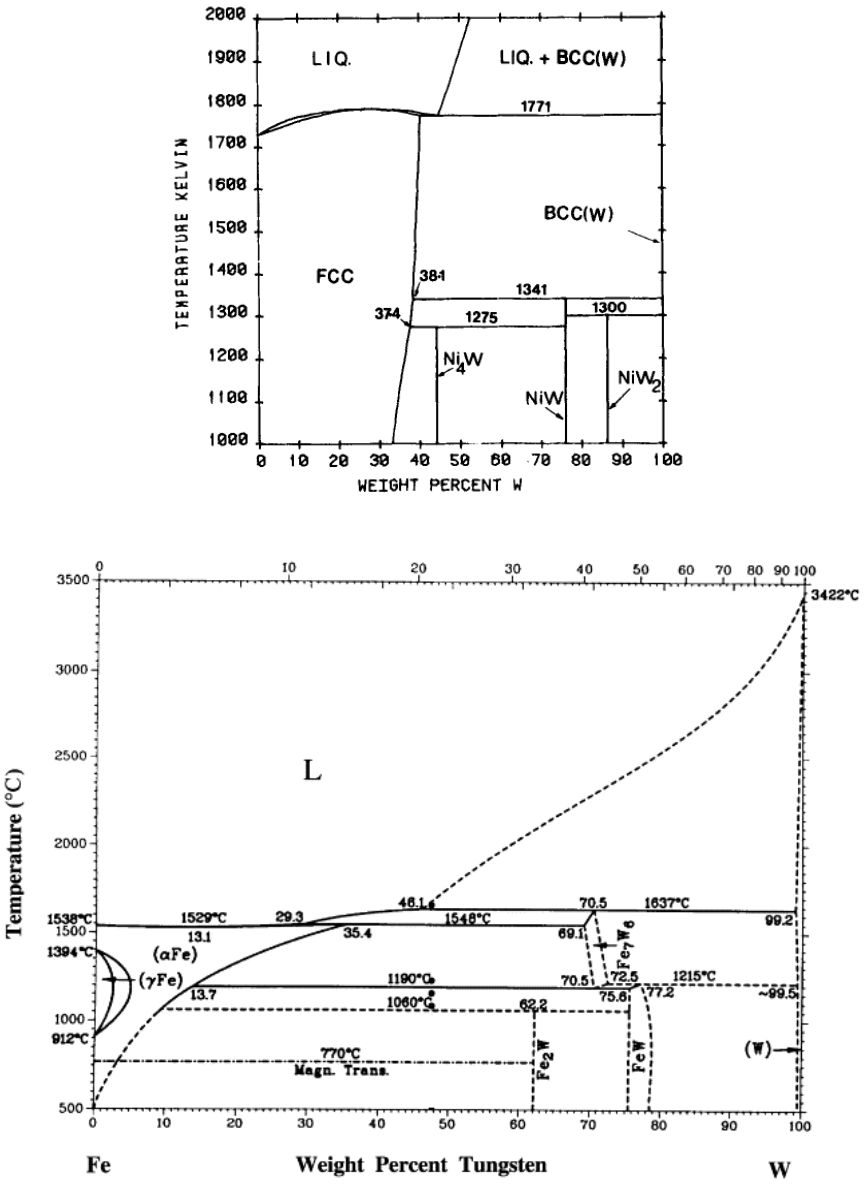

Figure 5. Binary phase diagrams**;** W-Ni binary phase diagram (up) and the W-Fe binary phase diagram (down) [12, 13].

However, as seen in the binary phase diagram of W-Ni given above there is high possibility of formation of intermetallics such as Ni_4W and NiW. These brittle intermetallic phases may form during cooling step of the sintering cycle due to temperature dependence of the solubility differences at the temperatures below 1275 °C and may decrease the mechanical properties of the high density tungsten based alloys. The possibility for precipitation increases with the amount of Ni due to the increase in the solubility of the tungsten for a given sintering temperature. However, it was reported that addition of iron to the alloy decreases the solubility of tungsten in nickel and prevents formation of the intermetallic phases. It was also found that a nickel to iron ratio of 7: 3 avoids intermetallic precipitation on cooling [14].

It was also reported that for W-Ni-Fe alloys having Ni:Fe ratio<1 were brittle due to the formation of stable μ (Fe_7W_6) phase. It was also given that for W-Ni-Fe alloys alloys having Ni:Fe ratio>4, another brittle phase as Ni_4W occur with a slow cooling rate from temperatures greater than approximately 950 °C. However, it is easy to resolutionize the Ni-W intermetallics in the binder matrix phase as compared to μ phase due to their lower peritectoid temperatures [15]. There is an also intermetallic free binary zones for the W-Ni-Fe alloy system defined in the previous studies [15] as 1000-1300 K for the Ni:Fe ratios of between 1 and 4.

The variation of Ni/Fe ratio not only affects the intermetallic formation but also the mechanical properties of the high density tungsten based alloys. Higher levels of W in the binder solution generally resulted in the superior mechanical properties [15]. The effect of composition especially for nickel to iron ratios on the microstructural and mechanical properties of the tungsten based alloys will be discussed again in this chapter.

After the liquid phase sintering process, final microstructure of the tungsten based alloys consists of two main phases as shown in Figure 1. Important parameters to be used for describing the microstructure of high density tungsten based alloys will be also explained in the following sections.

2.3 Microstructural Description of High Density Tungsten Heavy Alloys

As seen in Figure 1, tungsten based alloys are metal matrix composite structures and their microstructures, in terms of phases present, are characterized by some important microstructural properties. These properties can be given as % areal or volume fraction of phases (tungsten particles or binder matrix phase), contiguity of tungsten particles and average tungsten particle size.

2.3.1 Volume Fraction of Phases

Volume fraction of the phases is an important microstructural parameter which affects the mechanical properties of the tungsten based alloys. Measurements of the volume fraction of phases are based on different principles with different procedures [16, 17] including point counting methods. There is also an international standard describing a systematic manual point counting procedure for statistically estimating the volume fraction of an identifiable constituent or phase from sections through the microstructure by using a point grid [18].

Volume fraction of phases can also be performed by automated image analysis software. This method is also described by the international standard [19].

Processing conditions, raw materials used, post sintering operations including the thermo-mechanical treatments such as deformation and aging can affect the volume fraction of phases observed in the final microstructure. Figure 6 shows the typical reported volume fraction values for the Ni-Fe based tungsten based alloys having different weight percents. Volume fraction of the phases in the microstructure may affect the mechanical properties of high density tungsten based alloys directly or indirectly which will be explained in the following sections.

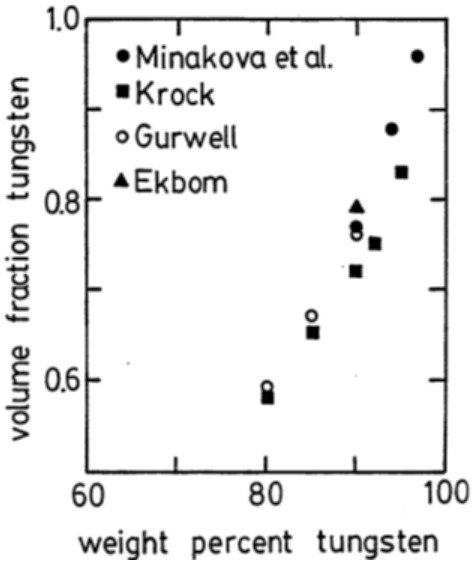

Figure 6. Typical volume fraction values of tungsten based alloys with various tungsten contents [5].

2.3.2 Contiguity of Solid Tungsten Particles

Another important microstructural parameter is the contiguity of tungsten particles. Contiguity is the measure of the solid-solid particles (measure of tungsten-tungsten interfaces) in the microstructure. The contiguity is also defined as the W-W interfacial area as an average fraction of the total interfacial area [20]. Contiguity of tungsten particles, C_w, is determined by counting the number of interphase boundary intercepts along a random test line placed on the metallographic image and by using the following equation [21],

$$C_w = \frac{2N_{WW}}{2N_{WW}+N_{WB}} \quad (2.1)$$

N_{WW} = Number of W-W interfaces as to unit length of test line
N_{WB} = Number of W-B (binder phase) interfaces as to length of test line

Mechanical properties are strongly dependent on the amount of W-W interfaces because these interfaces are the weakest parts in the microstructure [20].

Contiguity values and volume fractions of phases (binder matrix phase) are easily affected by the processing conditions and initial compositions [22]. Figure 7 and Table 1 show the variation of contiguity values and volume fractions of phases with the change in the amount of tungsten. As tungsten increases, contiguity of tungsten particles increases and volume fraction of binder matrix phase decreases as given in the figure. Even for the same composition, different sintering methods could also yield the different contiguity values, as given in Table 2.

Table 1. Variation in microstructural properties of different W-Ni-Fe alloys sintered at 1485 °C for 2 hours and heat treated at 1100°C under vacuum [23-24].

Composition in wt.%	Volume % of Binder phase	Contiguity	APS of W (μ)
97.5W-1.75Ni-0.75Fe	4	0.98	30
95W-3.5Ni-1.5Fe	10	0.45	34
92.5W-5.25Ni-2.25Fe	15	0.35	31
90W-7Ni-3Fe	20	0.21	31
87.5W-8.75Ni-3.25Fe	17	0.23	30
97.5W-1.25Ni-1.25Fe	4	0.80	30
95W-2.5Ni-2.5Fe	7	0.64	29
92.5W-3.75Ni-3.75Fe	11	0.51	27
90W-5Ni-5Fe	17	0.41	30
87.5W-6.25Ni-6.25Fe	17	0.45	19

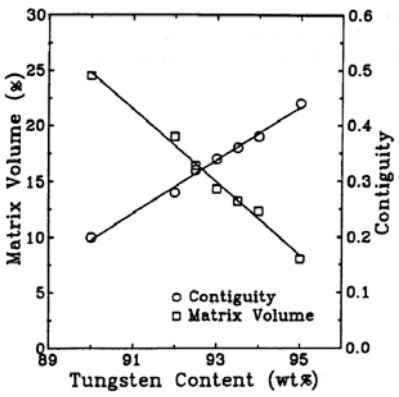

Figure 7. The variation of contiguity and binder matrix volume fraction with tungsten content [20].

Table 2. Variation in microstructural parameters and mechanical properties of 92.5W-6.4Ni-1.1Fe alloy which was sintered at 1500°C with conventional sintering furnace and microwave furnace [25].

Composition in Wt.%	Contiguity	APS of W (μ)	UTS (MPa)	El%
92.5W-6.4Ni-1.1Fe (by conventional furnace)	0.32	17.3	642	11.2
92.5W-6.4Ni-1.1Fe (by microwave furnace)	0.42	9.4	805	3.5

In order to achieve the maximum mechanical properties, contiguity of the tungsten particles should be controlled or reduced by the subsequent sintering operations. In high density tungsten based alloys, the ductility or the maximum elongation is strongly dependent on the contiguity values. A high contiguity in the microstructure induces a lower ductility [26]. It is easily seen in Figure 8 that although UTS of the alloys increases slightly, ductility decreases gradually as contiguity increases. Contiguity value of the alloy also affects impact strength as shown in Figure 9. As contiguity increases, impact strength of the alloy decreases for high density tungsten based alloys.

Due to the contiguity effect on the mechanical properties of the tungsten based alloys, modelling the relationship between the contiguity and other microstructural parameters and physical considerations in liquid phase sintering process are studied well in the literature [27, 28].

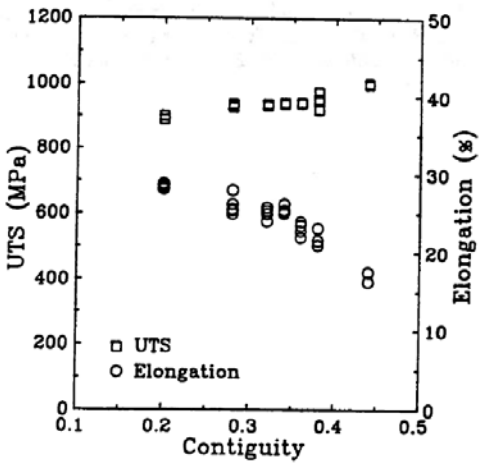

Figure 8. The variation of UTS and elongation of 93W-5.6Ni-1.4Fe alloy sintered at 1485 °C with contiguity [20].

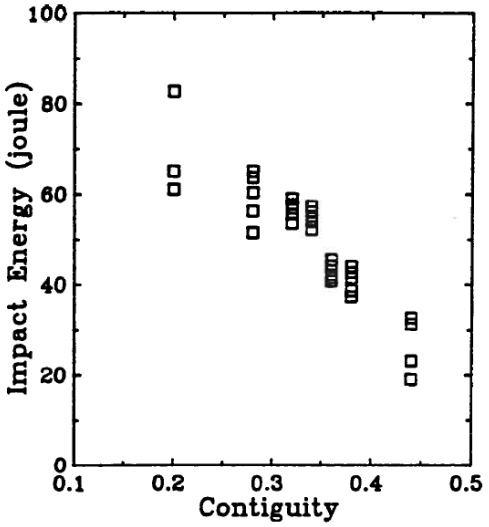

Figure 9. The variation of impact energy of 93W-5.6Ni-1.4Fe alloy sintered at 1485 °C with contiguity [20].

To sum up, only contiguity values are not enough and confidence to compare the studies or alloys, additional microstructural parameters are also needed to compare physical and mechanical properties. These microstructural parameters will be explained in detail in the following sections.

2.3.3 Particle Size of Solid Tungsten Particles

The coarsening of solid tungsten particles is observed during liquid phase sintering of the tungsten based alloys. This coarsening mechanism may be explained by the Ostwald ripening theory. In the Ostwald ripening mechanism, small particles dissolve in the matrix while bigger particles grow further [29]. The shrinkage of the W particles at the initial stages of sintering and increase in the amount of liquid phase can be calculated simply by level rule application. At this stage, i.e. during dissolution of W particles in the liquid matrix, kinetics is expected to obey the square root law ($X=kt^{1/2}$) as in any similar diffusional phenomena. Once the liquid matrix is saturated with the equilibrium amount of W, coarsening due to surface curvature dependent solubility occurs. This phenomenon also known as Ostwald ripening, is well documented in the literature [30 - 32] and because of its statistical nature coarsening phenomena obeys $t^{1/3}$ kinetics. Average particle radius will increase as the one third power of time and one third power of the equilibrium concentration of the W particle.
Due to this phenomena different particle sizes from almost zero to approximately twice of the average can be observed in the final microstructures of high density tungsten based alloys [6].

Any processing parameter such as tungsten content, sintering temperature and composition of the alloys affecting tungsten solid solubility can change average particle size of the microstructure. Therefore, measurement of average particle size is important to describe the sintering conditions applied to the alloy system.

As seen in the Figure 10, average particle size of tungsten particles increase with amount of tungsten. Further, coarsening rate constant also increases with the weight percent of tungsten [33-34].

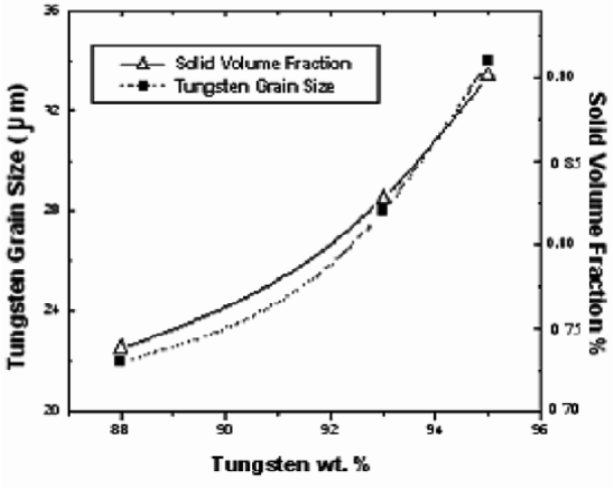

Figure 10. Variation of average particles size of tungsten particles with tungsten content for 88, 93 and 95 wt.% tungsten [33].

Average particle size is also affected by the starting composition and sintering time as well as sintering temperature. As observed in W-Ni-Cu alloy system, tungsten solubility in the binder matrix phase can be changed by varying the nickel to copper ratio in the composition. The solubility of tungsten in the matrix increases as nickel content increases in the binder matrix phase [14]. As a result of this, average particle size of tungsten particles increases as nickel to copper ratio in the binder matrix phase increases [35]. Figure 11 shows the variation of average particle size of tungsten particles with the sintering time and nickel to copper ratio. As can be seen, average particle size of tungsten in the alloys having nickel to copper ratio as 4 are always greater than average particle size of tungsten in the alloys having nickel to copper ratio as 1.5. It was also reported that average particle of tungsten particles increases with the sintering temperature [14].

Average particle size measurement of the tungsten particles, which can be performed on the metallographic cross section, is well documented in the literature [37].

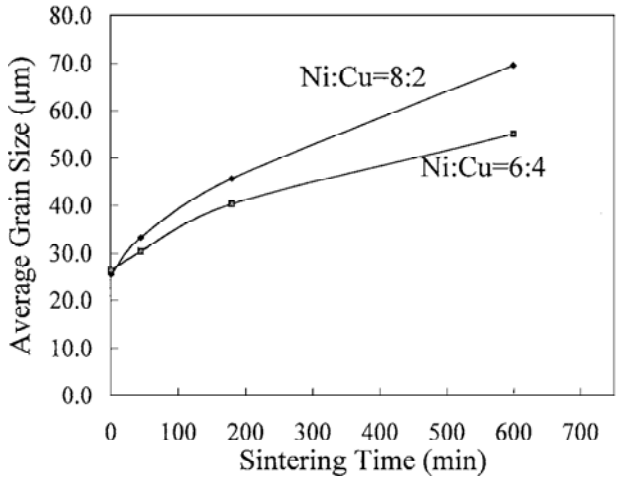

Figure 11. Average particle size variation with sintering time for 88W-Ni-Cu samples sintered at 1500°C during microgravity sintering [36].

Additionally, average particle size is also very important in order to determine the mechanical properties and failure behavior of the high density tungsten based alloys. As given in Figure 12, average particle size affects crack propagation behavior of the sintered alloys during tension testing. It was cited in the literature that the lower is the size of tungsten particle, higher is the tensile strength of tungsten based alloys. As the particle size decreased, the tensile fracture mode was found to change from interface failure to matrix failure and then to tungsten particle cleavage failure [38].

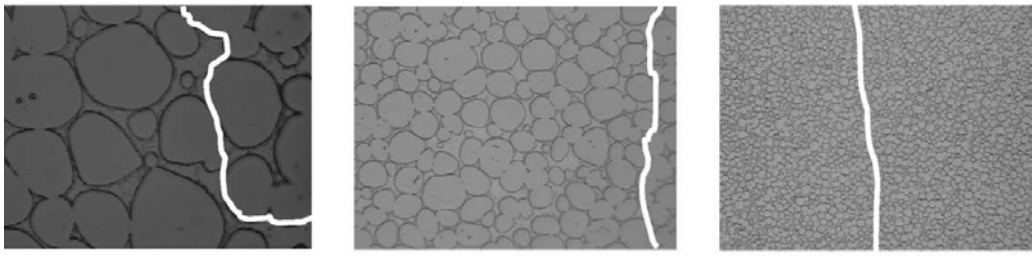

Coarser tungsten particle size leads to intergranular fracture which is interfacial failure.

Medium tungsten particle size leads to intergranular fracture which is matrix failure.

Fine tungsten particle size leads to granular fracture which is tungsten particle cleavage.

Figure 12. Schematic diagram showing the preferred path of fracture in high density tungsten based alloys with different particles sizes under tensile loading [38].

Other studies involving the modelling of the particle size coarsening dependency on the liquid content, particle coarsening under microgravity conditions and correlations between

the average particle size and contiguity with empirical mathematical expressions are also well documented in the literature [39-41].

Average particle size of solid tungsten particles has also effect on the mechanical properties of tungsten based alloys. For instance, yield strength of dual phase alloys (tungsten based alloys belong to this type of alloys) is found to be directly related to the inverse square root of average thickness of soft phase which is binder matrix phase between hard phase which is tungsten particles in the present case [42]. By using Hall-Petch equation [43], the relationship between yield strength and microstructural properties such as average tungsten particle size and binder matrix volume fraction can be given as [42, 44-47];

$$\sigma_y = \sigma_o + kGb\left[\frac{1-V_M}{DV_M}\right]^{1/2} \quad (2.3)$$

where σ_y is the yield strength of the alloy, σ_o is the intrinsic strength, k is a constant, G is the shear modulus, b is the Burgers vector, D is the average tungsten particle size and V_M is the binder matrix volume fraction.

According to this equation, yield strength of the tungsten based alloys increases with decrease in the average particle size of the tungsten particles and volume fraction of the binder matrix phase. On the contrary, it was also reported that mechanical properties in terms of stress-strain diagram are independent of binder matrix volume fraction for the alloys having tungsten contents in the range of 80 to 92 wt.% tungsten [48].

As mentioned before, the weakest part in the microstructure is the tungsten-tungsten interfacial area called as contiguity and contiguity values obtained in the final microstructure is directly related to the mechanical properties. As seen in Table 3, elongation is directly related to the contiguity for tungsten based alloys. Elongation decreases as contiguity increases in the microstructure.

Table 3. Variation in microstructural parameters and mechanical properties of mechanically alloyed 93W-5.6Ni-1.4Fe alloys with changes in sintering temperature [49]. The samples were sintered one minute under hydrogen, and heat treated at 1150°C for 1 hour under nitrogen.

Sintering Temperature (°C)	VF of BMP (%)	Contiguity	APS of W (μ)	UTS (MPa)	El. (%)	Hardness (HRC)
1445	12	0.70	5	893	1	28.7
1460	14.5	0.46	13	932	12.2	28.3
1470	15.3	0.43	16.8	924	13.8	28.1
1480	16.7	0.40	18.2	923	18.5	27.8

However, it was also reported that for the same composition, elongation is directly related to the average particle size of tungsten particles. The relationship between the average particle size of tungsten and the mechanical properties especially ductility of the tungsten based alloys is given in Table 4. As seen in this table, as average particle size increases, elongation of the alloys decreases with increase in contiguity.

Table 4. Variation in microstructural parameters and mechanical properties of 95W-3.5Ni-1.5Fe alloys with sintering time [50]. The alloys were sintered at 1480°C under wet hydrogen followed by a switch to dry argon for cooling and heat treated at 1100°C for 1 hour and water quenched.

Composition	Sintering Time	Contiguity	APS of W (μ)	UTS (MPa)	El. (%)
95W-3.5Ni-1.5Fe	30 minutes	0.511	18.9	930	18.2
	60 minutes	0.471	27.1	845	15.6
	600 minutes	0.25	45.1	836	14

It was also found that it is possible to change the average particle size of solid tungsten particles with the composition as seen in Table 5.

Table 5. Variation in microstructural parameters and mechanical properties of tungsten based alloys with binder composition [51]. The alloys were sintered at 1200°C under wet hydrogen. Alloys having a nickel to iron ratio of 6:4 or higher were heat treated at 1200°C for 2 hours under vacuum.

Composition	VF of BMP (%)	Contiguity	APS of W (μ)	UTS (MPa)	El. (%)
90W-5Ni-5Fe	27	0.238	16.2	910	20
90W-6Ni-4Fe	27	0.22	18.6	937	25
90W-7Ni-3Fe	27	0.211	17.6	937	36
90W-8Ni-2Fe	27	0.178	19.8	951	40
90W-9Ni-1Fe	29.5	0.153	19.3	965	40
90W-8Ni-2Co	28	0.133	19.8	1006	36
90W-9Ni-1Co	30.5	0.129	19.9	999	40

2.4 Mechanical Properties of Tungsten Based Alloys

If processed properly, tungsten based alloys can provide very high strength (1000- 1700 MPa) and very high ductility (10–30%) [52]. In order to produce high quality tungsten based alloys with better mechanical properties, important steps or parameters to be controlled in the production are given as follows [53];

a) Quality of powders (purity, etc.),
b) Powder mixing procedure,
c) Sintering cycle including heating and cooling steps,
d) Sintering atmosphere,
e) Post sintering heat treatments
f) Thermomechanical operations (eg. Swaging and heat treatment)

Especially for the military applications, the aim is to produce or develop alloys providing high penetration capability against target and maximum toughness in order to resist the impact at very high velocity. Factors which influence toughness and also the mechanical properties of tungsten based alloys are summarized in

Figure **13** given below;

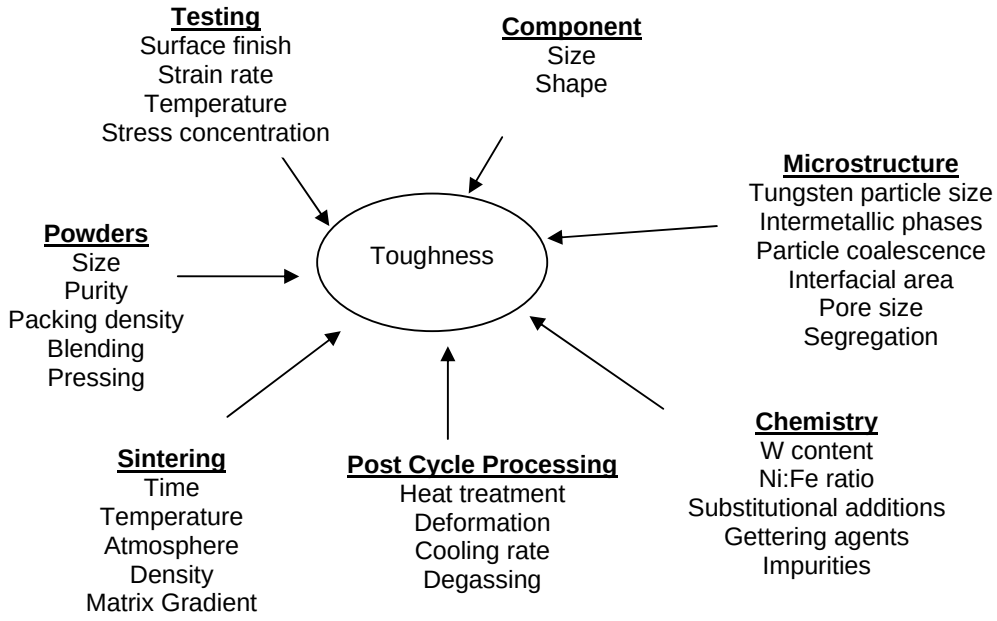

Figure 13. Important parameters affecting the toughness of tungsten based alloys [51, 54-55].

In order to achieve the required high mechanical properties, almost complete densification is needed. Presence of porosity due to incomplete or improper cooling (slow cooling may be needed in order to minimize the shrinkage effects [5]) from the sintering temperature can reduce the mechanical properties considerably.

Further, the evolution and size of porosity in the microstructure is also important. It was given that small spherical pores have little effect on mechanical properties whereas large pores resulting from coalescence or gas evolution especially observed in excessive sintered specimens and also greater than 0.5% porosity in the microstructure degrade the mechanical properties considerably, especially the ductility of tungsten based alloys [56]. The effect of porosity on ductility of the tungsten based alloys is given in Figure 14.

There are many reasons related to the sintering or processing conditions for incomplete densification or residual pores observed in the alloy which can be given as solidification or shrinkage micro pores at the cooling step of the sintering cycle, trapped gas in the pores, inadequate sintering times, very long sintering times and pores formed by some reactions occurred during the processing [57]. Therefore, it is very important to choose and modify the appropriate sintering atmosphere in order to reduce the pore content in the final microstructure. In the following part, effects of atmospheres and sintering time on the mechanical properties of tungsten based alloys will be discussed.

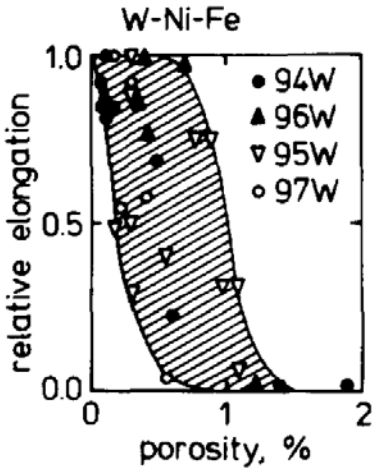

Figure 14. Effect of porosity on relative elongation for W Ni-Fe alloys with different tungsten contents [56].

2.4.1 Effect of Sintering Conditions

Hydrogen atmosphere is generally preferred for liquid phase sintering process of high density tungsten based alloys. Sintering under inert gas atmosphere gives unsatisfactory results in terms of physical and mechanical properties. Non-reducing atmospheres such as argon led to incomplete densification and lower mechanical properties. It was reported that incomplete densification under inert atmosphere is caused by the coarsening of tungsten particles more rapidly than the neck growth [58]. It was also noted that incomplete reduction of oxides may affect the wetting of liquid phase which may degrade the mechanical properties during sintering under argon atmosphere [57].

However, there are also some problems of sintering under dry hydrogen atmosphere. Unreduced oxygen coming from the tungsten into the binder matrix phase is released during the dissolution of tungsten particles. Dissolved hydrogen forms water vapor by reacting the oxygen in the matrix. Unfortunately, water vapor is insoluble in the binder matrix phase and water vapor pores occur. In case of long sintering times, these pores can grow by coalescence and ripening mechanism leading to low mechanical properties and lower sintered density. This problem can be solved by using wet hydrogen atmosphere in order to help the water vapor to diffuse to the surface of the compacts [59].

If a gas is trapped in the pores, the densification can be also be reduced by the increase in the gas pressure in the pore during the pore collapsing mechanism. There can be 3 different situations in terms of gas solubility character in the pore evolution mechanism,

1- An insoluble gas such as argon can be trapped,
2- A gas having high solubility and high diffusivity can be trapped,

3- Samples in which either solubility or diffusivity impedes the pore collapsing mechanism due to the gas pressure effect [59].

As explained before, if the sintering atmosphere is not reducing or is inert, gas trapped in the pores impair the pore closure mechanism and residual porosity becomes stabilized. Further, incomplete reduction inhibits the liquid penetration into the solid particles. Therefore, sintering under inert gases or non-reducing gases resulted in lower sintered densities. In the case of hydrogen trapped in the pores, i.e. gas having a high solubility and a high mobility through the matrix, the pressure occurred in the pores has a little effect on the densification rate.

Furthermore, pore degassing can also be conducted in order to reduce the gas pressure effect by changing atmosphere, for instance, changing hydrogen to argon atmosphere during sintering [59]. In addition to this pore degassing effect, changing sintering atmosphere from hydrogen to argon avoids the hydrogen embrittlement effect due to bcc crystal structure of tungsten in the tungsten based alloys [57].

Generally, it is better to choose the short sintering times rather than the long sintering times. A short sintering time like 30 minutes is optimum [55]. It is shown that long sintering times results in the pore coarsening by both diffusion and coalescence due to the rapid tungsten particle coarsening which results in the increase in the total pore content and decrease the mechanical properties. Further, long sintering times also induce the flattening of tungsten particles and decrease the contiguity of the microstructure [50, 55, 59].

Vacuum as a sintering atmosphere is also preferred for sintering of tungsten based alloys. The mechanical properties obtained by using the sintering atmosphere as a vacuum are quite reasonable and comparable to the mechanical properties obtained under the hydrogen atmosphere. However, vaporization of matrix occurs under vacuum which leads to decrease in mechanical properties in terms of embrittlement and a density increase especially for the alloys having tungsten content around 97 wt.%, as expected. Additionally sintering under vacuum atmosphere results in fast pore elimination (no gas trapped in the pores) which is leading to rapid and complete densification. As can be understood, in order to sinter under vacuum for the alloys having high tungsten contents it is better to choose short sintering times or choose the alloys having low tungsten content to minimize the binder matrix vaporization leading to embrittlement [57].

Figure 15 summarizes the effect of different atmospheres on the properties including the density of the tungsten based alloys. It should be noted that optimal sintering atmosphere shall be selected carefully in order to achieve the high mechanical properties. As seen in Figure 15, long sintering times is detrimental to the mechanical properties for all kind of atmospheres.

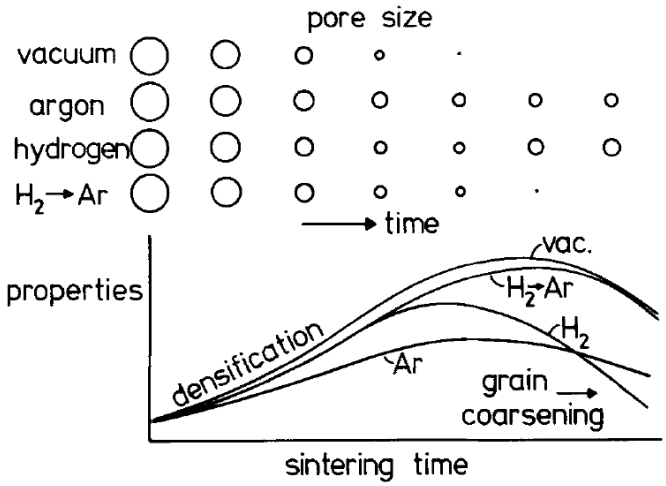

Figure 15. A Schematic plot of pore size and properties with sintering time for W-Ni-Fe alloys sintered under different atmospheres [59].

In order to reduce the amount of residual pores in the microstructure, cooling step of the sintering cycle is also very important. Slow cooling rates shall be used to minimize the shrinkage or solidification shrinkage at least up to liquidus temperature of the alloy caused by the shrinkage differences of solid and liquid phases [55].

As mentioned before, hydrogen removal is necessary in order to achieve higher mechanical properties. Therefore, vacuum heat treatment or switching to an inert gas atmosphere from hydrogen at the sintering cycle is applied to tungsten based alloys. As given in Figure 16, for the W-Ni-Fe alloys having different nickel to iron ratios are firstly subjected to sintering under hydrogen and exposed to the vacuum heat treatment for hydrogen removal operation after sintering process. It can be easily seen that heat treated alloys showed the higher elongation vales as compared to alloys which are not heat treated. Additionally, it was also noted that lower Ni/Fe ratios are less sensitive to hydrogen embrittlement [60].

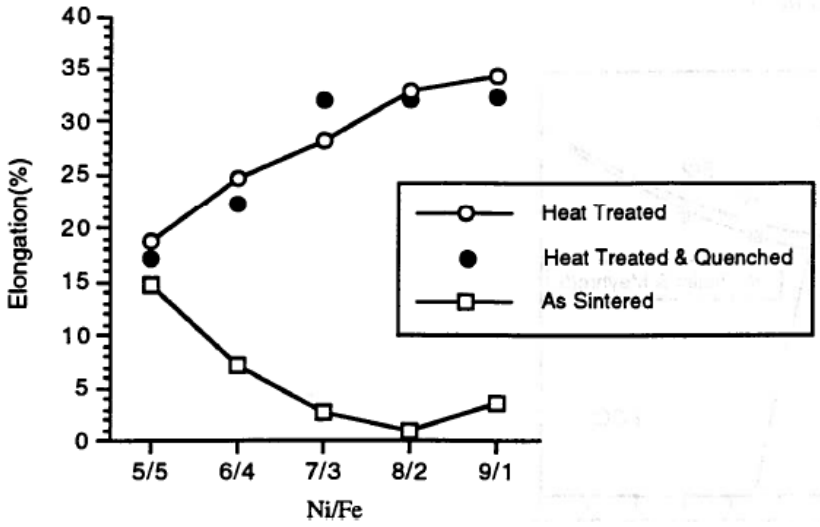

Figure 16. Variation of elongation with nickel/iron ratio in different heat treatment conditions for 93W-Ni-Fe alloys [60].

Purity of the powders and nickel to iron ratios in the starting composition have a significant effect on the mechanical properties and whole sintering process in terms of selection of post sintering operations. In the following part, effects of the purity of raw materials and composition variations as nickel to iron ratios on the mechanical properties of tungsten based alloys will be discussed.

2.4.2 Effect of Composition

Tungsten base alloys are typical composite materials that are composed of two main phases which are tungsten particles and binder matrix phase. In W-Ni-Fe alloys, binder matrix phase consists of nickel, iron and dissolved tungsten called as NiFe-rich phase. Binder matrix phase has a slight solubility, less than 3 wt.%, in the tungsten phase but tungsten has a high solubility, around 22 wt.% [61], in the binder matrix phase.

The mechanical properties of tungsten based alloys are dependent on the strength of the interface between the tungsten rich particles and binder matrix phase [38]. Mechanical properties of tungsten based alloys increases as the tungsten content in the binder matrix phase increases [15, 62].

Nickel to iron ratio in the initial composition changes the tungsten content in the solid solution binder matrix phase in the microstructure. As shown in Figure 17, weight % of tungsten increases as nickel to iron ratio in the initial composition increases. Furthermore, microstructural changes, especially volume percent of the binder matrix phase changes as nickel to iron ratio changes. As given in Table 6, volume percent of binder matrix phase increases with increases in nickel to iron ratio, leading to changes in the physical and mechanical properties. Tungsten particle coarsening also depends on the tungsten solubility in the binder matrix phase. Higher solubility of tungsten caused by the increase nickel

content in the matrix leads to higher average particle size of tungsten, lower contiguity and higher ductility in the tungsten based alloys [63].

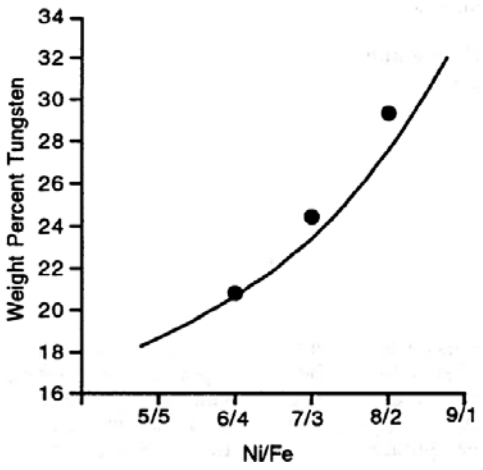

Figure 17. Variation of tungsten solubility in the binder matrix phase with nickel to iron ratio for 90W-Ni-Fe alloys sintered at 1400 °C [60].

Table 6. Variation of volume percent of the binder matrix phase with nickel to iron ratio [60].

Amount of Tungsten	Nickel to iron ratio			
	5/5	7/3	8/2	9/1
	Volume percent of binder matrix phase (%)			
90 wt.%W	22.5	22.8	23.2	24.1
93 wt.%W	16.3	16.5	16.8	17.4
96 wt.%W	9.7	9.8	9.9	10.3

Liquid phase sintering of W-Ni-Fe alloys is conducted at the temperatures above the liquidus temperature of the W-Ni-Fe ternary system. Therefore, any change in the ratio of nickel to iron affects the liquidus temperature of the system as given in Figure 18. Liquidus temperature increases as nickel to iron ratio increases in the composition.

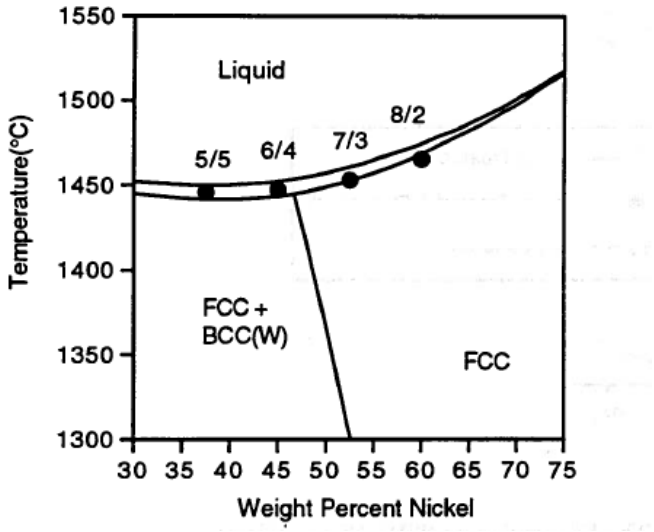

Figure 18. The Fe-Ni-W phase diagram with fixed tungsten content as 25 wt.% [60].

As mentioned before nickel to iron ratio is generally fixed to the ratio of 2.33 in order to prevent intermetallics formation on the cooling step of sintering cycle. In Figure 19, the effect of nickel to iron ratio on the mechanical properties of tungsten based alloys in terms of % elongation and tensile strength is given. As shown in Figure 19, fixing Ni to Fe ratio to 2.33 led to the limited mechanical properties. For the vacuum annealed samples, maximum tensile strength and elongation was obtained with a Ni/Fe ratio of 4, and for the vacuum annealed and quenched even better mechanical properties were achieved with a Ni/Fe ratio of 14. Further, unnotched charpy energy [64] of the samples increases up to around nickel to iron ratio of 2. In this study [15], tungsten based alloys having nickel to iron ratio between 1.5 and 5 were reported as intermetallic free alloys which is not in agreement with the previous findings in the literature.

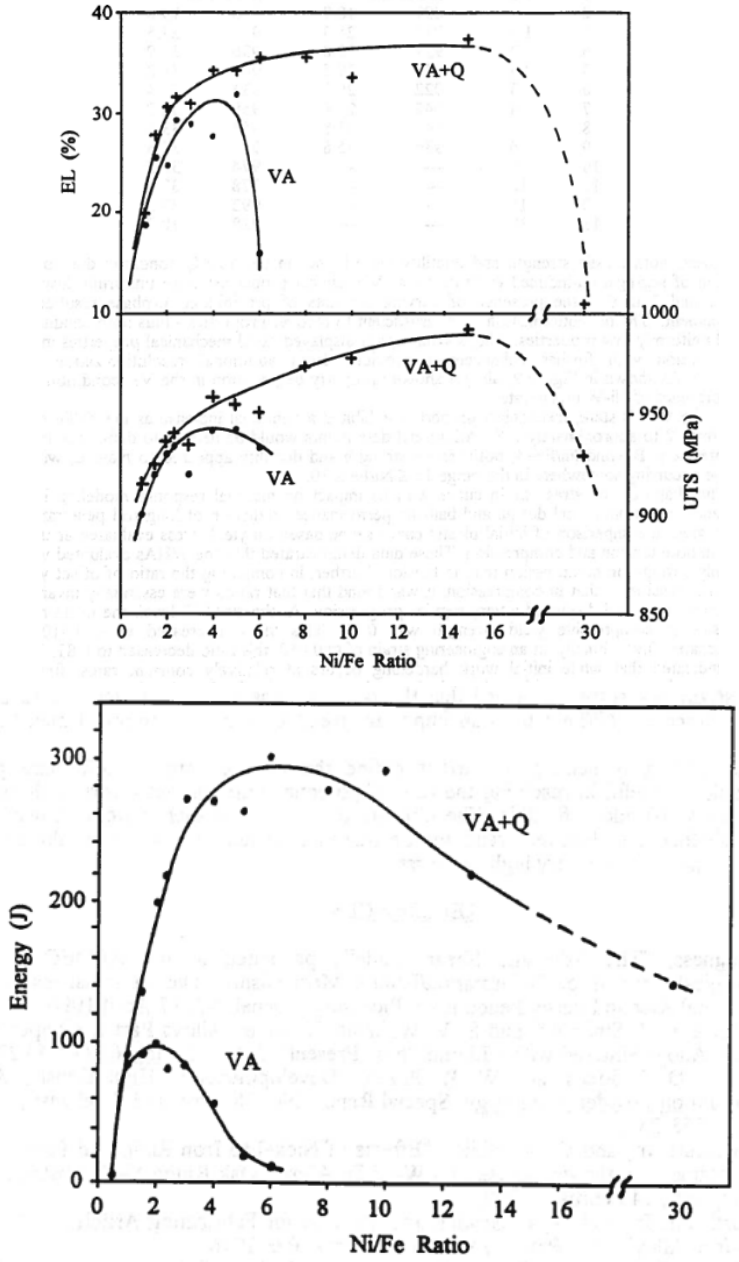

Figure 19. Variation of tensile strength, elongation and unnotched impact energy with Ni/Fe ratio for the 93W-Ni-Fe alloys with the nickel to iron ratio for 0.5< Ni/Fe< 30. VA, vacuum anneal is applied at 1050°C for 10 hours; VA + Q, vacuum anneal and quench, quenching is applied subsequent to annealing at 1100°C under N_2 for 2 hours [15].

It was also cited that yield strength of the alloys increases with increase in the nickel to iron ratio as given in Table 7.

Table 7. Variation of yield strengths obtained in tension and compression with nickel to iron ratio for the alloys having 93 wt.% tungsten [15].

Nickel to iron ratio	Compressive (MPa)			Tensile (MPa)		
	0.2%	1.0%	5.0%	0.2%	1.0%	5.0%
2.3	710	793	1030	655	717	827
4	731	807	1040	655	731	841
8	745	827	1060	689	752	862
15	772	855	1100	703	765	883

Mechanical properties of the tungsten based alloys are not only dependent on the nickel to iron ratio. The tungsten content has also a considerable effect on the mechanical properties as well as physical properties such as density of the alloys. As seen in Table 8, density and ultimate tensile strength increases as the tungsten content increases up to around 93 wt.%. However, ductility of the tungsten based alloys decreases considerably as the amount of tungsten increases. Similar results (see Figure 20) were also given in another study [65].

Table 8. Tensile and physical properties of tungsten based alloys having 88%, 93% and 95% wt.% tungsten sintered at 1500 °C for 30 min and vacuum annealed at 1100 °C for 8 hours [33].

Mechanical and physical properties of the alloys	Alloys compositions investigated		
	88W-8.4Ni-3.6Fe	93W-4.9Ni-2.1Fe	95W-3.5Ni-1.5Fe
Density (g/cm3)	16.60	17.52	17.98
Tensile strength (MPa)	894	996	916
Elongation (%)	30	23	11

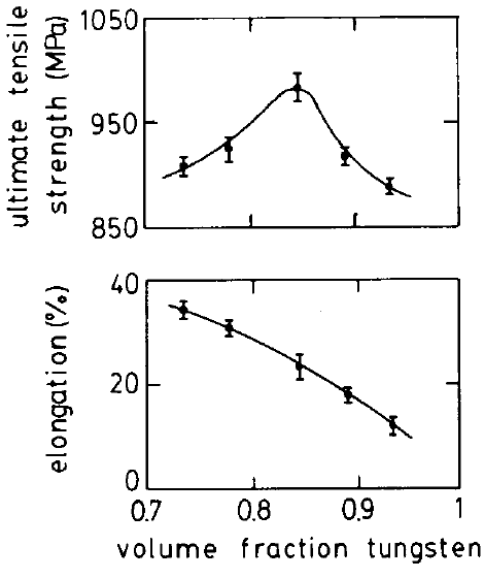

Figure 20. Variation of tensile strength and elongation with the weight percent of tungsten in the high density tungsten based alloys having 88 to 97 wt% tungsten sintered at 1480 °C for 30 minutes [66].

According to Humail et al. [33], in tungsten based alloys the variation in the mechanical properties might be due to changes in the tungsten particle size, volume fraction of binder matrix phase and weak W/W interfaces as contiguity differences obtained during the study. It was also concluded in this study that stronger binding energy between the NiFe rich phase and tungsten particles leads to a material having high mechanical properties by transferring the stresses between tungsten particles and binder matrix phase. The observed the maxima in the tensile strength of the alloys in this study can be explained as follows [65], up to 93wt.% tungsten, increase in the harder phase, which is tungsten particles, leads to increase in the strength of the alloy as in the rule of mixtures, however after 93wt.% tungsten a transition occurs in the fracture characteristic due to the increase in tungsten contiguity (see Figure 21) and after 93wt.% tungsten ductility of the alloys is dominated by the microstructure. As seen in Figure 21, contiguity of the tungsten particles also increases with increase in tungsten content which controls and dominates the ductility after a specific point in the microstructure.

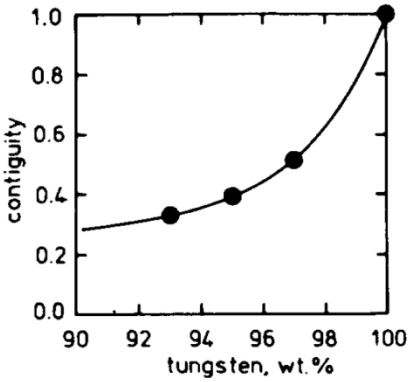

Figure 21. Variation of contiguity with tungsten content [56].

Yield strength and strain hardening coefficient values of tungsten based alloys are also affected by the amount of tungsten in the initial composition. As seen in Table 9, yield strength and strain hardening coefficient increase as tungsten increases. Strain hardening coefficient is important for the metallic materials in terms of workability and deformability. Strain hardening coefficient may vary from 0 which corresponds to a perfectly plastic solid to 1 which corresponds to an elastic solid [43]. The strain-hardening coefficient is very important for the workability of the metals, because this exponent indicates the measure of strengthening mechanism as the materials is strained [43, 66]. This coefficient is calculated from the true stress and true strain curve which will be discussed in detail in Chapter 3. The values of n range from 0.05 to 0.5 depending on the microstructure and the history of the heat treatment applied. Strain hardening coefficient also indicates the maximum uniform elongation that material can withstand before the necking or plastic instability. Further, strain hardening exponent guides the maximum reduction in cross sectional during the drawing process. As the value of strain hardening coefficient increases, final cross section area to which the metal can be reduced by drawing process decreases [66]. Determination of strain hardening coefficient of metallic materials in sheet are also described by the international standard [67].

Purity of the starting elemental powders may also affect the ductility and toughness of high density tungsten based alloys through the amount and segregation of the impurities such as carbon, phosphorus and sulfur to the boundaries in the microstructure. Segregation of these elements at the boundaries results in the degradation of mechanical properties, especially impact strength. It was reported that water quenching after heat treatment can prevent the segregation at the interphase boundaries [68]. Additionally, dry hydrogen use in debinding treatment is recommended in order to reduce the degradation effects of residual carbon on the mechanical properties, especially ductility, during the sintering operation of tungsten based alloys [69]. The segregation of impurity elements and measurement of these and its effect on the properties of tungsten based alloys are well documented in the literature [56, 69-75].

It was also noted that oxygen forming oxide films on the tungsten particles may lead to low cohesion between the solid particles and liquid phase during the liquid phase sintering process [76].

Table 9. Mechanical properties of different W-Ni-Fe alloys sintered at 1480 °C under hydrogen and argon atmosphere for 30 minutes [65].

Composition Ni/Fe=2.33	Yield Strength (MPa)	Tensile Strength (MPa)	Elongation (%)	Work Hardening Exponent
88W	565	907	34.6	0.48
90W	575	925	30.9	0.51
93W	596	986	23.4	0.56
95W	602	917	18.2	0.57
97W	612	888	12.4	0.58

2.4.3 Effect of Alloying Elements

Alloying addition such as molybdenum, rhenium, tantalum, or yttrium oxide, boron carbide and etc.to the high density tungsten based alloys are employed to increase the mechanical properties. Main purpose of this addition is to improve the mechanical properties without any post sintering operation such as swaging or any similar deformation processes. Unfortunately, embrittlement due to segregation or precipitation makes these efforts unsatisfactory [55]. More studies and experiments are needed to understand the effect of addition of these alloys on the strengthening mechanism.

There are two main mechanisms imposed by alloying additions which are grain refinement or inhibiting the coarsening of tungsten particle size as Hall–Petch type strengthening [43] and solid solution strengthening [43] in the binder matrix phase. On the other hand, mostly added element have lower density than the pure tungsten and alloying results in decrease in the sintered density of the alloys. Alloying additions and their effect on mechanical and physical properties of tungsten based alloy are well documented in the literature [77-82].

2.4.4 Effect of Post Sintering Operations

In order to change the mechanical properties and fracture behavior of tungsten based alloys, some specific treatments such as heat treatment and deformation might be conducted. In the following section studies on these treatments will be summarized.

2.4.4.1 Heat Treatment and Aging Behavior

As explained before, in order to prevent the intermetallic formation such as WNi_4 (β phase) during cooling, nickel to iron ratio is fixed to 2.33 (7/3) by many studies and researchers in the literature. It was also noted that for the higher nickel ratios (higher than 8/2), as sintered properties is lower due to formation of intermetallics [83]. However, controlled precipitation

of β phase at elevated temperatures can also be used to increase the mechanical properties. It was cited that the increase in strength after heat treatment is caused by the precipitation of β in the binder matrix phase and strain aging of tungsten particles which is due to the dislocation segregation of interstitial impurities such as C, N, O or H that can impede the dislocation motions [84, 85]. Further, the reaction kinetics of precipitation of β phase may be accelerated by the strain aging treatment [84-86]. Hardness variation of 93wt% tungsten based alloy with different nickel to iron ratio as a function of aging time is given in Figure 22. As seen from the figure that as aging time increases, hardness of the alloys having nickel to iron ratio of 7/3 decreases till the end of the process. However, for the alloys having nickel to iron ratio of 9/1, hardness decreases slightly at the beginning but then increases till the end of the process. Further, the difference in the hardness of the alloy is getting larger as the aging time increases. It was concluded that, aging mechanisms may differ with the nickel to iron ratio [84].

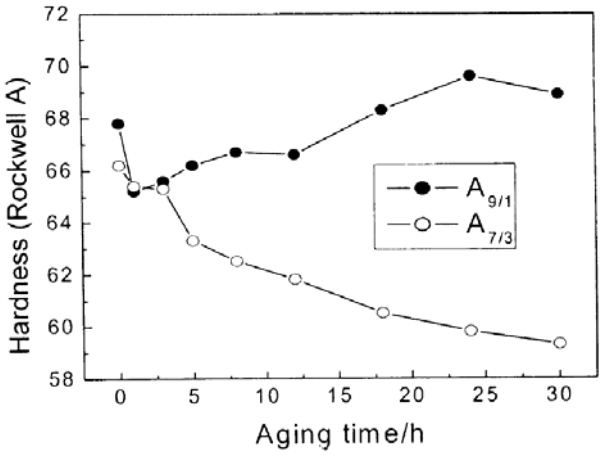

Figure 22. Variation of hardness of alloys with two different nickel to iron ratios and after 20% reduction with the aging time at 800 °C (alloys composition is 36 wt.% tungsten and rest is nickel-iron with different nickel to iron ratios, $A_{9/1}$ means that nickel to iron ratio is 9/1 and $A_{7/3}$ means that nickel to iron ratio is 7/3) [84].

Table 10 and Figure 23 show the variation of mechanical properties of tungsten based alloys having fixed nickel to iron ratio of 7/3 or 2.33. As clearly seen from the table, tensile strengths of both alloys increased and ductility of the alloys remained almost same upon subsequent heat treatment. For both type of alloys, tensile strength is maximum when aged at the temperature of 700 °C and ductility is maximum when aged at the temperature of 800 °C. At temperatures above 800 °C, tensile strength of alloys decreased and ductility of the alloys recovered. Additionally, hardness of the tungsten particles decreased rapidly at the temperatures above 800 °C (see Figure 23). This may be caused by recrystallization or recovery of the tungsten particles [85]. Due to this decrease in hardness, it is useless to apply the heat treatments to the tungsten based alloys at the temperatures above 800 °C. The changes in the deformed microstructure of the tungsten based alloys with aging temperature

in terms of observing the maximums or peaks in the mechanical properties up to a specific temperature and aging mechanism differing with nickel to iron ratio are discussed elsewhere [83-86].

Table 10. Variation in mechanical properties of two tungsten based alloys (90W and 93W with a fixed nickel to iron ratio of 7/3 or 2.33) with deformation and subsequent heat treatment [85].

Composition	Temperature	UTS (MPa)	Yield (MPa)	Elongation (%)
90W	Swaged condition	1135	1066	10.8
	700°C	1230	1090	12.2
	750°C	1180	1063	11.5
	800°C	1173	1042	12.4
93W	Swaged condition	1200	1166	7.6
	700°C	1360	1300	5.1
	750°C	1322	1240	6.0
	800°C	1250	1166	7.5

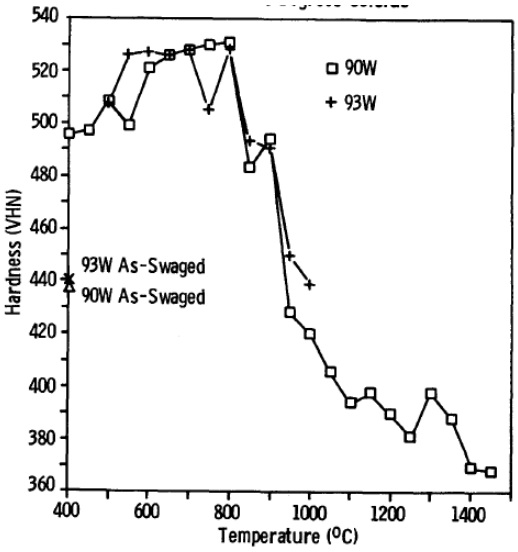

Figure 23. Variation of micro hardness of tungsten particles with the aging temperature for two tungsten based alloys having fixed nickel to iron ratio of 7/3 or 2.33 [85].

2.4.4.2 Deformation

Thermomechanical processes including deformation and subsequent heat treatment, such as swaging [85, 87-94], hydrostatic extrusion [95] and rapid hot extrusion [96] have been used to increase the mechanical properties of tungsten based alloys which will be used especially for the impact applications [97]. Work hardening caused by mechanical deformation is the main reason of the increase in strength and mechanical properties. At small deformations (up to ~15%), hardening is due to increase in the dislocation density of binder matrix phase, whereas at higher degree of deformations (more than ~15% deformation) hardening is due to tungsten particles [96]. Mechanical deformation also affects the microstructural features such as tungsten particle shape, contiguity and fracture properties of tungsten based alloys [91]. Deformation and heat treatment were also used to decrease the average particle size of tungsten particles [98].

As seen in Table 11, as deformation increases strength and hardness of the alloy increases but ductility decreases. Strength and hardness of the alloy increased due to the increase in dislocation density in the alloy [90]. It was also concluded that tungsten based alloys show strain aging behavior especially at the temperatures above 500 °C which can be considered as typical aging behavior explained in detail in the previous sections. Further, there are also 3 different precipitation mechanisms originating from heat treatment of tungsten based alloys as documented in the literature [91].

Table 11 Variation of mechanical properties of 90W-6Ni-2Fe-2Co alloy [90].

Condition	Reduction in Area (%RA)	UTS (MPa)	El. (%)	Hardness (HV30)
Sintered at 1450 °C for 2 hours	0	450	5	430
Heat treated at 1150 °C for 5 hours	0	750	18	435
Swaged-1	10	1348	10	490
Swaged-2	30	1378	9	502
Swaged-3	40	1430	9	530
Swaged-4	54	1560	7	540
Swaged-5	75	1646	6	610
Swaged and heat treated at 300 °C for 1 hour	54	1680	5	542
Swaged and heat treated at 500 °C for 1 hour	54	1740	3	560
Swaged and heat treated at 600 °C for 1 hour	54	1638	4	552
Swaged and heat treated at 700 °C for 1 hour	54	1450	7	520
Swaged and heat treated at 1100 °C for 1 hour	54	1025	5	495
Swaged and heat treated at 300 °C for 1 hour	75	1702	5	604
Swaged and heat treated at 500 °C for 1 hour	75	1823	5	630
Swaged and heat treated at 600 °C for 1 hour	75	1800	4	625
Swaged and heat treated at 700 °C for 1 hour	75	1500	8	590
Swaged and heat treated at 1100 °C for 1 hour	75	871	7	533

Generally speaking, if the alloys are properly sintered, there is no change in the sintered densities observed after plastic deformation [99]. On the other hand, there are some microstructural changes that may be observed after plastic deformation. Contiguity of tungsten particles may increase due to deformation up to specific point during swaging process. This can be explained as; tungsten particles are elongated and become the ellipsoidal shape after plastic deformation. Therefore, distance between tungsten particle is reduced which leads to higher contiguity [90, 91]. On the contrary, for the higher deformations, contiguity of the alloy reduces due to the separation of tungsten-tungsten

contacts or formation of microcracks filled with binder matrix phase [90-92]. Generally, swaging and heat treatment after deformation has no considerable effect on contiguity and average particle size of tungsten particles of high density tungsten based alloys [89-91].

Fracture characteristics of the tungsten based alloy also changes with the amount of deformation applied. As deformation increases, tungsten-tungsten boundary cohesion decreases and cleavage of tungsten particles increases as seen in Figure 24. Post deformation heat treatment also affects the fracture behavior of tungsten based alloys. At low temperatures, precipitation hardening occurs in the binder matrix phase and dominant fracture mechanism is decohesion of tungsten particles along the weak tungsten-tungsten interfaces. However, at the high heat treatment temperatures, this fracture behavior changes which can be correlated to the softening due to the dislocation recovery, coarsening of the precipitation and tungsten-tungsten interface precipitation. Therefore, dominant fracture path becomes tungsten cleavage at high temperatures again as seen in Figure 24 [91].

It was also cited that aging atmosphere affects the hardness of tungsten particles but not the hardness of binder matrix phase. This behavior is correlated with the different strain aging behavior of phases under argon or nitrogen in terms of inhibiting the dislocation movement by the interstitials atoms such as nitrogen and/or carbon atoms [89].

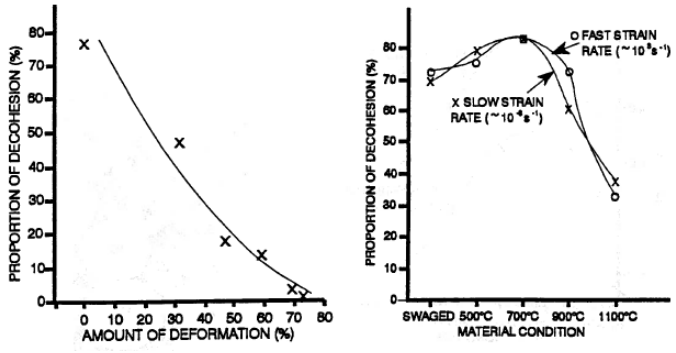

Figure 24. Variation of the amount of tungsten-tungsten cohesion at the fracture surfaces with the amount of deformation and heat treatment for 92.5W tungsten based alloy [91].

2.5 Fracture Behaviour of High Density Tungsten Based Alloys

The fracture behavior of tungsten based alloys and correlation with the microstructure and processing conditions was also studied by many researchers in the literature. First of all, in order to explain the fracture behavior of tungsten based alloys it is better to clarify the possible fracture paths observed in the high density tungsten based alloys. As given in Figure 25, there are four possible crack paths observed at the fracture surfaces of tungsten based alloys. These fracture or crack paths are given as; 1-Tungsten cleavage (transgranular failure), 2-tungsten-tungsten particles interface failure (intergranular), 3- tungsten-binder matrix interface failure and 4-binder matrix failure paths. Crack propagation and crack path

selection under tensile loading are directly related to a minimum fracture energy path or weakest path in the microstructure [65, 38]. For the case of alloys having lower mechanical properties, i.e., brittle alloys, mainly tungsten-matrix interfacial separation or failure is observed. Fracture during tensile testing might start at the interface failure if the interface between tungsten particles and the binder matrix phase is weak. For the case of alloys having higher mechanical properties, i.e., ductile alloys, little tungsten-binder matrix phase separation is observed but mostly tungsten cleavage and ductile failure of the binder matrix phase is observed. If the tungsten-binder matrix phase interface strength is strong enough, crack propagation might be impeded by the binder matrix phase. Additionally, intergranular failure or intergranular crack paths may be observed for both types (brittle and ductile) of alloys [5, 23, 38, 65]. It was also cited that tungsten-binder matrix phase separation or failure can be observed at tensile strengths up to 700 MPa for W-Ni-Fe alloys. However, tungsten particles cleavage failure can be observed for strengths exceeding 850 MPa for W-Ni-Fe alloys [38].

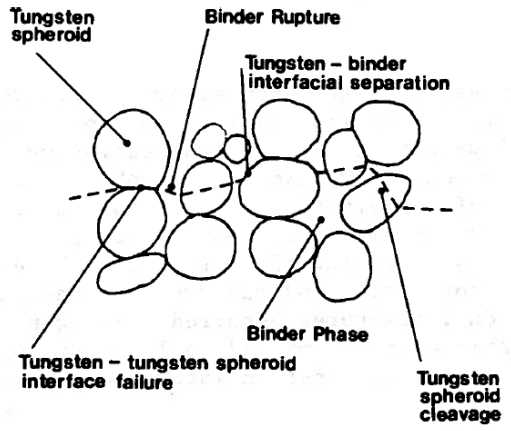

Figure 25. Schematic representation of the possible fracture paths of high density tungsten based alloys [65, 23].

As mentioned before, strength and ductility of tungsten based alloys are dependent on the strength of the tungsten-binder matrix interface [26, 38]. This interface strength can be affected by the impurity segregation to the boundaries, intermetallic formation such as Ni_4W, hydrogen content and residual porosity in the microstructure leading to degradation of mechanical properties [26]. Further, some microstructural properties such as the amount of tungsten which is related to the volume percent of binder matrix phase, contiguity and average particle size of tungsten particles also affect the fracture behavior of tungsten based alloys.

As tungsten content increases from 88 wt.% to 97 wt.%, meaning that volume percent of binder matrix phase is reduced, contiguity increases in the alloy composition, binder matrix phase failure decreases and tungsten-tungsten intergranular failure increases as shown in

Figure 26. It was also noted that as tungsten content increases from 88 wt.% to 97 wt.%, number of tungsten cleavage initially increases and then decreases [65].

Average particle size is also directly related to the fracture behavior of tungsten based alloys. As average particle size of tungsten particles decreases, tensile and yield strength increases and main fracture path transforms into transgranular cleavage from intergranular failure [38, 42].

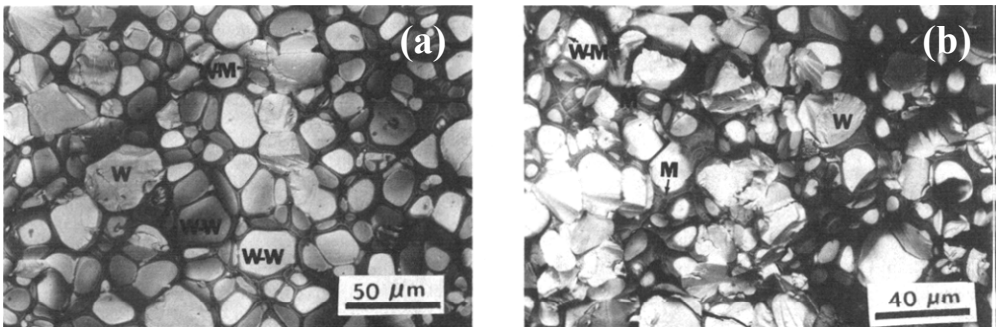

Figure 26. SEM micrographs of the fracture surfaces of alloys with fixed nickel to iron ratio of 7/3 containing (a) 93 pct W, and (b) 97 pct W sintered at 1480 °C for 30 min. W = tungsten cleavage, M = binder matrix rupture, W-W = tungsten-tungsten particle interface separation, and W-M = tungsten- binder matrix phase interface separation [65].

CHAPTER 3

1. EXPERIMENTAL PROCEDURE

In the present study, high density W-Ni-Fe alloys were produced by use of conventional powder metallurgy routes such as dry mixing, cold isostatic compaction and liquid phase sintering. The amount of tungsten was varied from 90 wt.% to 97 wt.% and the nickel to iron ratios was chosen as 2, 2.3 and 4.

The alloys produced were then subjected to microstructural, mechanical and thermal characterization through use of relevant techniques. The materials used in the study, the compositions of the W-Ni-Fe based high density alloys investigated, the experimental procedures applied in alloy preparation and the characterization studies carried out on the produced alloys will be introduced in detail in the following sections.

3.1 Alloy Preparation

3.1.1 Raw Materials Used in the Study

Elemental W, Ni and Fe powders with the characteristics given in Table 12, namely the average particle size, purity, shape and the source of the powders, were used in the present study. Carbon tape was used to handle powders during shape and size distribution analyses. The shape and relative size distribution of elemental powders are also presented in Figure 27.

Table 12. Characteristics of the W, Ni and Fe elemental powders used in this study.

Elemental Powder	Average Particle Size FSSS (μm)	Purity (wt.%)	Shape	Source and Sample Code
Tungsten Powder	4 - 5	99.9+	Polygonal	EUROTUNGSTENE AW 2123
Carbonyl Nickel Powder	4 - 5	99.85+	Spherical	VALE INCO TYPE 123
Iron Powder	5.2 - 6.4	99.5+	Spherical	WILLIAM ROWLAND CIP GRADE 5

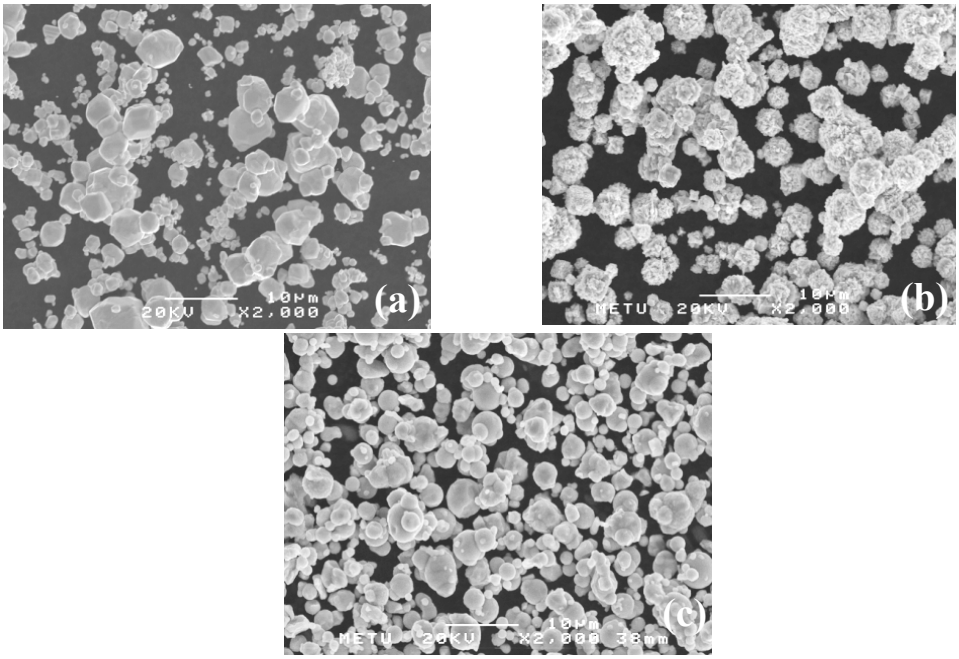

Figure 27. Shape and relative size distribution of elemental powders.
(a) Tungsten Powder, (b) Carbonyl Nickel Powder, (c) Iron Powder.

3.1.2 Alloy Systems Investigated

Elemental powders were weighed in a precision balance (CP3200S, Sartorius, Goettingen, Germany) to give the alloy compositions given in Table 13. The amount of tungsten and nickel to iron ratios were varied according to Table 13. W-Ni-Fe alloy samples were prepared through conventional powder metallurgy route of dry mixing, cold compaction and sintering, explained in detail in the following subsections.

3.1.3 Mixing and Isostatic Compaction of Powder Components of W-Ni-Fe Alloys

All mixing processes were conducted by using Turbula® Shaker Mixer (T2F, Glenn Mills, Switzerland) at a speed of 67 rpm in sealed PE containers for 45 minutes.

A cold isostatic press (CIP 42260, Flow Autoclave Engineers, USA) of 414 MPa capacity was used for isostatically compacting powder mixtures. Cylindrical specimens approximately 20 mm in diameter and 240 mm in height (around 1 kg in weight) were prepared by using polymeric wet bags under pressures around 300 MPa or 45,000 psi. Polymeric bags were fully filled with the mixed powder mixtures. After the compaction, green compacts gained the green densities in between 55 and 65% of the theoretical density. All green compacts had enough strength for the subsequent sintering operations.

Table 13. Nominal compositions of the investigated high density W-Ni-Fe Alloys.

Alloy Designation	Nickel to Iron Ratio	Composition in wt.%
90-1	2	90W-6.67Ni-3.33 Fe
90-2	2.3	90W-7Ni-3Fe
90-3	4	90W-8Ni-2Fe
93-1	2	93W-4.67Ni-2.33 Fe
93-2	2.3	93W-4.9Ni-2.1Fe
93-3	4	93W-5.6Ni-1.4Fe
97-1	2	97W-2Ni-1 Fe
97-2	2.3	97W-2.1Ni-0.9Fe
97-3	4	97W-2.4Ni-0.6Fe

3.1.4 Sintering and Heat Treatment Studies of W-Ni-Fe Alloys

Liquid phase sintering of W-Ni-Fe alloys was conducted at 1480 °C. Optimum sintering cycle was selected based on the literature and previous studies. The experimental procedure applied to W-Ni-Fe alloys is presented in Table 14.

Table 14. The experiment matrix applied to W-Ni-Fe alloys. The samples were sintered at 1480°C for 30 minutes.

Alloy	Sintering atmosphere		Heat treated at 1070 ºC for 120 minutes and water quenched	Deformation (%15 reduction in area)
	H_2+Ar	Vacuum		
90-1	√	-	√	-
90-2	√	√	√	√
90-3	√	-	√	-
93-1	√	-	√	-
93-2	√	-	√	√
93-3	√	-	√	-
97-1	√	-	√	-
97-2	√	-	√	-
97-3	√	-	√	-

As can be seen, two different sintering atmospheres were selected in order to study the optimum sintering cycle for the W-Ni-Fe alloys. Sintering cycles used in the study can be given as;

The sintering cycle (sintering cycle #1) was performed by using the atmosphere controlled sintering furnace (HT-1800M Vac, Linn High Therm Gmbh, Eschenfelden, Germany) by heating from room temperature to 1000 ºC at a rate of around 9°C/min under hydrogen atmosphere, holding for 30 minutes, heating to 1480 ºC at a rate of around 3°C/min under hydrogen atmosphere, holding for 30 minutes (20 minutes under hydrogen and 10 minutes under argon) and cooling to 1400 ºC at a rate around 5°C/min and furnace cooling to room temperature under commercially pure Ar. Dry hydrogen was used in the sintering experiments and dew point of the hydrogen gas was around -60 ºC.

In order to investigate the sintering atmosphere effect on the properties of the sintered tungsten based alloys, a vacuum sintering (sintering cycle #2) was performed to the 90-2 alloys. Sintering cycle #2 was completely same as sintering cycle #1 in terms of heating and cooling steps except for that reduction step was 90 minutes. Furthermore, sintering atmosphere was selected as vacuum, which was around $3.4x10^{-2}$ to $5.5x10^{-2}$ torr in a vacuum sintering furnace (VHSM-30, Jen Long Vacuum Industrial, Taiwan), for the whole sintering cycle including reduction step.

Heat treatment after sintering process was carried out in an atmosphere controlled furnace (ACF 110/6, Alser Teknik A.Ş., Ankara, Türkiye) under commercially pure nitrogen and heat treatment cycle was consisted of heating from room temperature to 1000 ºC at a rate of 10°C/min, heating from 1000 ºC to 1070 ºC at a rate of 7°C/min, holding for 120 minutes at this temperature and then water quenching was employed.

3.1.5 Cold Deformation

Selected specimens were cold worked at room temperature by rotary swaging with four hammers on the vertical GFM equipment (6F-4, Fenn Manufacturing, USA). In the forging operation, reduction in area of the samples was around 15%.

3.2 Structural Characterization

3.2.1 Density Measurements

The density measurements of the alloy specimens were carried out on the Basis of Archimedes' principle by using a precision balance (CP224S, Sartorius, Goettingen, Germany). Sintered ($\rho_{sintered}$) and green densities (ρ_{green}) of the samples were determined by using the equations (3.1 and 3.2) given below;

$$\rho_{sintered} = \frac{m_1}{m_1 - m_2} \rho_{xylene} \quad (3.1)$$

$$\rho_{green} = \frac{m_1}{m_3 - m_2} \rho_{xylene} \quad (3.2)$$

Where ρ_{xylene} is the density of the xylene which was taken as 0.86 gr/cm^3 in this study, m_1 is the sample weight in air, m_2 is the weight of the sample immersed in a beaker which was filled with xylene and m_3 is the weight of the sample saturated with xylene in air.

These experimentally determined densities were then compared to theoretical densities ($\rho_{theoretical}$), which were calculated by using equation (3.3) given below.

$$\frac{100}{\rho_{theoretical}} = \frac{W_W}{\rho_W} + \frac{W_{Ni}}{\rho_{Ni}} + \frac{W_{Fe}}{\rho_{Fe}} \quad (3.3)$$

Where W and ρ are the weight fraction and bulk density of the elemental powders respectively.

3.2.2 Microstructural Characterization

3.2.2.1 Microstructural Examination

The samples of W-Ni-Fe alloys cut from the undeformed part of tensile test samples were prepared by conventional metallographic techniques. Specimens were finally polished by using 0.3 μm alumina paste. Etching was carried out about 5 to 30 seconds by using Murakami's reagent which is composed of 10 g $K_3Fe(CN)_6$ (potassium ferricyanide), 10g NaOH, 100 ml H_2O.

Microstructural examination and fracture surface characterization of the alloy samples were carried out both under an optical microscope (Axioskop 2 Mat, Carl Zeiss Microscopy GmbH, Göttingen, Germany) and in a scanning electron microscope (SEM) (6400 JSM, Jeol, Japan) operated at 20 kV and the field emission SEM (Nova Nano 430, FEI Co. LTD., Eindhoven, Holland). Both secondary imaging and backscatter imaging modes were applied on all sintered specimens. Northern Tracor Energy Dispersive Spectroscopy (EDS) analysis system attached to the scanning electron microscope was used for the EDS analysis of the specimens, when needed. SEM micrographs of the samples were taken from at least 3 different regions of each sample.

3.2.2.1.1 Quantitative Metallographic Examinations

3.2.2.1.1.1 Contiguity Measurements

A 100*100 mm^2 line matrix was imposed on the micrographs taken by SEM at a magnification of 500x, as schematically given in Figure 28. Contiguity of tungsten particles was then determined by counting the number of interphase boundary intercepts along the test lines placed on the metallographic image and by using the following equation [21],

$$C_w = \frac{2N_{WW}}{2N_{WW}+N_{WB}} \quad (3.4)$$

N_{WW} = Number of W-W interfaces as to length of test line
N_{WB} = Number of W-B (binder matrix phase) interfaces as to length of test line

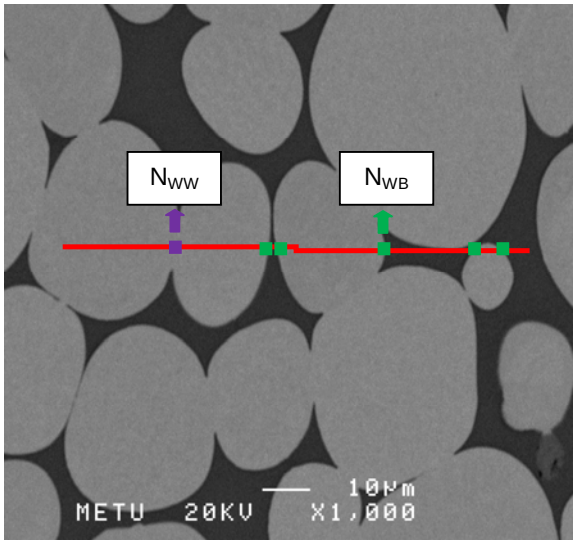

Figure 28. Schematically shown of contiguity measurements on SEM micrographs, higher magnification(x1000) instead of x500 was used in order to show the interface points easily in this figure.

3.2.2.1.1.2 Volume Percent of Binder Matrix Phase Analysis

Volume percent of binder matrix phase of the sintered alloys were determined by image analysis software (Axiovision Rel 4.8, Carl Zeiss Microscopy GmbH, Göttingen, Germany) on the micrographs taken by SEM at a magnification of 500x. SEM micrographs were converted into the black-white micrographs and then the volume percent of binder matrix phase was calculated by automated image analysis software as presented in Figure 29.

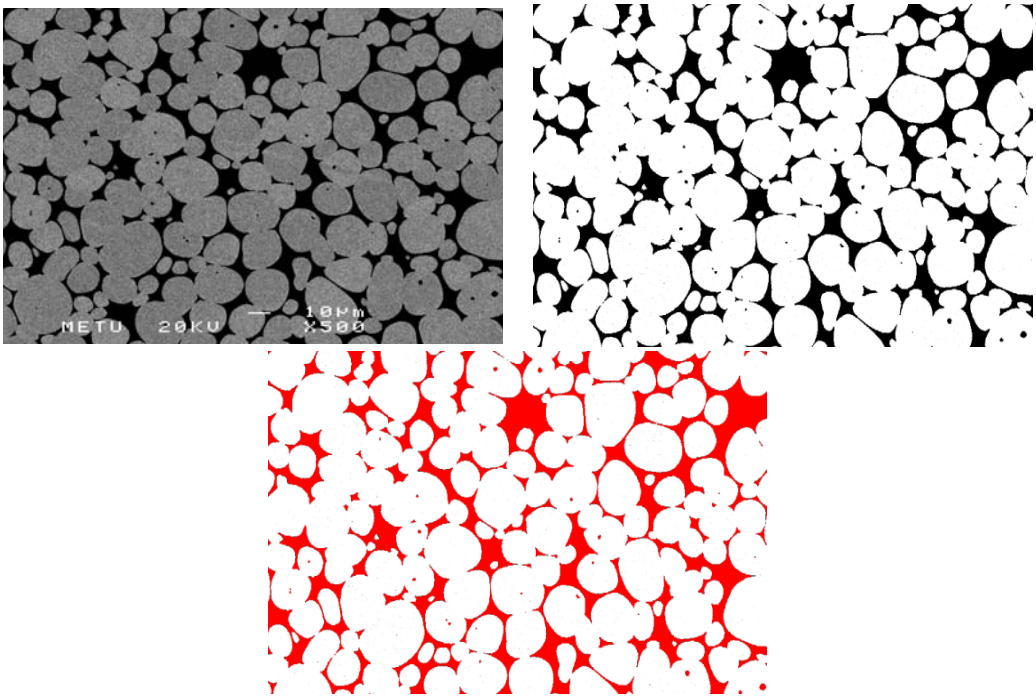

Figure 29. Volume percent of binder phase calculation processed by image analysis software, red area is binder matrix phase and white area is tungsten particles.

3.2.2.1.1.3 Average Particle Size Analysis

To calculate the average particle size of tungsten particles, tungsten particles are counted on the micrographs taken by SEM at a magnification of 500x, which are those used for volume percent of binder matrix phase calculations. Jeffries planimetric method was employed for the average particle size diameter measurements [100]. The procedure followed and schematically given in Figure 30 was; a circle with area of 5000-6500 mm^2 depending on the size of micrograph was drawn on the SEM micrographs. 500x magnification was selected so that at least 50 particles were present in the test area. Particles which are completely within the test area (n_1) and particles which are intersecting the test circle (n_2) are counted. The total of n_1 and n_2 are multiplied by the Jeffries factor, f, in order to calculate of the number of particles per square millimeters (N_A) according to the equation as follows;

$$N_A = f\left(n_1 + \frac{n_2}{2}\right) \tag{3.5}$$

f can be calculated for a given magnification (M) as follows;

$$f = \frac{M^2}{5000} \tag{3.6}$$

Finally, average particle diameter in millimeter (d) is calculated as follows,

$$d = \frac{1}{N_A^{0.5}} \tag{3.7}$$

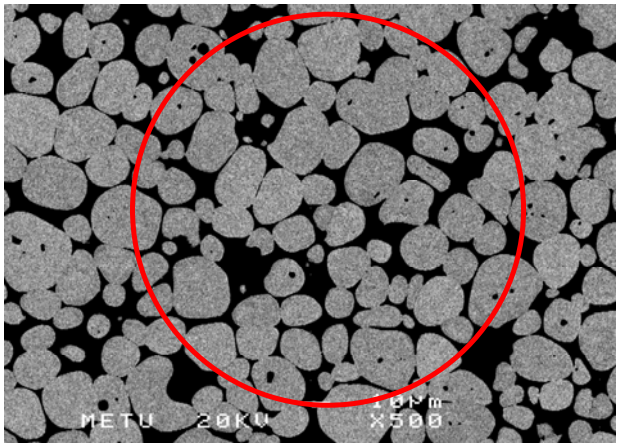

Figure 30. A schematic of average particle size measurement by using Jeffries planimetric method

3.2.3 X-Ray Diffraction

To determine the resultant phases in liquid phase sintered alloy samples, X-Ray diffractogrammes were taken by continuous scanning at 40 kV between 20° to 110° 2θ angles using Bruker X-Ray Diffractometer (D8 Advance, Bruker, Germany) with a scan rate of 1°/min, where Cu Kα was used as X-ray beam source.

3.2.4 DSC Examination

In order to investigate the possibility of third phase formation and to determine the liquidus and solidus temperatures, thermal analysis experiments were conducted on liquid phase sintered alloys by using Differential Scanning Calorimeter (DSC) (DSC-TGA Setaram Setsys Evolution 16-18, Setaram Instrumentation, Caluire, France). Heating and cooling cycles consisted of heating up to 1500 ºC at a rate of 10 ºC/min and cooling to 500 ºC at a rate of 10 ºC/min respectively under argon atmosphere.

3.2.5 Mechanical Testing

3.2.5.1 Tensile Test

In order to determine the mechanical properties of sintered tungsten based alloys, tension tests were carried out using 100 kN capacity universal tension-compression test machine (Instron 5582, Instron Co. LTD., Norwood, USA) on tensile specimens given in Figure 31 prepared as per ASTM E 8M [101] and tested with a crosshead speed of 0.5mm/min at room temperature. At least 3 specimens were tested and the average value was reported. 0.2 % offset method is used to determine the yield strength. Axial strain values were recorded by a video extensometer (Instron 2663-821, Instron Co. LTD., Norwood, USA). Strain hardening coefficient of the alloys were obtained from a fit of the experimental data to a power law

flow stress equation [43] used in homogeneous deformation zone of the stress-strain diagram as given below,

$$\sigma=\sigma_0+K\epsilon^n \quad (3.8)$$

where:

σ = true stress,
σ_0 = yield stress,
ϵ = true plastic strain,
K = strength coefficient, and
n = strain-hardening exponent

This equation is valid in the uniform plastic deformation zone of the samples which is the range between yield strength to ultimate tensile strength.

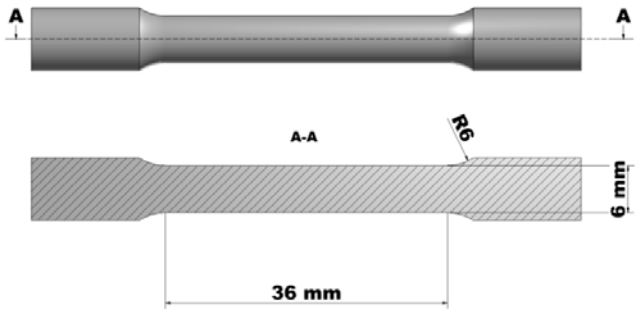

Figure 31. Dimensions of the tensile test specimen used in the mechanical characterization studies.

3.2.5.2 Hardness Tests

Micro hardness tester (Buehler, Illinois, USA) with loads lower than 1 kg was used to measure hardness of sintered compacts. Seven to ten indentations were taken for each sample and the average value was reported.

CHAPTER 4

RESULTS AND DISCUSSION

4.1 Effect of Sintering Conditions on the Properties of Tungsten Heavy Alloys

High density tungsten based alloys are metal matrix composite materials that are composed of two main phases which are tungsten particles and solid binder matrix phase with dissolved tungsten. These materials can provide very high strength (1000 – 1700MPa) and very high ductility (10 – 30%) [52] to the engineers or designers, if they are processed properly via powder metallurgy methods. These alloys are generally produced by liquid phase sintering process which is conducted at temperatures above the melting point of at least one of the binder matrix phase components.

Mechanical properties of high density tungsten based alloys are very sensitive to the residual pore content in the microstructure and particular sintering parameters during processing. Especially, ductility of these alloys is greatly reduced by the porosity content greater than 0.5% in the microstructure [56]. Porosity formation in the microstructure may be attributed to the improper cooling from the sintering temperature [5], incomplete reduction of oxides that inhibits the wetting of binder phase to the tungsten particles, trapped gas in the pores, inadequate sintering times, very long sintering times and pores formed by some reactions such as water vapor formation during the processing [57]. Hydrogen is generally used as a sintering atmosphere for the sintering of tungsten based alloys since non-reducing atmospheres such as argon results in incomplete reduction of oxides, incomplete densification and inferior mechanical properties [58]. However, hydrogen embrittlement effect after sintering under hydrogen may also be observed for tungsten based alloys if there is no subsequent heat treatment conducted under inert gases or vacuum [57, 102]. In the case of hydrogen embrittlement, reduction in mechanical properties has been explained by the weakening effect of hydrogen on the interfacial strength between the tungsten particles and binder matrix phase [102]. Therefore, post sintering operations such as heat treatment under inert gases or vacuum are generally performed in order to remove the hydrogen in the microstructure. Additionally, sintering atmosphere can also be changed from hydrogen to inert gases such as argon during the sintering process in order to reduce the hydrogen embrittlement effect [59, 103]. This action may also enhance the pore closure during the liquid phase sintering process which may lead to higher densification in the microstructure.

In order to observe the effect of sintering atmosphere on the mechanical properties, some sintering experiments including different atmosphere cycles were performed in the present study. For these sintering optimization studies, 90W-7Ni-3Fe alloy composition was selected to compare the achieved mechanical properties to those reported in the literature.

For the composition of 90W-7Ni-3Fe, Ni:Fe ratio was kept as 2.33 in order to avoid the precipitation on cooling as reported in the literature [14]. Sintering temperature was selected as 1480°C which is higher than the eutectic temperature for this selected composition [14].

Firstly, samples were sintered according to the sintering cycle #1 given in the experimental procedure part, where whole cycle was performed under hydrogen and there was no subsequent heat treatment performed after sintering. In this cycle samples achieved densities above 99 % of the theoretical, but with very poor mechanical properties. Some of the samples were broken even in the machining step of the specimen preparation. The poor mechanical properties obtained after sintering cycle #1 were related to the hydrogen embrittlement effect. Therefore, a step to change the sintering atmosphere was added to the sintering cycle, where liquid phase sintering at 1480°C was initially conducted under hydrogen, followed by sintering 10 minutes under argon. Alternatively, in order to eliminate the heat treatment process due to hydrogen embrittlement and to decrease the gas consumption during liquid phase sintering process, vacuum (sintering cycle #2) was selected as the sintering atmosphere.

Densities and mechanical properties of the alloys sintered under two different conditions are given in Table 15. Sintering under hydrogen and argon led to a density of 99.5 % theoretical, whereas sintering under vacuum led to a lower density of 98.5 % theoretical. This lower density of the alloys sintered under vacuum may be attributed to the absence of reduction step. In the vacuum sintering cycle, hydrogen was not used for the reduction of oxides. Due to this, reduction of oxides might not be completed which affected the wetting properties of the liquid formed during the liquid phase sintering process leading to the lower density, since, wetting of liquid decreases as the oxide stability of the tungsten particles increases [9].

Table 15. Comparison of density and mechanical properties of 90W-7Ni-3Fe alloy sintered at 1480°C under different atmospheres.

Properties	Hydrogen and argon	Vacuum
Density (%)	99.5 ± 0.5	98.5 ± 0.5
UTS (MPa)	889±12	587±13
% Elongation	28±2	3.3±1.2

The mechanical properties of the samples sintered under hydrogen and argon are comparable with the mechanical properties reported in the literature [65]. On the other hand, considerably lower mechanical properties were achieved with liquid phase sintering of 90W-7Ni-3Fe alloy at 1480°C under vacuum. This may be attributed to the lower density (~98.5%) achieved under vacuum (Table 15). In a similar study by Bose et.al [57], 90W-

7Ni-3Fe alloy was sintered under hydrogen up to 1300 °C for the reduction of oxides and then under vacuum to give tensile strength of 913 MPa and 32% elongation.

Mechanical properties of tungsten based alloys are also dependent on the interfacial strength between the tungsten particles and binder matrix phase [38]. Crack propagation and crack path selection under loading occurs along the weakest path in the microstructure [38, 65]. For the case of brittle alloys, mainly tungsten-matrix interfacial separation or failure is observed. Fracture during tensile testing might start at the interface failure if the interface between tungsten particles and the binder matrix phase is weak. For the case of ductile alloys, little tungsten-binder matrix phase separation is observed but mostly tungsten cleavage and ductile failure of the binder matrix phase is observed. If the tungsten-binder matrix phase interface strength is strong enough, crack propagation might be impeded by the binder matrix phase [5, 26, 38, 65]. Practically, tungsten-binder matrix phase separation can be accompanied with tensile strengths up to 700 MPa and tungsten particles cleavage failure can be accompanied with strengths exceeding 850 MPa for Ni-Fe based tungsten alloys [38].

Fracture surfaces of the liquid phase sintered alloys sintered under two different sintering conditions in the present study are given in Figure 32. Analysis of the fracture surfaces showed that the main fracture mechanism in the vacuum sintered alloys with a tensile strength of 587 MPa is intergranular failure and tungsten–binder matrix separation. In contrast, main fracture mechanism in the alloys sintered under hydrogen and argon with a tensile strength of 889 MPa is tungsten cleavage. Additionally, large pores after sintering can be observed on the fracture surfaces of the vacuum sintered alloys which probably is due to insufficient oxide reduction during sintering leading to inferior mechanical properties.

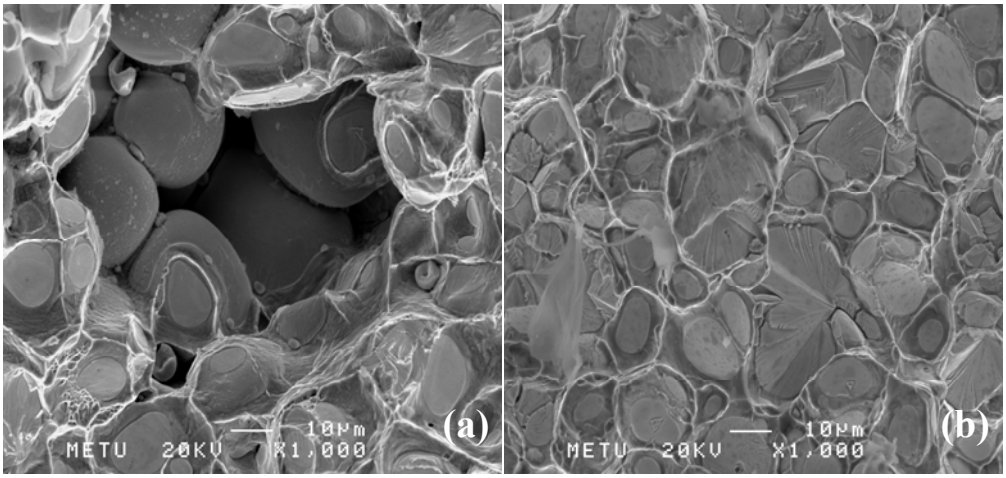

Figure 32. Fracture surfaces of the 90W-7Ni-3Fe alloy liquid phase sintered at 1480°C for (a) 30 minutes under vacuum, (b) 20 minutes under hydrogen and 10 minutes under argon.

The cracks usually start at the weakest points in the microstructure which are usually the tungsten-tungsten interfaces in tungsten based alloys [20, 26, 102]. As seen on the fracture

surfaces of the vacuum sintered samples, cracks initiated on the tungsten-tungsten interfaces propagated along the tungsten-binder matrix phase interface. Large areas of binder matrix phase separation and decohesion was also observed since interfacial strength between the tungsten and binder phase was very weak and not enough to impede the crack propagation and keep the alloy's structural integrity leading to very inferior mechanical properties. The decrease in the interfacial strength was correlated to the residual porosity in the microstructure and the incomplete oxide reduction.

On the other hand, in the specimens sintered under hydrogen and argon atmosphere, reduction under hydrogen during the sintering process appeared to increase the cohesive strength of the tungsten-binder matrix phase interface causing the main fracture mechanism to be tungsten cleavage. Additionally, propagation of cracks initiated at the tungsten-tungsten interface was inhibited by the binder matrix phase leading to superior mechanical properties.

It is also known that hydrogen embrittlement occurs by weakening of the tungsten - binder matrix interface [102] which makes the material very brittle. In the alloys suffering from the hydrogen embrittlement, main fracture mechanism becomes tungsten intergranular failure and decohesion of tungsten-binder matrix phase [102]. In the alloys sintered under hydrogen and argon atmosphere (sintering cycle #1), high density (99.5%) and high ductility (28.3%) showed that this process is adequate in order to perform sufficient reduction of oxides and eliminate the hydrogen embrittlement effect.

The results of this optimization study indicated that in order to the achieve better mechanical properties comparable to the values reported in the literature, reduction of oxides must be performed under the hydrogen atmosphere and then atmosphere should be converted from hydrogen to argon to prevent hydrogen embrittlement. Therefore, sintering cycle #1 was selected as the appropriate sintering cycle to be conducted in this study.

4.2 Effect of Composition on the Properties of Tungsten Heavy Alloys

The main objective of this thesis is to investigate the effect of composition and post sintering treatments on the microstructure and mechanical properties of liquid phase sintered W-Ni-Fe based tungsten heavy alloys. In this section, the effect of composition and in the next section, the effect of post sintering treatments will be discussed. This section is divided in two main topics: effect of tungsten content and effect of binder phase composition.

4.2.1 Tungsten Content

In two-phase tungsten heavy alloys, tungsten is the principal phase of the microstructure. The amount of tungsten usually changes from 90 to 98 wt.% resulting in density varying between 17 and 18.5 g/cm^3. Change in the amount of tungsten may lead to different microstructural properties which give rise to the variations in mechanical properties. It has been reported that as tungsten content increases, contiguity of tungsten particles increases and volume fraction of binder matrix phase decreases [20]. Contiguity and volume fraction of binder matrix phase affect the mechanical properties, especially the ductility, greatly in tungsten based alloys [49].

In order to investigate the effect of tungsten content on microstructural and mechanical properties, three alloys of the composition 90W-7Ni-3Fe, 93W-4.9Ni-2.1Fe and 97W-2.1Ni-0.9Fe, all with a Ni/Fe ratio of 2.33 were selected.

After liquid phase sintering process with the sintering cycle discussed in Section 4.1, densities above 98.5% theoretical were achieved. SEM micrographs of the three alloys are given Figure 33. The microstructure consists of round nearly spherical tungsten particles embedded in nickel based binder phase. EDX analyses showed that binder matrix phase for 93W-4.9Ni-2.1Fe was composed of 50.76Ni-22.42Fe-26.82W. The tungsten solubility in the binder matrix phase was found to be higher than the value reported in similar studies in the literature [33, 60]. This difference was believed to be due to the procedures of the measurement technique. Additionally, composition of the matrix phase of 90 wt%W and 97 wt%W alloys were similar to that of the 93W alloy, and this result is compatible with the study by Humail et al [33].

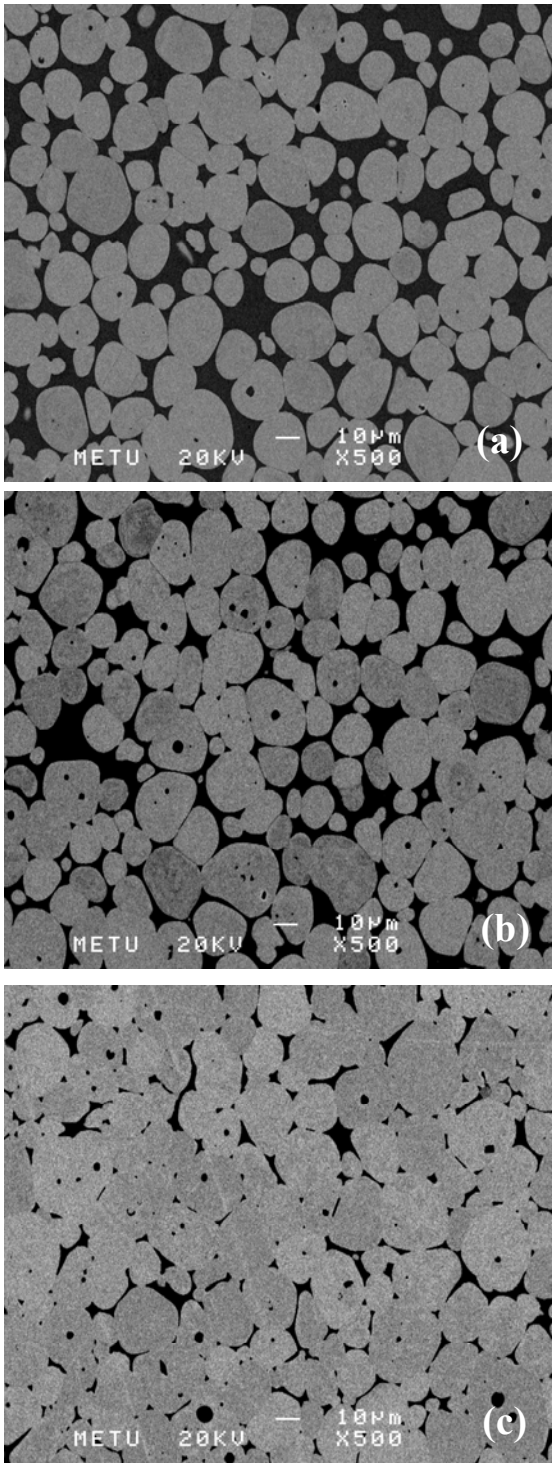

Figure 33. SEM micrographs of the alloys sintered at 1480 °C for 30 minutes.
a) 90W-7Ni-3Fe, b) 93W-4.9Ni-2.1Fe c) 97W-2.1Ni-0.9.

Microstructural properties of 90W-7Ni-3Fe, 93W-4.9Ni-2.1Fe and 97W-2.1Ni-0.9 alloys are given in Table 16. Volume fraction of the binder phase, which initially was 20%, 14.5 % and 6.5 % for the alloys studied before W dissolution (initial volume percent of binder phase was calculated according to the rules of mixture principle), was found to change to 22.2%, 14.9 % and 6.5% with the increase in tungsten content from 90W to 97W. Similar changes in the volume fraction of binder phase with increase in tungsten content have been reported in the literature [20]. The difference between the initial volume fraction of binder phase without tungsten dissolution and the volume fraction of binder phase with the dissolved tungsten decreased with increase in tungsten content from 90W to 97W. For the alloys of 97W, it was observed that volume percent of the binder phase remained approximately same although its weight fraction increases. This result was correlated with the low amount of binder phase which resulted in the low dissolution of tungsten.

Table 16 also indicated that the increase in the tungsten amount has led to increase in the contiguity of tungsten particles from 0.24 to 0.53. It has been reported that contiguity of tungsten particles increases with the tungsten content which might be attributed to the increase in the number of irregular tungsten particles which gives rise to increased tungsten-tungsten solid contact area per unit volume [33, 56]. The increase in the contiguity of tungsten particles with increase in the tungsten content is also in agreement with the previous studies [20, 23, 26, 33, 65].

Table 16. Comparison of microstructural properties of 90W-7Ni-3Fe, 93W-4.9Ni-2.1Fe and 97W-2.1Ni-0.9 alloys sintered at 1480 °C for 30 minutes.

Alloys	Volume Fraction (%)	Contiguity	APS of W (microns)
90W-7Ni-3Fe	22±1	0.24±0.02	16.7±0.6
93W-4.9Ni-2.1Fe	14.9±0.1	0.33±0.06	17.2±0.1
97W-2.1Ni-0.9Fe	6.5±1	0.53±0.02	17.6±1

It was also observed that with the increase in the tungsten content, there seems to be a slight increase from 16.7μm to 17.6μm in the average particle size of tungsten. In liquid phase sintering process, the coarsening of solid tungsten particles is observed due to the Ostwald ripening mechanism in which small particles dissolve in the matrix while bigger particles grow further due to the difference in surface curvature dependent solubility [29]. Kinetics of this process is directly related to the process of tungsten dissolution in the matrix and the equilibrium binder matrix composition. Ostwald ripening is well documented in the literature [30-32] and because of its statistical nature coarsening phenomena obeys $t^{1/3}$ kinetics. Average particle radius will increase as the one third powder of time and one third power of

the equilibrium tungsten concentration of the binder matrix [6]. Therefore, kinetics of the coarsening of the tungsten particles may be directly correlated with the sintering process parameters such as sintering temperature, sintering time and binder matrix composition.

In a study by Humail et al [33], it has been reported that average tungsten particle size increased from ~22 μm to ~32 μm with increase in tungsten content from 88wt% to 95 wt%. In that study [33], samples of 88W-8.4Ni-3.6Fe, 93W-4.9Ni-2.1Fe and 95W-3.5Ni-1.5Fe were sintered at 1500°C for 30 minutes under hydrogen atmosphere and were subsequently heat treated in vacuum at a temperature of 1100°C for 8 hours. Tungsten particle coarsening observed was relatively much more (~22 μm to ~32 μm) when compared with our study (16.7μm to 17.6μm) and this might be due to the higher sintering temperature used. Sintering temperature has a considerable effect on the tungsten particle coarsening as reported in the literature [49]. In that study on an alloy of 93W-5.6Ni-1.4Fe, average particle size of tungsten particles increased from 5 μm to 18.2 μm with a decrease in contiguity as the sintering temperature increased from 1445°C to 1480°C which might be due to the larger tungsten solubility at higher temperatures [49].

In another study, it was also reported [65] that the average particle size of tungsten increased from 17 μm to 23 μm when the tungsten content is increased from 90 wt% to 97wt% in alloys with a Ni to Fe ratio of 2.33 in the binder matrix. This increase in the average tungsten particle size has been explained by the increase in the volume percent of tungsten phase which reduces the distance between the particles [9, 65]. In this study [65], in order to achieve these results, sintering atmosphere after 1300 °C was selected as wet hydrogen (dew point was around +20°C) and cooling rate was selected as 3K/min down to 1420°C under argon. After sintering process, heat treatment was conducted under argon at 1100 °C for 1 hour. In the present study, the dew point of the hydrogen gas used in the sintering cycle was around -60°C and cooling rate was selected as 5°C /min down to 1400°C. The difference observed in the coarsening rate of tungsten particles may be attributed to the different amount of water vapor in the hydrogen gas during sintering since wet hydrogen inhibits the water vapor formation resulted from the reaction between the hydrogen and oxide in the microstructure which promotes the densification and particle coarsening [57] Additionally, coarsening of tungsten particles while tungsten content increased from 90wt.% to 97wt.% might be also correlated with slower cooling rate which provides more time for the tungsten particle coarsening the liquid phase sintering process.

Mechanical properties of the alloys are given in Table 17. Tensile strengths and elongations of 90W-7Ni-3Fe and 93W-4.9Ni-2.1Fe alloys are comparable to the values reported in the literature. However, tensile strength and elongation of 97W-2.1Ni-0.9Fe alloy which were 735 MPa and 4.08%, respectively are lower than the tensile strength (~815MPa) and ductility (~10%) of 97W-2.1Ni-0.9 in a similar study by Bose et. al. [57]. In order to achieve these properties, wet hydrogen atmosphere (dew point around 0°C) for sintering of 97W-2.1Ni-0.9 alloys was used instead of dry hydrogen atmosphere [57]. Under the light of these observations, it can be also concluded that wet hydrogen can also be used in order to achieve better mechanical properties.

Table 17. Comparison of mechanical properties of 90W-7Ni-3Fe, 93W-4.9Ni-2.1Fe and 97W-2.1Ni-0.9 alloys sintered at 1480 °C for 30 minutes.

Alloys Sintered	UTS (MPa)	%El	Yield (MPa)	Hardness (HV0.01)	n Coefficient	Strength Coefficient (K)
90W-7Ni-3Fe	889±12	28±2	580±12	352±23	0.62±0.01	1458±30
93W-4.9Ni-2.1Fe	898±16	23±3	595±11	368±13	0.63±0.02	1504±26
97W-2.1Ni-0.9Fe	735±3	4±0.5	613±6	372±12	0.70±0.08	1557±405

The peak trend in the ultimate tensile strength was also observed at the composition of 93W-4.9Ni-2.1Fe while the tungsten increased from 90W alloy to 97W alloy which is comparable to the previous studies [33, 59, 65]. Slight increase of the ultimate tensile strength from 90wt%W alloy to 93wt%W alloy might be attributed to the increase in the harder tungsten phase [65] according to the rule of mixtures as expected [104]. However, the decrease in ultimate tensile strength after 93W has also been observed as in similar studies [33, 59, 65, 93]. This decrease in the ultimate tensile strength has been explained by the lower ductility dictated by the increased contiguity with increase in the tungsten content which also resulted in a change in the fracture mode as explained in the following section [65].

After the peak strength, which is around 93W, contiguity of the microstructures increased sharply from 0.33 to 0.53 which lead to an increase in the crack initiation sites as well as very low binder matrix phase content that inhibits the crack propagation in the microstructure. Therefore, contiguity dominated the mechanical properties and yielded very poor mechanical properties.

The three stages of fracture process in tungsten based alloys is given as : 1-cracks opening at the tungsten-tungsten interface and the inhibiting of propagation of cracks by the matrix, 2-transfer of plastic deformation from binder matrix phase to the tungsten particles, 3-catastrophic failure of the sample with the transgranular fracture of tungsten particles [93]. It can be concluded that after a specific amount of tungsten, propagation of cracks initiated at the weakest points as tungsten-tungsten interface could not be inhibited due to low amount of binder matrix composition as it is in 97W-2.1Ni-0.9Fe. Additionally, stress transfer from binder matrix phase might not be performed successfully and the catastrophic failure of the specimens occurred. In other words, the process of the slip band forming and transgranular crack initiation at the nearby tungsten particles due to the subsequent deformation carried out through the work hardened binder matrix phase might not be performed properly due to the increase in contiguity observed from 90W to 97W alloy. This change in fracture mode with

increasing tungsten content manifested itself as a reduction in ductility from 28% to 4% as the tungsten content is increased from 90 wt.% to 97wt.%.

It was also observed that yield strength and hardness of the alloys increased as tungsten content increases. According to the modified Hall-Petch equation ($\sigma_y \alpha \left[\frac{1-V_M}{DV_M}\right]^{1/2}$) [43], yield strength is directly related with the decrease in the average particle size of the tungsten particles and volume fraction of the binder matrix phase [42-47]. In the present study, since there was only a slight increase in the average particle size of tungsten, i.e. remained almost same, increase in yield strength and hardness of the alloys should be related with the reduction in the volume fraction of the binder matrix phase from 22% to 6.5% with increasing tungsten content which is in agreement with similar studies [65].

Stress-strain diagrams of the liquid phase sintered alloys are given in Figure 34. Two different types of tensile behavior were observed for the alloys investigated. 90W-7Ni-3Fe alloy yielded the maximum elongation and showed necking behavior. 93W-4.9Ni-2.1Fe alloy also exhibited necking behavior but at slightly less elongation as compared to 90W-7Ni-3Fe. On the other hand, 97W-2.1Ni-0.9 alloy showed no necking with limited ductility. This difference in the stress-strain diagrams of the alloys has been explained by the increase in the number of cracks occurred at tungsten-tungsten interfaces under tensile loading which might be attributed to the increase in contiguity and decrease of the amount of binder matrix phase from 90W to 97W alloy [93]. The amount of binder matrix phase decreases and contiguity increases as tungsten content increases. Matrix phase has a major role in terms of inhibiting the crack propagation during tensile loading as mentioned before. Microstructure with high tungsten-tungsten contacts meaning lower binder matrix phase might not neither reduce the formation of crack initiation nor decrease the crack propagation rate. As a result of this, limited ductility was observed for the alloy 97W-2.1Ni-0.9.

It can be observed from the stress-strain diagrams that deformation behavior of the liquid phase sintered alloys change considerably in terms of ductility and plastic instability which results in an increase in the strain hardening coefficient from 0.62 to 0.70 as the amount of tungsten increases from 90 wt% to 97 wt%. It is known that strain hardening coefficient is a measure of the stretch formability of a material. The larger strain hardening coefficient indicates that the material can be deformed and stretched more before the tension instability or the start of necking. Additionally, elastic spring-back of the material increases with the strength coefficient [105].

The increase in the strain hardening coefficient as the tungsten content increases was comparable to the results reported in a similar study [65], in which strain hardening coefficients of the alloys sintered at 1480°C for 30 minutes increased from 0.51 to 0.58 as tungsten content increase from 90 wt.% to 97 wt.% with a Ni to Fe ratio of 2.33 in the binder matrix. The increase in strain hardening coefficient corresponding to an increase in the resistance to tension instability with increasing tungsten content has been explained by the decrease in the binder matrix resistance to crack propagation under tensile loading. The classic mechanical models were not of much use to explain the stress–strain response of the tungsten based alloys due to the difference in deformability of binder matrix phase and tungsten particles. Therefore, strain hardening coefficient of the alloys measured in the present study is quite different than the strain hardening coefficient of a one phase alloy.

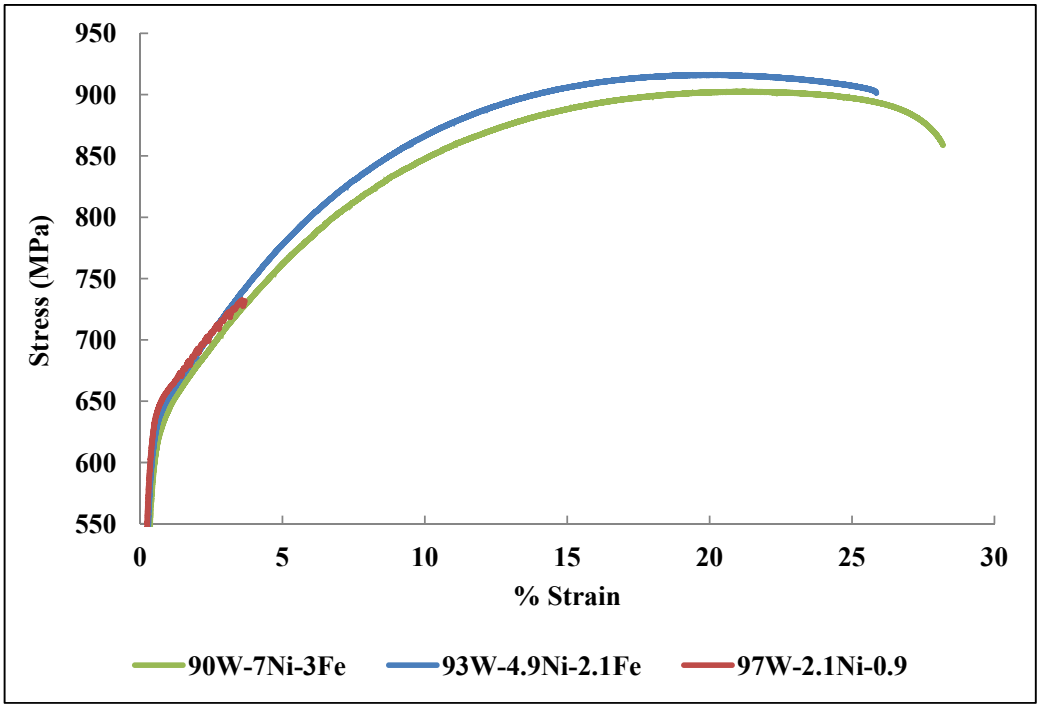

Figure 34. Engineering stress-strain curves of the alloys sintered at 1480 °C for 30 minutes a) 90W-7Ni-3Fe, b) 93W-4.9Ni-2.1Fe c) 97W-2.1Ni-0.9.

Tungsten based alloys are two phase metal matrix composites composed of two main phases which are tungsten particles (hard phase) and binder matrix phase (soft phase). The deformation of two phase structures can be analysed in four stages [106]. First stage is the elastic deformation of both phases, second stage is plastic deformation of the soft phase, third stage is the plastic deformation of both phases and the final stage is the fracture of the hard phase or decohesion of the interface between the phases. Although limited information is found in the literature, it is known that in two phase composite materials, if the amount of the harder phase is above 70 volume percent, than deformation is mainly controlled by the properties of the harder phase [43]. Harder phase is tungsten particles in the present study. At the beginning of the deformation in the present study, while the binder matrix phase deforms plastically tungsten particles are deformed elastically. After the strain hardening of binder matrix, deformation should have been transferred to tungsten particles [93]. However, this deformation transfer mechanism changes as the tungsten content is increased from 90 wt.% to 97 wt.%. As the amount of the binder matrix phase decreased, deformation mechanism of the alloy approached to that of almost pure tungsten during plastic deformation under tensile loading. The increase in the strain hardening coefficient might be attributed to the rapid strain hardening of limited amount of binder matrix phase which decrease the ductility considerably and the increase the resistance to tension instability.

It has been reported that in both mechanical models of composite materials, which assumes equal strain or equal stress in both phases, strength of the alloy increases with the increase in the amount of the hard phase [106]. It is also well known that pure tungsten has the highest elastic modulus as compared to its alloys which result in the highest elastic spring-back

properties. It was observed that average strength coefficients of the alloys (K) increased from 1458 MPa to 1557 MPa as tungsten content increased from 90 wt.% to 97wt.%.

Fracture surfaces of the liquid phase sintered alloys were given in Figure 35. It is known that the fracture behavior of tungsten based alloys is directly correlated with the microstructure. There are four possible crack paths observed in tungsten based alloys: 1-Tungsten cleavage (transgranular failure), 2-tungsten-tungsten particles interface failure (intergranular), 3-tungsten-binder matrix interface failure and 4-binder matrix failure paths. Crack initiation, propagation and crack path selection under tensile loading are directly related to a minimum fracture energy path or weakest path in the microstructure [38, 65]. Mainly tungsten-matrix interfacial separation or failure leads to inferior mechanical properties (meaning brittle alloys) due to the weak interface strength between the tungsten particle and binder matrix phase. Conversely, little tungsten-binder matrix phase separation is observed but mostly tungsten cleavage and ductile failure of the binder matrix phase is observed for the alloys having better mechanical properties (meaning ductile alloys). If the tungsten-binder matrix phase interface is strong enough, crack propagation might be impeded by the binder matrix phase. Nevertheless, intergranular failure or intergranular crack paths may be observed for both types (brittle and ductile) of alloys [5, 20, 26, 38, 65].

All four possible crack types were observed on the fracture surfaces of the liquid phase sintered alloys. Careful examination of the fracture surfaces has shown that the amount of tungsten cleavage on the fracture surfaces of 90W-7Ni-3Fe alloy is more than that in 97W-2.1Ni-0.9 alloy since dominant fracture paths of the cracks changed from tungsten cleavage to tungsten-tungsten particle interface failure as tungsten increased in the composition. This was expected because cracks initiated at the tungsten-tungsten interface propagated easily under the tensile loading since contiguity increased with the increase tungsten content. It is known that higher contiguity yields less elongation in liquid phase sintered alloys since tungsten-tungsten are the weakest parts in the microstructure and can be regarded as nucleation sites of the cracks [23, 26, 33, 93]. Additionally, blocking the crack propagation becomes more difficult due to decrease in the % volume fraction of binder matrix phase with the tungsten increase in the composition. This observation is in good agreement with the previous studies in the literature showing that a brittle tungsten based alloy exhibits more tungsten-binder matrix phase separation. Cracks generally occur at the tungsten-tungsten interfacial area and if there is not enough crack hindering effect of binder matrix phase due to increase in the amount of tungsten, cracks propagates transgranularly as observed in 97W alloy [26, 65].

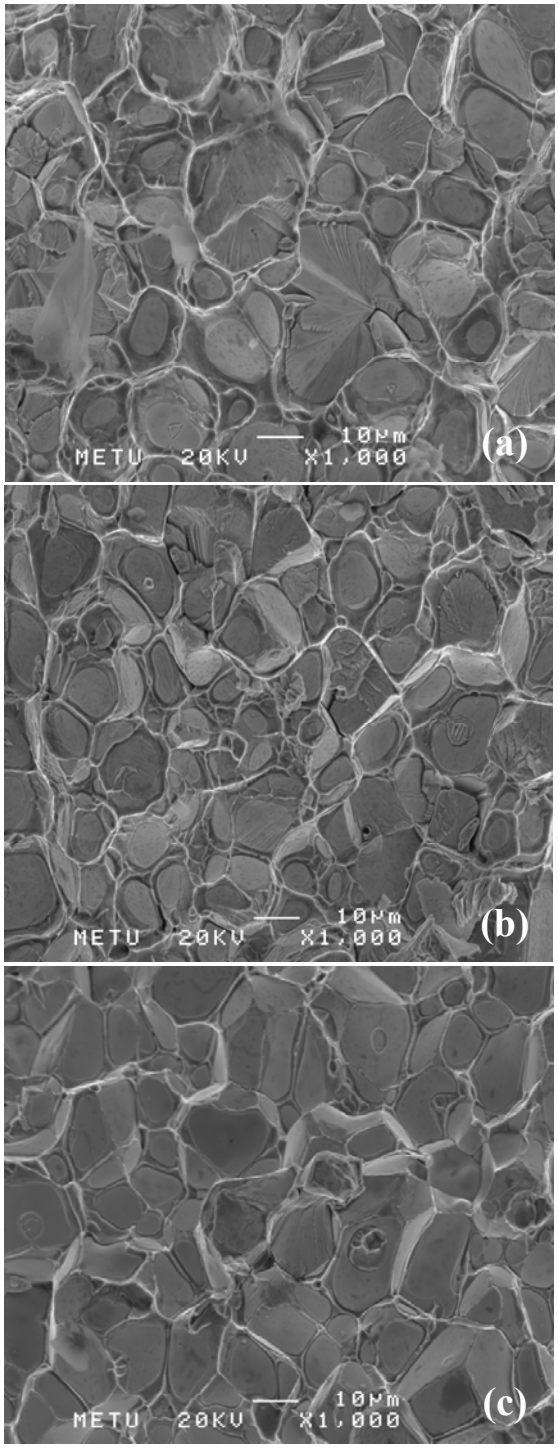

Figure 35. Fracture surfaces of the alloys sintered at 1480 °C for 30 minutes a) 90W-7Ni-3Fe, b) 93W-4.9Ni-2.1Fe c) 97W-2.1Ni-0.9.

4.2.2 Binder Phase Composition

The mechanical properties of W-Ni-Fe two phase metal matrix composites depend largely on the interface strength between the tungsten particles and binder matrix phase [38]. It has been reported that mechanical properties of tungsten based alloys increases as the tungsten content in the binder matrix phase increases [15, 62]. Therefore, the strength of this interface is predominantly controlled by the equilibrium tungsten solubility in the binder matrix phase. Tungsten solubility in the binder matrix phase is commonly affected by sintering parameters such as sintering temperature, cooling rate, etc. and composition of the liquid phase sintered alloys. Especially, Ni/Fe ratio set the tungsten solubility in the binder matrix phase in any fixed sintering cycle.

It has been cited that some important microstructural properties such as volume fraction of binder phase, contiguity of tungsten particles and average particle size of tungsten which affect the mechanical properties of tungsten based alloys, are influenced by tungsten solubility in the binder matrix phase [63].

According to the liquidus projection and phase diagram of the ternary of W-Ni-Fe alloys given in Figure 36, melting point of the alloy and tungsten solubility increase as Ni/Fe ratio increases in the binder matrix phase in any tungsten based alloy [60]. As seen in Figure 36, solubility of the tungsten in the binder phase increases while Ni increases in the composition. Arrows were drawn on the figures in order to mark the change in liquidus temperature of binder matrix phase and tungsten solubility with respect to Ni content for 3 investigated alloys. Volume fraction of the binder matrix phase increases due to this increase in the solubility, in other words; amount of liquid phase increases with Ni/Fe ratio during liquid phase sintering process.

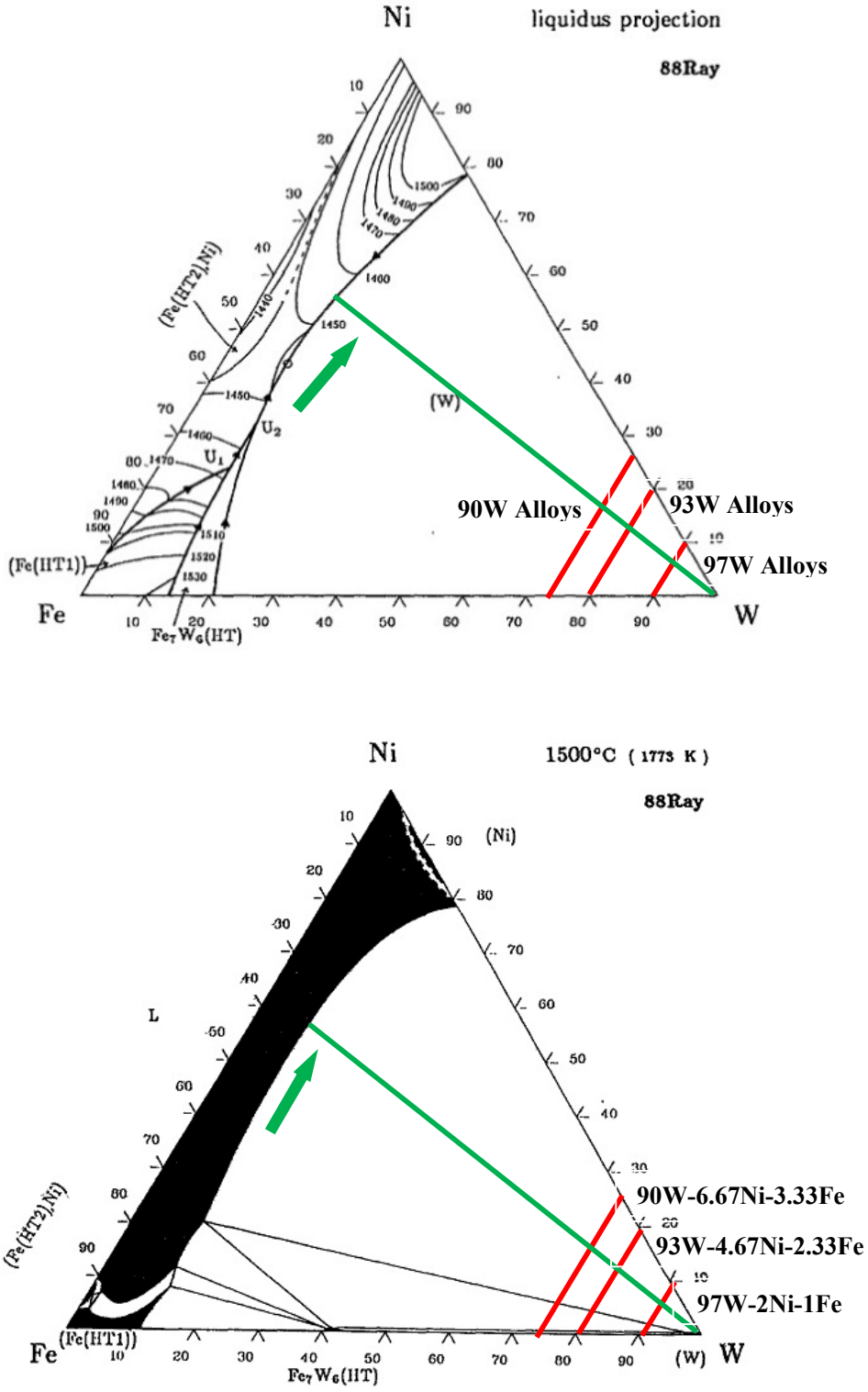

Figure 36. Liquidus projection (upper side) and 1500 °C isothermal section of W-Ni-Fe ternary phase diagram (lower side). Percentages are given in atomic percent [107].

Increase in tungsten solubility in the binder matrix phase enhances the liquid phase spreading and penetration along the tungsten particles which induces the faster diffusion within the binder matrix phase [22, 9]. Thus, high tungsten solubility in the binder matrix phase results in lower contiguity in the final microstructure [22].

Average tungsten particle size also depends on the tungsten solubility in the binder matrix phase as well as the tungsten content. It has been reported that coarsening rate and hence the average particle size of tungsten increases as tungsten content increases due to the fact that diffusion distance between the tungsten particles through the liquid matrix is reduced [65, 108].

Since, the equilibrium concentration tungsten in the liquid binder phase determines the effective mobility and rate of Ostwald ripening, they decrease with an increasing Fe/Ni ratio in the 92W-Ni-Fe alloy [109]. Coarsening is mainly affected by three factors, which are diffusivity of tungsten in the binder matrix, sintering temperature (Arrhenius type dependency) and the equilibrium tungsten solubility [110]. Therefore, it can be stated that higher the tungsten solubility, the larger is the tungsten particle size in the final microstructure.

It has been reported that deformation behavior of W-Ni-Fe alloys is also affected by the binder matrix composition since initial deformation mainly occurs in the binder matrix phase which is rapidly strain hardened under tensile loading [111]. Therefore, strain hardening, deformation behavior and fracture behavior of tungsten based alloys is greatly affected by the binder matrix phase.

The effect of binder phase composition on the microstructural properties of liquid phase sintered tungsten heavy alloys is given in Table 18. It was observed that volume fraction of binder phase increased slightly as Ni/Fe ratio increased in the binder matrix phase for the alloys of 90W and 93W as expected. This result is in agreement with the previous studies [23, 60] and ternary phase diagram data. However, for the alloys which contain 97W, a change was not observed in volume fraction of binder phase with increase in Ni/Fe ratio. This as well as the relatively lower density of the 97wt%W alloy with Ni/Fe ratio of 4 may be attributed to the lower amount of binder matrix phase which led to the difficulties in the volume percent measurements of both phases.

Table 18 indicates that there was no obvious change in the contiguity of tungsten particles as Ni/Fe ratio increased in the binder matrix phase. In a similar study [23], contiguity of tungsten particles was observed to decrease from 0.41 to 0.21 as the Ni/Fe ratio increased from 1 to 2.33 for 90W-5Ni-5Fe and 90W-7Ni-3Fe alloys sintered at 1485°C for 2 hours and heat treated at 1100°C under vacuum. Similar change in contiguity had also been observed in samples which contain 92.5W. This difference may be attributed to the slightly higher sintering temperature and considerably longer sintering time applied to the alloy samples which also led to an increase (~ 3% to 4%) in the volume fraction of binder matrix phase. In addition, it is known that contiguity has a strong dependence on the volume fraction of tungsten particles [20]. Microstructural characterization of the samples showed that contiguity was mainly affected by the volume fraction of tungsten if there is sufficient tungsten solubility in the binder matrix phase.

Table 18. Comparison of microstructural properties of 90W, 93W and 97W alloys with different Ni/Fe ratios sintered at 1480 °C for 30 minutes.

Alloy	Volume Fraction (%)	Contiguity	Average Particle Size of W (μm)	Relative Density (%)
90W-Ni/Fe Ratio				
2	21 ± 2	0.25 ± 0.03	16.5 ± 0.5	99 ± 0.5
2.3	22± 1	0.24 ± 0.02	16.70 ± 0.6	99.5 ± 0.5
4	23± 2	0.26 ± 0.03	17.4 ± 1.1	99.5 ± 0.5
93W-Ni/Fe Ratio				
2	14.3 ± 0.5	0.34 ± 0.07	15.8 ± 0.2	99 ± 0.5
2.3	14.9 ± 0.1	0.33 ± 0.06	17.20 ± 0.1	99.5 ± 0.5
4	16 ± 1	0.36 ± 0.06	17.40± 0.1	99.5 ± 0.5
97W-Ni/Fe Ratio				
2	6.7 ± 0.7	0.53 ± 0.01	17.60 ± 0.5	99.5 ± 0.5
2.3	6.5 ± 1	0.53 ± 0.02	17.60 ± 1	98.5 ± 0.5
4	6.7 ± 0.7	0.54 ± 0.03	16.2 ± 0.2	97.5 ± 0.5

There was also a slight increase in the average size of tungsten particles with increase in Ni/Fe ratio in the binder phase for the liquid phase sintered 90W and 93W alloys. This increase may be attributed to the increase in the tungsten solubility in the binder matrix phase which led to faster particle coarsening kinetics [110].

On the other hand, this trend of slight increase in the average particle size of tungsten with increase in Ni/Fe ratio was not observed for 97W alloys. It is well known that %volume of liquid as binder matrix phase is directly related to the rate of liquid phase sintering process and the final microstructure [9]. This due to the fact that liquid phase during the process forms a fast diffusion or mass transport path which affects the all stages of liquid phase sintering process. Therefore, lower amount of binder matrix phase makes the full densification difficult in terms of the lower rate of mass transportation [112]. In the 97W alloys, volume fraction of binder matrix phase is about %6.5 and is relatively lower than the other two alloys, 90Wand 93W.

It was also observed that as Ni/Fe ratio in the binder matrix phase increased, %relative densities of the 97W alloys decreased, which may be explained by the change in the liquidus temperature of binder matrix phase of the alloys [60]. It is well known that sintering temperature is a critical parameter during the liquid phase sintering process. Liquid phase sintering is conducted at temperatures above the melting point of the additive metals such Ni, Fe or Co or their alloys [52]. It was reported that liquidus temperature of a tungsten based alloy with a Ni/Fe ratio of 4 is about 10°C higher than liquidus temperature of a tungsten

based alloy with a Ni/Fe ratio of 2.33 [60]. This increase in liquidus temperature of binder matrix phase was caused by the increase in the solubility of tungsten in the binder matrix phase. The tungsten content of the binder phase compositions determined by EDS analysis is given in Table 19. The results show that the tungsten content in the binder matrix phase increases with the increase in Ni/Fe ratio and is comparable to the previous studies [60].

Table 19. Comparison of binder matrix composition of 90W, 93W and 97W alloys with different Ni/Fe ratios sintered at 1480 °C for 30 minutes.

Alloy	Ni in wt%	Fe in wt%	W in wt%
90W-Ni/Fe Ratio			
2	49.59	23.36	27.05
2.3	51.26	20.54	28.2
4	54.29	13.2	32.51
93W-Ni/Fe Ratio			
2	50.6	23.73	25.66
2.3	50.63	21.07	28.3
4	54.1	13.06	32.85
97W-Ni/Fe Ratio			
2	52.13	22.16	25.72
2.3	53.63	19.42	26.96
4	55.24	12.14	32.62

DSC data of the 97W alloys is given in Figure 37. DSC cooling curves clearly revealed that liquidus temperature of the ternary W-Ni-Fe alloy increased with the increase in Ni/Fe ratio to 4 in the binder matrix phase. The liquidus temperature of 97 W alloy with a Ni/Fe ratio of 4 is about 1480°C, which is closer to the sintering temperature used in the experiments. Hence, for the 97W-2.4Ni-0.6Fe alloy, sintering temperature is not high enough for obtaining high density samples. Such a reduction in density for 97W alloys led to lower mechanical properties in this alloy [9, 112] due to lower amount of binder phase as explained above. Similar change in the liquidus temperature to 1480°C, has also been observed for the 90W and 93W alloys which has Ni to Fe ratio of 4. However, the higher amount of liquid phase in 90W and 93W alloys led to better densification and mechanical properties.

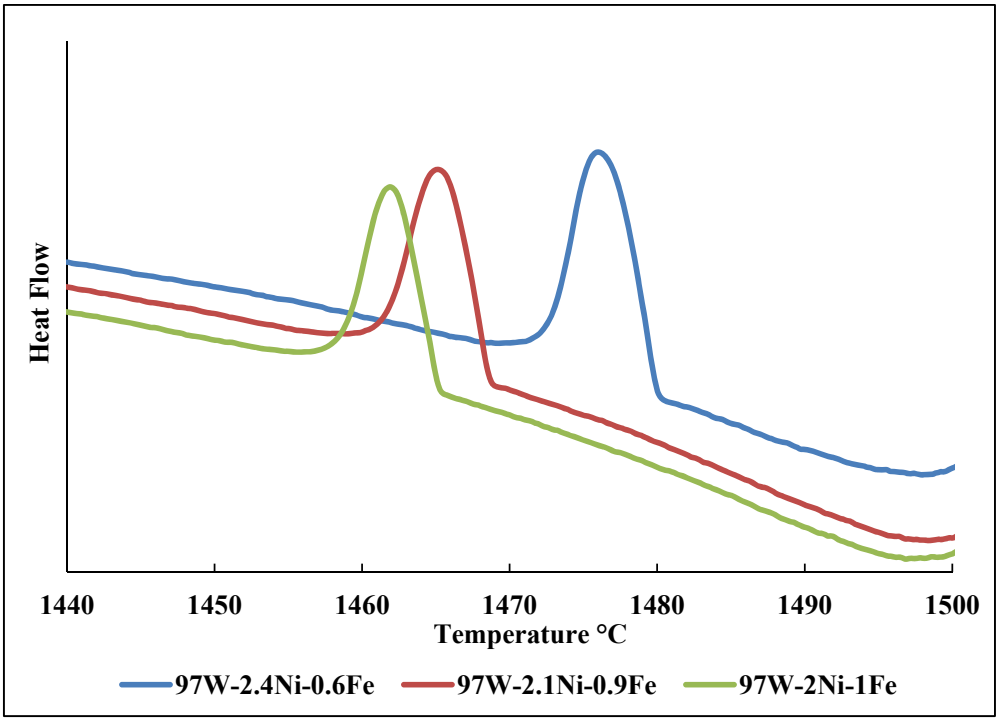

Figure 37. Comparison of DSC cooling curves of the alloys sintered at 1480 °C for 30 minutes.

The mechanical properties of liquid phase sintered alloys were given in Table 20. Mechanical properties of the alloys with fixed Ni/Fe ratio of 2.33 with different amounts of tungsten were discussed in the previous section. Therefore, in this section only the effect of Ni/Fe ratio on the mechanical properties of the alloys with a Ni/Fe of 2 to 4 will be discussed for each alloy group.

Table 20. Comparison of mechanical properties of 90W, 93W and 97W alloys with different Ni/Fe ratios sintered at 1480 °C for 30 minutes.

Alloy	Yield (MPa)	UTS (MPa)	% Elongation	Hardness (HV 0.1)	n Coefficient
90W-Ni/Fe Ratio					
2	641 ± 48	944 ± 54	21 ± 7	377 ± 10	0.62 ± 0.02
2.3	580 ± 12	889 ± 12	28 ± 2	352 ± 23	0.62 ± 0.01
4	584 ± 12	893 ± 29	18 ± 5	474 ± 11	0.63 ± 0.01
93W-Ni/Fe Ratio					
2	603 ± 13	899 ± 15	20 ± 3	376 ± 22	0.64 ± 0.01
2.3	595 ± 11	898 ± 16	23 ± 3	368 ± 13	0.63 ± 0.02
4	630 ± 25	769± 138	6 ± 7	404 ± 60	0.72 ± 0.01
97W-Ni/Fe Ratio					
2	612 ± 14	816 ± 10	7 ± 0.4	372 ± 14	0.74 ± 0.06
2.3	613 ± 6	735 ± 3	4 ± 0.5	372 ± 12	0.70 ± 0.08
4	602 ± 21	660 ± 30	2 ± 0.4	404 ± 38	0.52 ± 0.04

It has been reported that addition of iron prevents formation of the intermetallic phases by decreasing the solubility of tungsten in binder matrix phase. It was also found that a nickel to iron ratio of 7: 3 avoids intermetallic precipitation on cooling [14]. Therefore, as mentioned before Ni/Fe ratio in the binder matrix is generally fixed to 2.33 or 7/3 for the sintering studies on tungsten based alloys.

In order to observe the phases present in the microstructure, XRD analysis and DSC thermal analysis were performed on the alloys. X-ray diffraction patterns of the samples showed that all the alloys consist of body centered cubic tungsten phase and face centered cubic Ni-Fe-W binder phase (Figure 38). Similarly, DSC data did not show the presence of a third phase in the alloys studied. Hence, it can be stated that with the processing conditions selected, there is no intermetallic phase formation in the microstructure of the alloys with a Ni/Fe ratio between 2 and 4 during the cooling stage after the liquid phase sintering process. This result is in agreement with the previous studies on tungsten based alloys [15, 83, 84].

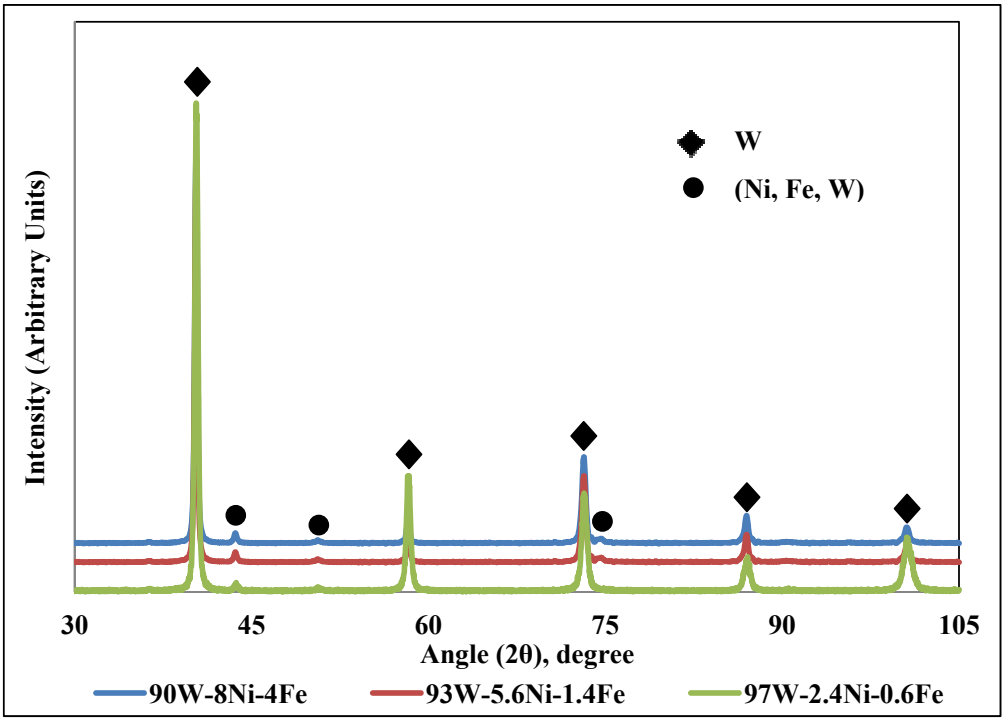

Figure 38. X-ray diffraction patterns of the alloys sintered at 1480 °C for 30 minutes. JCPDS number for W: 004-0806, JCPDS number for (Ni, Fe, W): 004-0850.

In tungsten heavy alloys Ni/Fe ratio in the binder phase is generally fixed to 2.33 or 7/3, in order to achieve the optimum mechanical properties. However, as given in Table 20, 90W, 93W and 97W, alloys having Ni/Fe ratio as 2 gave the highest tensile strength and yield strength in the as in sintered condition. Ductility of the alloys increased from 21 to 28 and from 20 to 23, respectively for the alloys with 90W and 93W with the little increase in Ni/Fe ratio from 2 to 2.3 due to the increase in the tungsten solubility in the binder phase (see Table 19) which led to stronger interface between the tungsten particles and binder phase. Stronger interface has also led to the increase in hardness of all alloys. However, although tungsten solubility increased as Ni/Fe ratio increased up to 4, ductility values of alloys were greatly reduced from 28 to 18 for 90W alloys and from 23 to 6 for 93W alloys. Additionally, there was also a decrease in tensile strength with increase in Ni/Fe ratio to 4 for the alloys with 93W. This decrease in mechanical properties might be due to higher liquidus temperature (~1480°C) of the alloys with a Ni/Fe ratio of 4, which does not give enough chemical homogeneity because of the the sintering temperature which is 1480°C and closer to the liquidus temperature of binder matrix phase.

Ni/Fe ratio increase in binder phase had different effects on the mechanical properties of 97W alloys as compared to 90W and 93W alloys. Densification and mass transportation rate decreased due to the increase in the liquidus temperature and the low binder phase content which led to slower densification [9, 112]. Therefore, as Ni/Fe ratio increased in binder

phase, densification might require higher sintering temperature and more time and absence of these led to decrease in the mechanical properties with increase in Ni/Fe ratio.

After careful examination of mechanical properties of the alloys given in Table 20, it can be concluded that there is no need to fix the Ni/Fe ratio to 2.33. Since, mechanical properties are quite similar for the alloys with Ni/Fe ratio as 2 and 2.33. Especially for the 93wt% W alloys, mechanical properties in terms of tensile strength, yield strength, % elongation, hardness and n coefficient properties are almost same. Besides, Ni/Fe ratio as 2 is better than the ratios of 2.3 and 4 for the alloys of 97W according to the mechanical properties for the sintering cycle having low sintering temperatures as in the present study.

On the other hand, Table 19 also revealed that there is a necessity of post-sintering sintering heat treatment after the liquid sintering process especially for the alloys with a Ni/Fe ratio as 4. Since, standard deviations of the mechanical properties achieved are too large to discuss or compare the results with the other alloys.

4.3 Effect of Post Sintering Operations on the Properties of Tungsten Heavy Alloys

In this section, the effect of post sintering treatments on the microstructure and mechanical properties of tungsten heavy alloys will be discussed. This section is divided in two main topics: the effect of heat treatment and the effect of deformation.

4.3.1 Heat Treatment

It has been reported that heat treatment of tungsten based alloys is utilized to remove the hydrogen embrittlement effects, to increase the homogeneity in the chemical composition, to prevent impurity segregation or precipitation on the interfaces, and to change some microstructural properties such as contiguity [20, 57, 59, 60, 68, 103, 113]. Generally, heat treatment consists of quenching from the specified temperature into water, oil or argon [113].

In some studies [20, 114-115] cyclic heat treatments were also applied to tungsten based alloys in order change the microstructure, especially the contiguity. Contiguity was reduced after the heat treatment and this reduction in contiguity has been explained by penetration of the binder matrix phase into the tungsten interface area to decrease the thermal stress caused by the differences in thermal expansion coefficients during the heat treatment [114, 115]. As mentioned in the earlier sections, contiguity affects the mechanical properties especially ductility greatly in tungsten based alloys [49] since tungsten-tungsten interfacial areas are the weakest points in the microstructure [20, 26]. It was also known that contiguity decreases with increase in the volume fraction of binder phase [20].

Mechanical properties of tungsten based alloys such as impact strength or toughness are also greatly affected by the contiguity variation in the microstructure. As contiguity decreased, toughness increased [20, 114]. However, tensile strength and ductility are not greatly affected the contiguity variation in the microstructure for the alloys having same compositions [20].

Heat treatment including the water quenching process, affects contiguity as well as the chemical homogeneity in the binder phase and increase the interfacial strength between the

tungsten particles and binder matrix phase. It has been reported that the tungsten particles are more in the binder matrix phase and dispersed more homogeneously in the alloys cooled rapidly than that in the alloys cooled slowly [113].
In order to observe the effects of heat treatment on microstructural and mechanical properties of liquid phase sintered tungsten heavy alloys, the samples were annealed under nitrogen at 1070 °C for 120 minutes and then water quenched. It was clearly observed that the treatment affected the contiguity values and the volume fraction of matrix phases in the microstructure of 90W and 93W alloys. However, these effects could not be noticed clearly for the alloys of 97W. This difference may be attributed to the low amount of binder matrix phase which led to the difficulties in the volume percent measurements of both phases.

Figure 39 and Figure 40 indicated that volume fraction of the binder phase increased and contiguity of the liquid phase sintered alloys was reduced after the heat treatment.

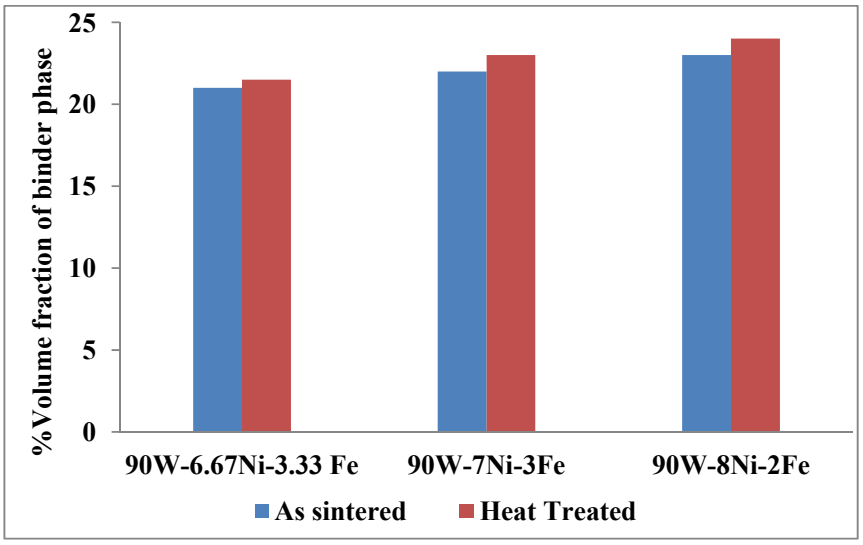

Figure 39. Comparison of volume fraction of 90W alloys with a Ni/Fe ratio varied from 2 to 4 sintered at 1480 °C for 30 minutes and sintered at 1480 °C for 30 minutes and heat treated at 1070°C for 120 minutes.

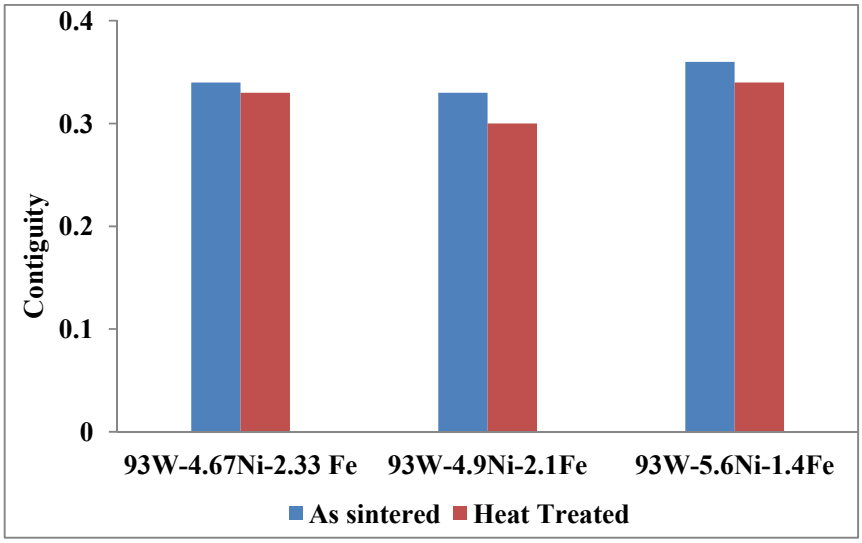

Figure 40. Comparison of contiguity of 93W alloys with a Ni/Fe ratio varied from 2 to 4 sintered at 1480 °C for 30 minutes sintered at 1480 °C for 30 minutes and heat treated at 1070°C for 120 minutes.

The decrease in the contiguity and increase in volume fraction of binder phase with heat treatment is in agreement with the literature [20, 114, 115]. These changes in the microstructural properties might be attributed to the heat treatment including water quenching process which led to the penetration of binder phase between the tungsten particles in the microstructure due to the difference in thermal expansion coefficients of tungsten particles and binder matrix phase.

It was also observed that tensile strengths of the liquid phase sintered alloys were not much correlated to the ductility. It is well known that ductility is more sensitive to the microstructure as compared to tensile strength [20, 26]. This statement is verified by the results obtained as given in Figure 41 and Figure 42. Furthermore, it was also observed that tensile strength of the alloys were not significantly affected by the heat treatment since tensile strength of the alloys was mainly governed by the rule of mixtures rather than the bonding strength between the phases which means that tensile strength is directly related to the amount of harder phase, i.e., tungsten particles. On the contrary, heat treatment considerably changed the ductility of the alloys as given in Figure 42. For instance, % elongation increase from 18% to 33% after the heat treatment applied to the alloys of 90W-8Ni-4Fe.

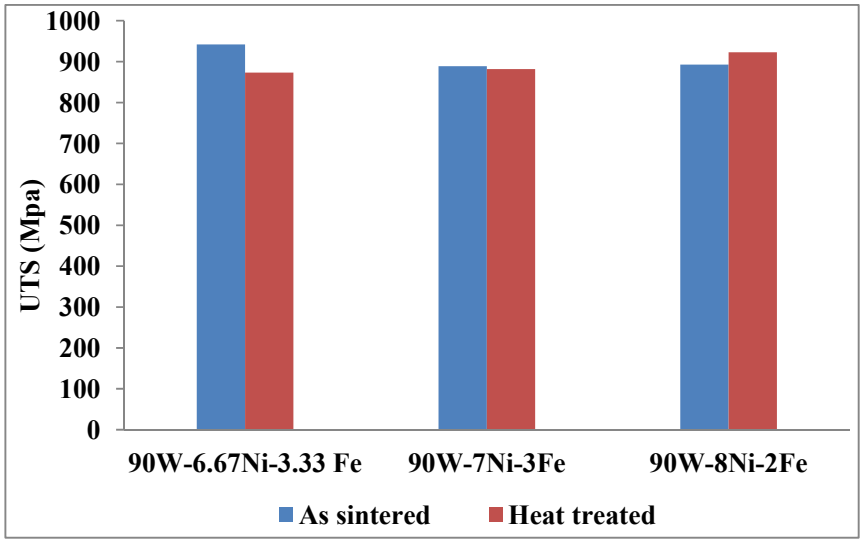

Figure 41. Comparison of tensile strengths of 90W alloys with a Ni/Fe ratio varied from 2 to 4 sintered at 1480 °C for 30 minutes and sintered at 1480 °C for 30 minutes and heat treated at 1070°C for 120 minutes.

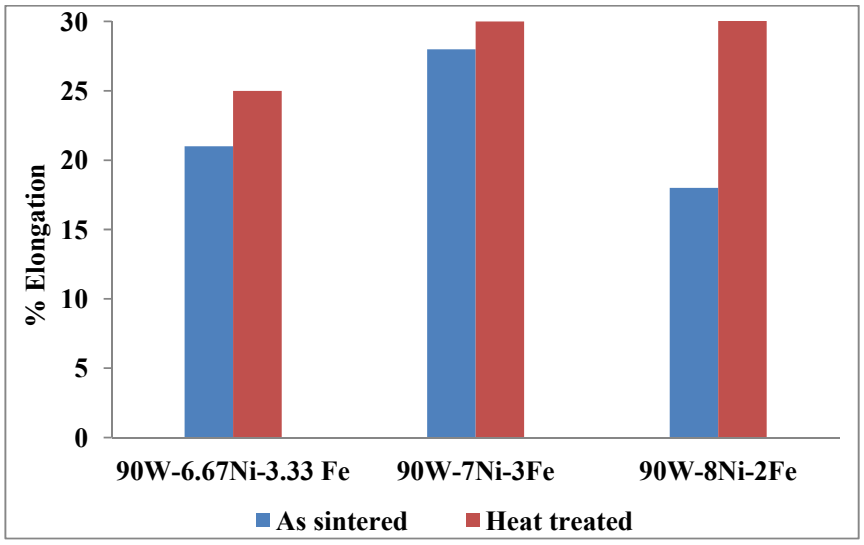

Figure 42. Comparison of % elongation of 90W alloys with a Ni/Fe ratio varied from 2 to 4 sintered at 1480 °C for 30 minutes and sintered at 1480 °C for 30 minutes and heat treated at 1070°C for 120 minutes.

The increase in elongation with heat treatment might be correlated to the change in the crack propagation mechanisms in the alloys. It was clearly observed that number of tungsten cleavage increased after the heat treatment applied as seen in Figure 43. Examinations also showed that the main difference in the crack propagation is the role of the binder phase in

inhibiting the crack propagation. Due to the heat treatment, binder matrix phase might have achieved compositional homogenity which led to more resistance to crack propagation, which gives rise to more tungsten cleavage inplace of binder phase fracture and therefore better ductility.

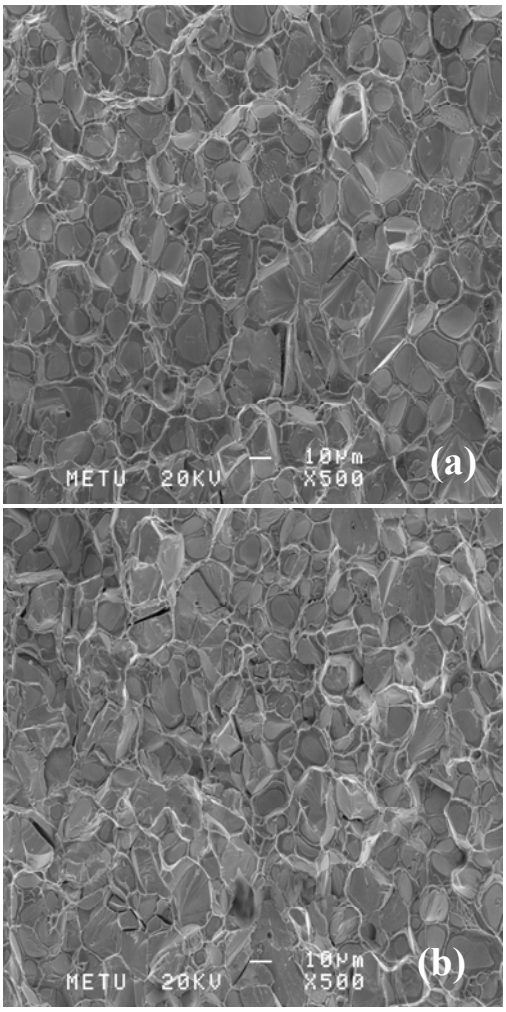

Figure 43. Fracture surfaces of the 90W-8Ni-4Fe alloys a) sintered at 1480 °C for 30 minutes b) sintered at 1480 °C for 30 minutes and heat treated at 1070°C for 120 minutes.

Table 21 which tabulates basic microstructural parameters in heat treated alloys showed that volume percent of binder matrix phase increased as Ni/Fe ratio increased for all alloys as expected. This increase may be attributed to the increase in the tungsten solubility as reported in the similar studies [23, 60].

Table 21. Comparison of microstructural properties of 90W, 93W and 97W alloys with different Ni/Fe ratios sintered at 1480 °C for 30 minutes and heat treated at 1070°C for 120 minutes.

Alloy	Contiguity	%Volume Fraction	Average Particle Size of W (μm)	%Relative Density
90W-Ni/Fe Ratio				
2	0.23 ± 0.08	21.5 ± 1.60	16.30 ± 0.4	99 ± 0.5
2.3	0.22 ± 0.02	22.9 ± 1.2	16.20 ± 1	99 ± 0.5
4	0.25 ± 0.01	23.7 ± 0.5	15.90 ± 0.2	99.5 ± 0.5
93W-Ni/Fe Ratio				
2	0.33 ± 0.06	14.5 ± 0.2	16.70 ± 0.3	99 ± 0.5
2.3	0.30 ± 0.02	14.8 ± 0.6	17.50 ± 0.6	99.5 ± 0.5
4	0.34 ± 0.01	17.5 ± 1.4	17.90 ± 0.5	99.5 ± 0.5
97W-Ni/Fe Ratio				
2	0.52 ± 0.03	6.7 ± 0.6	17.7 ± 0.4	99 ± 0.5
2.3	0.54 ± 0.01	6.6 ± 0.5	17.8 ± 0.1	99 ± 0.5
4	0.52 ± 0.02	6.5 ± 0.8	18.2 ± 0.6	97.5 ± 0.5

The EDS analysis showed that the amount of tungsten in the binder matrix phase increased with the increase in Ni/Fe ratio for heat treated alloys. Therefore, amount of liquid become higher which led to the increase in the liquid volume fraction due to the fact that tungsten solubility increases with increase in Ni/Fe ratio as given in Table 22.

Table 22. Comparison of binder matrix composition of 90W, 93W and 97W alloys with different Ni/Fe ratios sintered at 1480 °C for 30 minutes and heat treated at 1070°C for 120 minutes.

Alloy	Ni in wt%	Fe in wt%	W in wt%
90W-Ni/Fe Ratio			
2	51.46	24.86	23.68
2.3	52.88	21.05	26.06
4	12.83	56.6	30.57
93W-Ni/Fe Ratio			
2	51.38	23.06	25.56
2.3	52.22	21.1	26.68
4	55.2	12.7	32.1
97W-Ni/Fe Ratio			
2	52.04	22.88	25.08
2.3	54.21	18.75	27.04
4	57.72	11.94	30.35

X-ray diffraction patterns of the heat treated alloys showed that all the alloys consist of tungsten phase and Ni–Fe–W binder phase (Figure 44). Furthermore, DSC data did not show the presence of a third phase in the alloys studied. This result is in agreement with the previous studies on tungsten based alloys [15, 83, 84].

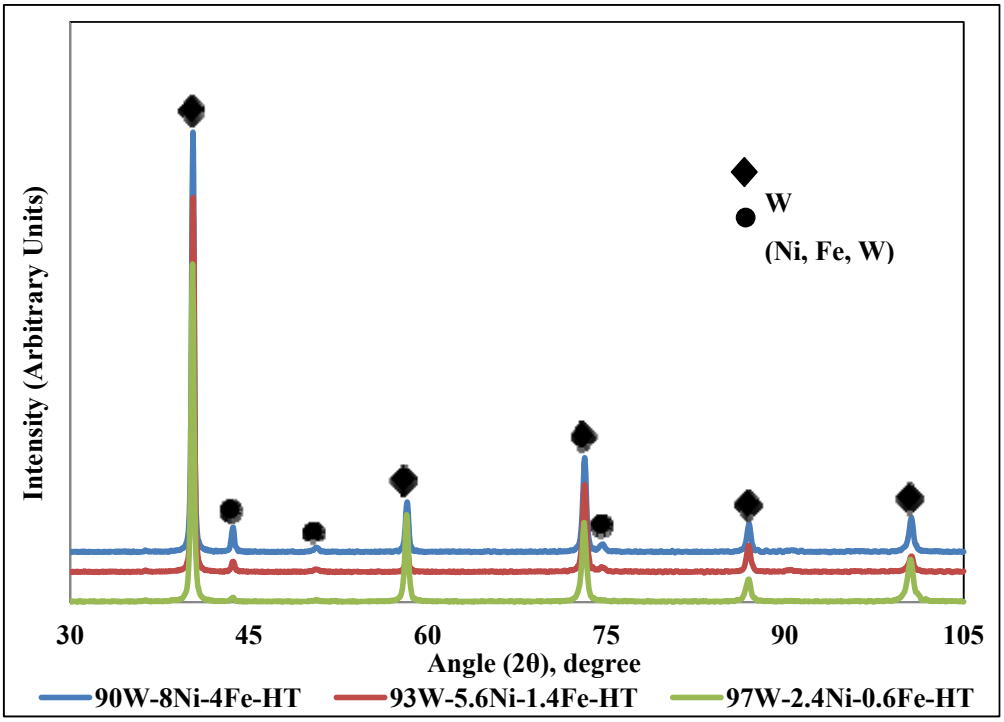

Figure 44. X-ray diffraction patterns of the alloys sintered at 1480 °C for 30 minutes and heat treated at 1070°C for 120 minutes. HT means heat treated.
JCPDS number for W: 004-0806, JCPDS number for (Ni, Fe, W): 004-0850.

The mechanical properties of liquid phase sintered and heat treated alloys were given in Table 23. The mechanical properties of W-Ni-Fe alloys are generally dictated by the interface strength between the tungsten particles and binder matrix phase [38]. W-Ni-Fe alloys are typical metal matrix composites in which interfacial strength is dominated by the tungsten solubility. It is well known that that mechanical properties of tungsten based alloys increases as the tungsten content in the binder matrix phase increases [15, 62]. It can be summarized as mechanical properties such as ultimate tensile strength, yield strength, hardness, ductility and deformation characteristics of the matrix alloy are greatly affected by the tungsten solubility in the binder matrix phase [116].

This relation between the tungsten solubility and the mechanical properties might be explained by the interactions between the tungsten atoms as solute atoms and dislocations that can be considered as solid solution strengthening of binder matrix phase. Tungsten atoms act as obstacles in the binder matrix phase to the dislocation motion which might increase the tensile strength and hardness of the alloys [43, 116].

Table 23. Comparison of mechanical properties of 90W, 93W and 97W alloys with different Ni/Fe ratios sintered at 1480 °C for 30 minutes and heat treated at 1070°C for 120 minutes.

Alloy	UTS (MPa)	Yield (MPa)	% Elongation	Hardness (HV 0.1)	n Coefficient
90W-Ni/Fe Ratio					
2	873 ± 7	564 ± 7	25.1 ± 1.14	379 ± 10	0.58 ± 0.01
2.3	883 ± 5	565 ± 2	30 ± 2.76	358 ± 18	0.57 ± 0.01
4	923 ± 10	590 ± 2	33 ± 3.5	386 ± 26	0.55 ± 0.02
93W-Ni/Fe Ratio					
2	892 ± 9	575 ± 12	22 ± 3.2	372 ± 27	0.56 ± 0.01
2.3	899 ± 4	578 ± 4	25 ± 0.5	375 ± 43	0.56 ± 0.02
4	940 ± 4	614 ± 5	26 ± 4	373 ± 50	0.56 ± 0.02
97W-Ni/Fe Ratio					
2	808 ± 32	569 ± 27	7 ± 0.4	395 ± 11	0.60 ± 0.03
2.3	803 ± 10	606 ± 3	5.1 ± 0.2	398 ± 13	0.58 ± 0.01
4	752 ± 14	592 ± 8	4 ± 1	415 ± 38	0.56 ± 0.04

Table 23 indicated that ultimate tensile strength, yield strength, % elongation increased with the increase in the Ni/Fe ratio for 90W and 93W alloys. This result is in agreement with the similar studies [15]. In this study, yield strength of the 93W alloys increased as Ni/Fe ratio in the binder matrix phase increased. It can be stated as in order to improve the mechanical properties of tungsten based alloys, the solubility of the tungsten in the binder matrix phase shall be increased, since tungsten atoms served as obstacles to the dislocation motion in terms of interactions which led to higher mechanical properties.

However, similar tungsten solubility effect on the mechanical properties could not be observed for 97W alloys. This might be correlated to the lower sintered density of the alloys and incomplete densification due to the increase in the liquidus temperature of binder matrix phase resulted from the increase in Ni/Fe ratio. These alloys having 97wt.% tungsten might need more time or higher sintering temperature in order to achieve the complete densification. Therefore, Ni/Fe ratio effect on the mechanical properties could not be observed clearly due to these reasons.

Additionally, one might expect high work hardening coefficient with the increase in tungsten solubility in the binder matrix phase. Surprisingly, it was observed that there was no significant change in the strain hardening coefficient of the alloys having same amount of tungsten after the heat treatment. This result is in agreement to the similar study [116].

4.3.2 Deformation

Deformation is an effective process to improve the mechanical properties of tungsten based alloys. The main reason for the increase in the strength of the deformed alloy is strain hardening. At deformations up to 15% in reduction in area, strengthening effect is generally

due to the increase in the dislocation density of binder phase [90, 97]. Generally, at small deformations which are lower than 20% in reduction in area, there is no significant change in average particle size of tungsten [89-91] while tungsten particles are elongated and become ellipsoidal after the deformation which leads to an increase in contiguity of tungsten particles because distance between tungsten particle is reduced normal to the deformation direction [90-91].

Deformation generally does not affect the sintered densities of the properly processed alloys [99]. However, in the case low sintered densities, deformation might be used to improve the mechanical properties of the liquid phase sintered alloys by the help of strain hardening of binder phase and pore closure effect due to the deformation [97].

Fracture behavior of the liquid phase sintered tungsten based alloys was also affected by the deformation applied. Interfacial strength between the tungsten particles and binder phase increases with deformation which lead to increase the number of tungsten cleavages in the fracture surfaces of the liquid phase sintered tungsten based alloys [91, 97].

Liquid phase sintered 90W-7Ni-3Fe and 93W-4.9Ni-2.1Fe alloys were cold worked at room temperature by rotary swaging with four hammers. In the forging operation, reduction in area of the samples was around 15%.

Microstructural properties of the sintered and swaged alloys were given in
Table **24**. It was observed that there was no change in densities of the liquid phase sintered alloys since all alloys were properly processed and gained the theoretical density greater than 99%.

Average particle size of tungsten particles was remained almost same after plastic deformation as seen in
Table **24**. This is in agreement in the previous studies in the literature. It has been reported that there was no significant changes observed at the deformations up to 30% reduction in area [89]. In a similar study by Katavic et. al. [89], 92.5W-5Ni-2.5Fe-0.26Co was deformed at different degrees of reduction from %5 to %30, average particle size was not changed significantly due to deformation for this alloy.

However, contiguity of the tungsten particles increased and volume fraction of binder phase decrease with the deformation in the present study. These results are in agreement to the previous studies in the literature [89, 91]. The decrease in the volume fraction of binder phase and increase in the contiguity has been explained by the fact that tungsten particles were getting close together, which led to increase the tungsten-tungsten interfacial area that resulted in the decrease in the volume fraction of binder phase. Swaging process produced inhomogeneous deformation in the microstructure which led to decrease in the volume fraction of binder phase. Additionally, the shape of the tungsten particles did not change too much due to low amount of deformation which is around 15% reduction in area. In contrast, it has been also reported that contiguity decreased with the annealing at 1150 °C for 5 h and deformation after heat treatment [90]. In this study, liquid phase sintered 90W-6Ni-2Fe-2Co were swaged and contiguity value decreased from approximately 0.33 of the as sintered sample to 0.17 of 30% swaged sample. This decrease in the contiguity has been explained by

the separation of tungsten–tungsten interfacial areas due to the applied stress formed during swaging process [90].

Table 24 Comparison of microstructural properties of 90W and 93W sintered at 1480 °C for 30 minutes and swaged up to reduction in area of %15.

Microstructural Parameter	90W-7Ni-3Fe		93W-4.9Ni-2.1Fe	
	Sintered	Sintered and swaged	Sintered	Sintered and swaged
Relative density (%)	99.5	99.4	99.3	99.5
Average Particle Size	16.7±0.6	16.9±0.1	17.2±0.1	17.2±0.1
%Volume Fraction of Binder Phase	22±1	18.4±2.2	14.9±0.1	13.5±0.80
Contiguity	0.24±0.02	0.26±0.05	0.33±0.06	0.39±0.06

Mechanical properties of the sintered and swaged alloys were given in Table 25. The mechanical properties obtained after the swaging process of the liquid phase sintered alloys were comparable to mechanical properties given in a similar study [85] in which 90W-7Ni-3Fe alloy with 18% swaging. It was clearly observed that, tensile strength and hardness of the alloys were improved due to the swaging process, but % elongation (ductility) was reduced. This increase in the strength might be attributed to the increase in the dislocation density which led to work hardening in the alloys [43, 90].

Table 25. Comparison of mechanical properties of 90W and 93W sintered at 1480 °C for 30 minutes and swaged up to reduction in area of %15.

Mechanical Property	90W-7Ni-3Fe		93W-4.9Ni-2.1Fe	
	Sintered	Sintered and swaged	Sintered	Sintered and swaged
Elongation (%)	28±2	10±2	23±3	10±2
Tensile strength (MPa)	889±12	1157±6	898±16	1147±24
Hardness (HV0.1)	352±23	473±30	370±32	482±27

Scanning electron micrographs of the fracture surfaces of the liquid phase sintered and swaged samples are given in Figure 45. Analysis of the fracture surfaces showed that, cleavage of tungsten particles, intergranular tungsten particle fracture and ductile binder phase failure were the fracture modes for the both alloys. Swaging process led to increase the binder matrix failure with the consequence of the strain hardening. It can be stated that the deformation process increased the dislocation density of the alloy and this led to higher tensile strength and lower ductility due to work hardening mechanism.

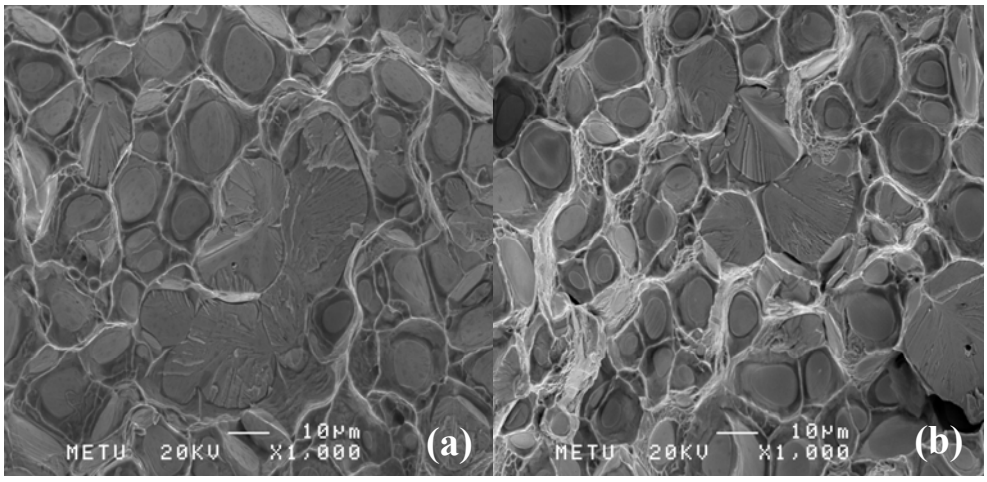

Figure 45. Fracture surfaces of the liquid phase sintered 90W-7Ni-3Fe a) sintered at 1480 °C for 30 minutes b) swaged up to 15% reduction in area.

CHAPTER 5

CONCLUSIONS

In this thesis the effect of processing conditions (hydrogen or vacuum), tungsten content (90W, 93W, 97W), binder phase composition (Ni/Fe ratio of 2, 2.33 and 4) and post sintering treatments (heat treatment and swaging) on the microstructure and mechanical properties of liquid phase sintered tungsten heavy alloys have been investigated. The main conclusions of the study are :

1. Sintering under hydrogen or vacuum were employed for the optimization studies of the selected tungsten based alloys. It was found that reduction of oxide films formed around the metal powder must be performed by using hydrogen during the sintering cycle in order to have better interface strength between the tungsten particles and binder matrix phase which led to better mechanical properties. Additionally, changing sintering atmosphere from hydrogen to argon during sintering cycle may be used instead of post-sintering heat treatment in order to remove the hydrogen embrittlement effect observed on the tungsten based alloys.

2. The variation in tungsten content of the selected tungsten based alloys with a Ni/Fe ratio of 2.33 showed that as tungsten content increased with a decrease in ductility of the alloys due to sharp increase in contiguity. Furthermore, the peak trend in ultimate tensile strength at around 93wt% was also observed. After this point, microstructure properties such as contiguity dictated the mechanical properties. Ductility and tensile strength were reduced as tungsten increased after the peak point which led to transformation of dominant fracture mechanism from the tungsten cleavage to intergranular fracture. Additionally, 97W alloys showed no tension instability prior to fracture due to lower fracture strains resulted from the higher contiguity value. Moreover, average particle size of tungsten increased as tungsten content increased due to the increase in coarsening rate of tungsten particles.

3. In the study, Ni/Fe ratios varied from 2 to 4 for the selected tungsten based alloys. It was observed that tungsten solubility in the binder phase increased as Ni/Fe ratio increased in the composition. Volume fraction of binder phase increased with the increase in Ni/Fe ratio. Furthermore, as Ni/Fe ratio increased, liquidus temperature of binder matrix phase increased due to higher solubility of tungsten in binder phase phase which led to lower sintered density and incomplete densification for 97W alloys. Additionally, the necessity of heat treatment for the homogenity in the composition increased which led to high standard deviations in the mechanical properties as Ni/Fe ratio increased. The XRD and DSC measurements of the samples showed that the microstructure of tungsten based alloys consists of two phases: pure bcc tungsten particles embedded in fcc Ni rich binder phase (Ni-Fe-W).

4. The samples were heat treated at 1070 °C for 2 hours under nitrogen atmosphere. It was found that after heat treatment standard deviations of the mechanical properties were reduced due to the higher chemical homogeneity in the binder phase composition as well as reduction in contiguity and increase in volume fraction binder matrix phase. After heat treatment, it was observed that as Ni/Fe ratio increased, interfacial cohesive strength increased between the tungsten particles and binder phase due to higher tungsten solubility which led to increase in mechanical properties such as tensile strength, yield strength and % elongation. Furthermore, it was also found that ductility was more sensitive to the variations in the microstructure as compared to other mechanical properties.

5. Rapid plastic deformation after liquid phase sintering process by using rotary swager with four hammers were applied to the selected tungsten based alloys. It was observed that swaging process produced inhomogeneous deformation in the microstructure which led to decrease in the volume fraction of binder phase. It was also found that deformation operation increased contiguity of tungsten particles in the microstructure due to the reduction in distance between tungsten particles. It was also observed that tensile strength and hardness of the alloys increased due to higher dislocation density in the microstructure and cohesive strength between the tungsten particles and binder phase which led to increase the amount of matrix failure in the fracture surfaces of the alloys as well as number of transgranular tungsten failures.

REFERENCES

[1] G. H. S. Price, C. J. Smithells, S. V. Williams, Copper-Nickel-Tungsten Alloys: Sintered with a Liquid Phase Present, Journal of the Institute of Metals. 62 (1938) 239-264.

[2] T. Kerry, Tungsten (Elements), Benchmark Books, New York (2003).

[3] E. Lassner, W. D. Schubert, Tungsten Properties, Chemistry, Technology of the Element, Alloys, and Chemical Compounds, Kluwer Academic / Plenum Publishers, New York (1999).

[4] Powder Metal Technologies and Applications (electronic files), ASM Handbook, Volume 7, ASM International (1998).

[5] B. H. Rabin, Microstructure and Tensile Properties of Liquid Phase Sintered Tungsten Nickel Iron Composites, Ph. D. Thesis, Rensselaer Polytechnic Institute (1986).

[6] N. K. Çalışkan, Powder Metallurgy of High Density W-Ni-Cu Alloys, M. Sc. Thesis, Middle East Technical University (2006).

[7] Quintus Isostatic Pressing Handbook, ASEA Metallurgy. (1984) 4-5.

[8] Z. Esen, Production and Characterization of Porous Titanium Alloys, Ph. D. Thesis, Middle East Technical University (2007).

[9] R. M. German, Liquid Phase Sintering, Plenum Press, New York (1985).

[10] R. M. German, S. Farooq, C. M. Kipphut, Kinetics of Liquid Phase Sintering, Materials Science and Engineering A. 105-106 (1988) 215-224.

[11] R. M. German, P. Suri, S. J. Park, Review: Liquid Phase Sintering, Journal of Materials Science. 44 (2009) 1-39.

[12] A. F. Guillermet, L. Östlund, Experimental and Theoretical Study of the Phase Equilibria in the Fe-Ni-W System, Metallurgical and Materials Transactions: A. 17 (1986) 1809-1823.

[13] MC. Chou, CF. Chu, ST. Wu, Phase Transformations of Electroplated Amorphous Iron-Tungsten-Carbon Film, Materials Chemistry and Physics. 78 (2003) 59-66.

[14] J. Liu, R. M. German, Rearrangement Densification in Liquid-Phase Sintering, Metallurgical and Materials Transactions: A. 32 (2001) 3125-3131.

[15] S. G. Caldwell, Variation of Ni/Fe Ratio in W-Ni-Fe Alloys: A Current Perspective in: A. Bose, R. J. Dowding (Eds.), Proceedings of the First International Conference on Tungsten and Tungsten Alloys, Metal Powder Industries Federation. (1992) 89-96.

[16] J. H. Hilliard, J. W. Cahn, An Evaluation of Procedures in Quantitative Metallography for Volume-Fraction Analysis, Transactions of the Metallurgical Society of AIME. 221 (1961) 344-352.

[17] J. Gurland, Application of Quantitative Microscopy to Cemented Carbides, Practical Applications of Quantitative Metallography, ASTM STP 839, J. L. McCall, J. H. Steele, Jr. (Eds.), American Society for Testing and Materials. (1984) 65-84.

[18] ASTM E 562, Standard Test Method for Determining Volume Fraction by Systematic Manual Point Count (2008).

[19] ASTM E 1245, Practice for Determining the Inclusion or Second-Phase Constituent Content of Metals by Automatic Image Analysis (2008).

[20] KS. Churn, JW. Nob, HS. Song, EP. Kim, S. Lee, WH. Back, The Effect of Contiguity on the Mechanical Properties of 93W-5.6Ni-1.4Fe Heavy Alloy, in: A. Bose, R. J. Dowding (Eds.), Proceedings of the First International Conference on Tungsten and Tungsten Alloys, Metal Powder Industries Federation. (1992) 397-406.

[21] J. Gurland, An Estimate of Contact and Continuity of Dispersions in Opaque Samples, Transactions of the Metallurgical Society of AIME. 221 (1966) 642-646.

[22] V. Srikanth, G. S. Upadhyaya, Contiguity Variation in Tungsten Spheroids of Sintered Heavy Alloys, Metallography. 19 (1986) 437-445.

[23] R. L. Woodward, R. G. O'Donnell, Microstructural Influences on the Ductility of Tungsten Alloys, in: A. Bose, R. J. Dowding (Eds.), Proceedings of the First International Conference on Tungsten and Tungsten Alloys, Metal Powder Industries. (1992) 389-396.

[24] R. L. Woodward, R. G. O'Donnell, The Composition and Temperature Dependence of The Mechanical Properties of Tungsten Alloys, Metallurgical Transactions: A. 21 (1990) 744-748.

[25] A. Upadhyaya, S. K. Tiwari, P. Mishra, Microwave Sintering of W–Ni–Fe Alloy, Scripta Materialia. 56 (2007), 5-8.

[26] K. S. Churn, R. M. German, Fracture Behavior of W-Ni-Fe Heavy Alloys, Metallurgical Transactions: A. 15 (1984) 331-338.

[27] R. M. German, The Contiguity of Liquid Phase Sintered Microstructures, Metallurgical Transactions: A. 16 (1985) 1247-1252.

[28] J. Liu, R. M. German, Microstructural Parameters Related to Liquid-Phase Sintering, Metallurgical Transactions: A. 31 (2000) 2607-2614.

[29] S. J. Park, J. M. Martin, J. F. Guo, J. L. Johnson, R. M. German, Grain Growth Behavior of Tungsten Heavy Alloys Based on the Master Sintering Curve Concept, Metallurgical Transactions: A. 37 (2006) 3337-3346.

[30] J. M. Lifshiftz, V. V. Slyozov, The Kinetics of Precipitation from Supersaturated Solid Solutions, Journal of Physics and Chemistry of Solids. 19 (1961) 35-50.

[31] C. Wagner, Zeitschrift Fur Elektrochemie. 65 (1961) 581-591.

[32] J. C. Cahn, In the Mechanism of Phase Transformations in Crystalline Solids, Institute of Metals Monograph No.33, Institute of Metals. London (1961).

[33] I. S. Humail, F. Akhtar, S. J. Askari, M. Tufail, X. Qu, Tensile Behavior Change Depending on the Varying Tungsten Content of W-Ni-Fe Alloys, International Journal of Refractory Metals and Hard Materials. 25 (2007) 380-385.

[34] J. H. Jean, C. H. Lin, Coarsening of Tungsten Particles in W-Ni-Fe alloys, Journal of Materials Science. 24 (1989) 500-504.

[35] A. Upadhyaya, R. M. German, Shape Distortion in Liquid-Phase-Sintered Tungsten Heavy Alloys, Metallurgical Transactions: A. 29 (1998) 2631-2638.

[36] P. Lu, R. M. German, Multiple Grain Growth Events in Liquid Phase Sintering, Journal of Materials Science. 36 (2001) 3385-3394.

[37] ASTM E112, Standard Test Methods for Determining Average Grain Size (2012).

[38] J. Das, U. R. Kiran, A. Chakraborty, N. E. Prasad, Hardness and Tensile Properties of Tungsten Based Heavy Alloys Prepared by Liquid Phase Sintering Technique, International Journal of Refractory Metals and Hard Materials. 27 (2009) 577-583.

[39] J. L. Johnson, L. G. Campbell, S. J. Park, R. M. German, Grain Growth in Dilute Tungsten based alloys During Liquid Phase Sintering Under Microgravity Conditions, Metallurgical Transactions: A. 40 (2009) 426-437.

[40] R. M. German, E. A. Olevsky, Modeling Grain Growth Dependence on the Liquid Content in Liquid-Phase-Sintered Materials, Metallurgical Transactions: A. 29 (1998) 3057-3067.

[41] J. Liu, Z. Z. Fang, Quantitative Characterization of Microstructures of Liquid-Phase-Sintered Two-Phase Materials, Metallurgical Transactions: A. 35 (2004) 1881-1888.

[42] H. J. Ryu, S. H. Hong, W. H. Baek, Microstructure and Mechanical Properties of Mechanically Alloyed and Solid-state Sintered Tungsten Heavy Alloys, Materials Science and Engineering A. 291 (2000) 91-96.

[43] G. E. Dieter, Mechanical Metallurgy, SI Metric edition, McGraw-Hill Book Company (1988).

[44] S. H. Hong, H. J. Ryu, Processing, Microstructure, and Mechanical Properties of Mechanically Alloyed Tungsten Heavy Alloy, Journal of Metastable and Nanocrystalline Materials. 15-16 (2003) 665-672.

[45] U. R. Kiran, A. Panchal, M. Sankaranarayana, T. K. Nandy, Tensile and Impact Behavior of Swaged Tungsten Based Alloys Processed by Liquid Phase Sintering, International Journal of Refractory Metals and Hard Materials. 37 (2013) 1-11.

[46] H. J. Ryu, S. H. Hong, Effects of Sintering Conditions on Mechanical Properties of Mechanically Alloyed Tungsten Heavy Alloys, Metals and Materials International. 7 (2001) 221-226.

[47] S. H. Hong, H. J. Ryu, Combination of Mechanical Alloying and Two-Stage Sintering of a 93W-5.6Ni-1.4Fe Tungsten Heavy Alloy, Materials Science and Engineering A. 344 (2003) 253-260.

[48] R. H. Krock, L. A. Shepard, Mechanical Behavior of the Two-Phase Composite, Tungsten-Nickel-Iron, Transactions of the Metallurgical Society of AIME. 227 (1963) 1127-1134.

[49] DK. Kim, S. Lee, H. J. Ryu, S. Hyunghong, JW. Noh, Correlation of Microstructure with Dynamic Deformation Behavior and Penetration Performance of Tungsten Based Alloys Fabricated by Mechanical Alloying, Metallurgical and Materials Transactions: A. 31 (2000) 2475-2489.

[50] R. M. German, A. Bose, S. S. Mani, Sintering Time and Atmosphere Influences on the Microstructure and Mechanical Properties of Tungsten Heavy Alloys, Metallurgical and Materials Transactions: A. 23 (1992) 211-219.

[51] T. J. McCabe, Microstructure Morphology Aspects and the Relationship to Mechanical Properties of Tungsten Alloys, in: A. Bose, R. J. Dowding (Eds.), Proceedings of the First International Conference on Tungsten and Tungsten Alloys, Metal Powder Industries Federation. (1992) 407-418.

[52] A. Upadhyaya, Processing Strategy for Consolidating Tungsten Based Alloys for Ordnance Applications, Materials Chemistry and Physics. 67 (2001) 101-110.

[53] R. J. Dowding, M. C. Hogwood, L. Wong, R. L. Woodward, Tungsten Alloy Properties Relevant to Kinetic Energy Penetrator Performance, in: A. Bose, R. J. Dowding (Eds.), Proceedings of Second International Conference on Tungsten and Refractory Metals, Metal Powder Industries Federation. (1994) 3-10.

[54] R. M. German, J. E. Hanafee, S. L. DiGiallonardo, Toughness Variation with Test Temperature and Cooling Rate for Liquid Phase Sintered W-3.5Ni-1.5Fe, Metallurgical Transactions A. 15 (1984) 121-128.

[55] R. M. German, Critical Developments in Tungsten Heavy Alloys, in: A. Bose, R. J. Dowding (Eds.), Proceedings of the First International Conference on Tungsten and Tungsten Alloys, Metal Powder Industries Federation. (1992) 3-14.

[56] D. V. Edmonds, Structure/Property Relationships in Sintered Heavy Alloys, International Journal of Refractory Metals and Hard Materials. 10 (1991) 15-26.

[57] A. Bose, R. M. German, Sintering Atmosphere Effects on Tensile Properties of Heavy Alloys, Metallurgical and Materials Transactions: A. 19 (1988) 2467-2476.

[58] I. H. Moon, J. H. Kim, M. J. Suk, K. M. Lee, J. K. Lee, Observation of W Particle Growth in a W Powder Compact During Sintering in a Non-Reducing Atmosphere, International Journal of Refractory Metals and Hard Materials. 11 (1992) 309-315.

[59] R. M. German, K. S. Churn, Sintering Atmosphere Effects on the Ductility of W-Ni-Fe Heavy Metals, Metallurgical and Materials Transactions: A. 15 (1984) 747-754.

[60] J. R. Spencer, J. A. Mullendore, The Effect of Nickel:Iron Ratios on the Mechanical Properties, Microstructure and Processing of W-Ni-Fe Alloys, in: A. Bose, R. J. Dowding (Eds.), Proceedings of the First International Conference on Tungsten and Tungsten Alloys, Metal Powder Industries. (1992) 111-118.

[61] Y. B. Zhu, Y. Wang, X. Y. Zhang, G. W. Qin, W/NiFe Phase Interfacial Characteristics of Liquid-Phase Sintered W-Ni-Fe Alloy, International Journal of Refractory Metals and Hard Materials. 25(2007) 275-279.

[62] E. W. Kennedy, Influence of Microstructure on Fracture Characteristics and Tensile Properties of Two Tungsten Heavy Alloys, in: A. Bose, R. J. Dowding (Eds.), Proceedings of the Second International Conference on Tungsten and Refractory Metals, Metal Powder Industries. (1994) 101-110.

[63] A. Bose, R. M. German, Matrix Composition Effects on the Tensile Properties of Tungsten-Molybdenum Heavy Alloys, Metallurgical and Materials Transactions: A. 21 (1990) 1325-1327.

[64] ISO 5754, Sintered Metal Materials, Excluding Hardmetals-Unnotched Impact Test Piece (1993).

[65] B. H. Rabin, R. M. German, Microstructure Effects on Tensile Properties of Tungsten-Nickel-Iron Composites, Metallurgical and Materials Transactions: A. 19 (1988) 1523-1532.

[66] Mechanical Testing and Evaluation (electronic files), ASM Handbook, Volume 8, ASM International (2000).

[67] ASTM E 646, Standard Test Method for Tensile Strain-Hardening Exponents (n-values) of Metallic Sheet Materials (2007).

[68] Y. Lifu, C. Huaiqing, Q.Suwen, G. Qiuvan, Study on Impurity Segregation in W-Ni-Fe Alloys, in: A. Bose, R. J. Dowding (Eds.), Proceedings of the First International Conference on Tungsten and Tungsten Alloys, Metal Powder Industries. (1992) 265-272.

[69] Y. S. Zu, S. T. Lin, Optimizing the Mechanical Properties of Injection Molded W-4.9%Ni-2.1%Fe in Debinding, Journal of Materials Processing Technology. 71 (1997) 337-342.

[70] A. Asher, L. Borukhin, R. Gero, Effects of Phosphorus Impurities on the Mechanical Properties of Tungsten-Based Heavy Metal and Analytical Methods for Its Control, in: A. Bose, R. J. Dowding (Eds.), Proceedings of the First International Conference on Tungsten and Tungsten Alloys, Metal Powder Industries. (1992) 257-264.

[71] D. V. Edmonds, P. N. Jones, Interfacial Embrittlement in Liquid-Phase Sintered Tungsten Heavy Alloys, Metallurgical and Materials Transactions: A. 10 (1979) 289-295.

[72] C. Lea, B. C. Muddle, D. V. Edmonds, Segregation to Interphase Boundaries in Liquid-Phase Sintered Tungsten Alloys, Metallurgical and Materials Transactions: A. 14 (1983) 667-677.

[73] B. C. Muddle, D. V. Edmonds, Interfacial Segregation and Embrittlement in Liquid Phase Sintered Tungsten Alloys, Metal Science, 17 (1983) 209-218.

[74] E. Fortuna, K. Sikorski, K. J. Kurzydlowski, Experimental Studies of Oxygen and Carbon Segregation at the Interfacial Boundaries of a 90W-7Ni-3Fe Tungsten Heavy Alloy, Materials Characterization. 52 (2004) 323-329.

[75] L. B. Ekbom, The Distribution and Influence of Impurities in Tungsten Heavy Metals, International Journal of Refractory Metals and Hard Materials. 10 (1991) 155-159.

[76] F. V. Lenel, Sintering in the Presence of a Liquid Phase, The American Institute of Mining, Metallurgical and Petroleum Engineers, New York Meeting. (1948) 878-905.

[77] P. B. Kemp, R. M. German, Grain Growth in Liquid-Phase-Sintered W-Mo-Ni-Fe Alloys, Journal of the Less-Common Metals. 175 (1991) 353-368.

[78] W. S. Lee, T. Y. Chan, The Effects of Molybdenum Content on the Dynamic Properties of Tungsten-based Heavy Alloys, Materials Science Forum. 534-536 (2007) 1293-1296.

[79] KH. Lin, CS. Hsu, ST. Lin, Variables on the Precipitation of an Intermetallic Phase for Liquid Phase Sintered W-Mo-Ni-Fe Heavy Alloys, International Journal of Refractory Metals and Hard Materials. 20 (2002) 401-408.

[80] T. J. McCabe, J. J. Valencia, D. Zhao, Effect of Boron Additions on the Impact Strength Behavior of Tungsten Heavy Alloys, in: A. Bose, R. J. Dowding (Eds.), Proceedings of the Second International Conference on Tungsten and Refractory Metals, Metal Powder Industries. (1994) 77-92.

[81] V. Srikanth, G. Harshe, R. M. German, Effect of Molybdenum Addition to W-Ni-Fe-B4C Nonconventional Hard Materials, in: A. Bose, R. J. Dowding (Eds.), Proceedings of the First International Conference on Tungsten and Tungsten Alloys, Metal Powder Industries. (1992) 205-212.

[82] W. Qingquan, Z. Binru, L. Guobiao, Z. Guoan, L. Heyi, Effect of Molybdenum Addition on Properties and Microstructure of W-Ni-Fe Heavy Alloys, in: A. Bose, R. J. Dowding (Eds.), Proceedings of the First International Conference on Tungsten and Tungsten Alloys, Metal Powder Industries. (1992) 431-436.

[83] L. Ronghua, H. Jihua, Y. Sheng, Z. Jun, Strain Aging Precipitation Behavior of β Phase in W-Ni-Fe Ternary System, Journal of Materials Science Letters. 22 (2003) 397-398.

[84] R. Li, J. Huang, S. Yin, J. Zhao, Aging Behaviours of W-Ni-Fe Ternary Alloys with High Ni-to-Fe Ratios, Journal of Materials Science and Technology. 19 (2003) 631-633.

[85] R. J. Dowding, K. J. Tauer, Strain Aging in Tungsten Heavy Alloys, Scripta Metallurgica et Materialia. 25 (1991) 121-126.

[86] D. Rittel, I. Roman, Ductility and Precipitation in Sintered Tungsten Alloys, Materials Science and Engineering. 82 (1986) 93-99.

[87] D. Rittel, R. Levin, A. Dorogoy, On The Isotropy of the Dynamic Mechanical and Failure Properties of Swaged Tungsten Heavy Alloys, Metallurgical and Materials Transactions: A. 35 (2004) 3787-3795.

[88] A. Sunwoo, S. Groves, D. Goto, H. Hopkins, Effect of Matrix Alloy and Cold Swaging on Micro-tensile Properties of Tungsten Heavy Alloys, Materials Letters. 60 (2006) 321-325.

[89] B. Katavic, Z. Odanovic, M. Burzic, Investigation of the Rotary Swaging and Heat Treatment on the Behavior of W and Gamma Phases in PM 92.5W-5Ni-2.5Fe-0.26Co Heavy Alloy. Materials Science and Engineering A. 492 (2008) 337-345.

[90] U. R. Kiran, A. S. Rao, M. Sankaranarayana, T. K. Nandy, Swaging and Heat Treatment Studies on Sintered 90W-6Ni-2Fe-2Co Tungsten Heavy Alloy. International Journal of Refractory Metals and Hard Materials. 33 (2012) 113-121.

[91] A. R. Bentley, M. C. Hogwood, The Effect of Mechanical Deformation and Heat Treatment on the Microstructural Characteristics of Two Tungsten Heavy Alloys, in: A. Bose, R. J. Dowding (Eds.), Proceedings of the First International Conference on Tungsten and Tungsten Alloys, Metal Powder Industries Federation. (1992) 419-430.

[92] W. Leonard, L. Magness, Jr. , Improving Mechanical Properties of Tungsten Heavy Alloy Composites Through Thermomechanical Processing, in: A. Bose, R. J. Dowding (Eds.), Proceedings of the First International Conference on Tungsten and Tungsten Alloys, Metal Powder Industries. (1992) 127-134.

[93] R. Gero, L. Borukhin, I. Pikus, Some Structural Effects of Plastic Deformation on Tungsten Heavy Metal Alloys, Materials Science and Engineering A. 302 (2001) 162-167.

[94] U. R. Kiran, A. Panchal, M. Sankaranarayana, T. K. Nandy, Tensile and Impact Behavior of Swaged Tungsten Based Alloys Processed by Liquid Phase Sintering, International Journal of Refractory Metals and Hard Materials. 37 (2013) 1-11.

[95] Z. H. Zhang, F. C. Wang, S. K. Li, L. Wang, Deformation Characteristics of the 93W-4.9Ni-2.1Fe Tungsten Heavy Alloy Deformed by Hydrostatic Extrusion. Materials Science and Engineering A. 435-436 (2006) 632-637.

[96] X. Gong, J. L. Fan, F. Ding, M. Song, B. Y. Huang, J. M. Tian, Microstructure and Highly Enhanced Mechanical Properties of Fine-grained Tungsten Heavy Alloy After One-pass Rapid Hot Extrusion, Materials Science and Engineering A. 528 (2011) 3046-3052.

[97] N. K. Çalışkan, N. Durlu, Ş. Bor, Swaging of Liquid Phase Sintered 90W-7Ni-3Fe Tungsten Heavy Alloy, International Journal of Refractory Metals and Hard Materials. 36 (2013) 260-264.

[98] G. R. Goren-Muginstein, A. Rosen, The Effect of Cold Deformation on Grain Refinement of Heavy Metals, Materials Science and Engineering A. 238 (1997) 351-356.

[99] B. Katavic, M. Nikacevic, Properties of the Cold Swaged and Strain Aged P/M 91W-6Ni-3Co Heavy Alloy, Second International Conference on Deformation Processing and Structure of Materials. (2005) 135-140.

[100] G. F., Vander Voort, Grain Size Measurement, ASTM STP 839, J. L. McCall, J. H. Steele, Jr. (Eds.), American Society for Testing and Materials, Philadelphia. (1984) 85-131.

[101] ASTM E8/E8M, Standard Test Methods for Tension Testing of Metallic Materials (2009).

[102] H. K. Yoon, S. H. Lee, S. -J. L. Kang, D. N. Yoon, Effect of Vacuum Treatment on Mechanical Properties of W-Ni-Fe Heavy Alloy. Journal of Materials Science. 18 (1983) 1374-1380.

[103] J. Das, G. A. Rao, S. K. Pabi, Microstructure and Mechanical Properties of Tungsten Heavy Alloys, Materials Science and Engineering A. 527 (2010) 7841-7847.

[104] K. K. Chawla, Composite Materials: Science and Engineering Publisher, Springer (1998).

[105] M. R. Akbarpour, A. Ekrami, Effect of Ferrite Volume Fraction on Work Hardening Behavior of High Bainite Dual Phase (DP) Steels, Materials Science and Engineering A. 477 (2008) 306-310.

[106] J. Lian, Z. Jiang, J. Liu, Theoretical Model for the Tensile Work Hardening Behaviour of Dual-phase Steel, Materials Science and Engineering A. 147 (1991) 55 - 65.

[107] Handbook of Ternary Alloy Phase Diagrams, ASM International (1995).

[108] J. H. Jean, C. H. Lin, Coarsening of Tungsten Particles in W-Ni-Fe alloys, Journal of Materials Science. 24 (1989) 500-504.

[109] S. Young-Duh, A. Sung-Tae, D. N. Yoon, Chemically Induced Migration of Liquid Film in W-Ni-Fe alloy, Acta Metallurgica. 33 (1985) 1907-1910.

[110] D. A. Porter, K. E. Easterling, Phase Transformations in Metals and Alloys, Taylor & Francis (1992).

[111] R. S. Coates, K. T. Ramesh, The Rate-dependent Deformation of a Tungsten Heavy Alloy, Materials Science and Engineering A. 145 (1991) 159-166.

[112] R. M. German, L. L. Bourguignon, B. H. Rabin, Microstructure Limitations of High Tungsten Content Heavy Alloys, Journal of Metals. 37 (1985) 36-39.

[113] B. Katavic, Z. Odanovic, Investigation of Deformation and Heat Treatment Effects on Properties of PM 92.5W-5Ni-2.5Fe Heavy Alloys, Powder Metallurgy. 47 (2004) 191-199.

[114] DK. Kim, S. Lee, JW. Noh, Dynamic and Quasi-static Torsional Behavior of Tungsten Heavy Alloy Specimens Fabricated Through Sintering, Heat-treatment, Swaging and Aging, Materials Science and Engineering A. 247 (1998) 285-294.

[115] HS. Song, JW. Noh, WH. Baek, SJ. L. Kang, BS. Chun, Undulation of W/matrix Interface by Resintering of Cyclically Heat-treated W-Ni-Fe Heavy Alloys, Metallurgical and Materials Transactions: A. 28 (1997) 485-489.

[116] K. E. Knipling, G. Zeman, J. S. Marte, S. M. Kelly, S. L. Kampe, Effect of Dissolved Tungsten on the Deformation of 70Ni-30Fe Alloys, Metallurgical and Materials Transactions: A. 35 (2004) 2821-2828.

CURRICULUM VITAE

PERSONAL INFORMATION

Surname, Name: Çalışkan, Necmettin Kaan
Nationality: Turkish (TC)
Date and Place of Birth: 28 October 1980, Tarsus/ Mersin
Marital Status: Married
Phone: +90 312 590 92 09
Mobile Phone: +90 532 654 67 97
Fax: +90 312 590 91 48
e-mail: kaan.caliskan@tubitak.gov.tr

EDUCATION

Degree	Institution	Year of Graduation
PhD	METU Metallurgical and Materials Engineering	2013
MSc	METU Metallurgical and Materials Engineering	2006
BS	METU Metallurgical and Materials Engineering	2003
High School	Arı Fen High School, Ankara	1998

WORK EXPERIENCE

Year	Place	Enrollment
2004- Present	Tübitak Sage	Chief Researcher
2002 Summer	Selnikel A.Ş.	Intern Student
2001 Summer	Asil Çelik A.Ş.	Intern Student

FOREIGN LANGUAGES

Advanced English, Basic German

PUBLICATIONS

1. N. K. Çalışkan, N. Durlu, Ş. Bor, Swaging of Liquid Phase Sintered 90W–7Ni–3Fe Tungsten Heavy Alloy,Int. Journal of Refractory Metals and Hard Materials. 36 (2013) 260-264.

2. N. K. Çalışkan, N. Durlu, Ş. Bor, The Effect of Tungsten Content On the Mechanical Properties of Liquid Phase Sintered Tungsten Based Alloys, 16.Uluslararası Metalurji ve Malzeme Kongresi. (2012) 81-88.

3. N. K. Çalışkan, N. Durlu, Ş. Bor, Sıvı Fazlı Sinterlenen W-Ni-Cu Alaşımlarında Soğutma Hızının Mekanik Özelliklere Etkisi, 6. Uluslararası Toz Metalurji Konferansı. (2011) 520-524.

4. N. K. Çalışkan, N. Durlu, Ö. Soyer, Ş. Bor, W-Ni-Fe Alaşımlarında Bağlayıcı Faz Bileşiminin Mekanik Özelliklere Etkisi, 6. Uluslararası Toz Metalurji Konferansı. (2011) 544-548.

5. N. K. Çalışkan, Ö. Soyer, Delici Mühimmatlarda Kullanılan Yüksek Mukavemetli Çeliklere Genel Bakış, 5.Savunma Teknolojileri Kongresi. (2010) 2 487-494.

6. N. K. Çalışkan, N. Durlu, Ş. Bor, Tungsten Esaslı Ağır Alaşımların Toz Metalurjisi Teknikleri ile Üretimi, 5.Savunma Teknolojileri Kongresi. (2010) 1 79-86.

7. N. K. Çalışkan, N. Durlu, Ş. Bor, Zırh Delici Mühimmatlarda Kullanılan Tungsten Ağır Alaşımlarının (WHA, İng.) Ülkemizdeki ve Dünyadaki Durumunun Değerlendirilmesi, 4. Savunma Teknolojileri Kongresi. (2008) 2 9-16.

8. M. K. Pehlivanoğlu, N. K. Çalışkan, Kızılötesi Güdümlü Mühimmatlarda Kubbe/Pencere Uygulamalarında Kullanılan Kızılötesi-Geçirgen Malzemeler ve Üretim Teknolojileri, 14. Uluslararası Metalurji ve Malzeme Kongresi. (2008) 1052-1064.

9. N. K. Çalışkan, N. Durlu, Ş. Bor, Yüksek Yoğunluklu W (90 Ağ.%)-Ni-Cu Alaşımlarında Kompozisyon Değişimlerinin Sinterleme Davranışı ve Mikroyapısal Özellikler Üzerindeki Etkileri, 14. Uluslararası Metalurji ve Malzeme Kongresi. (2008) 810-817.

10.N. K. Çalışkan, M. K. Pehlivanoğlu, Ş. Bor, Effect of Composition On the Sintering Behavior and Microstructure of W (90 Wt%)-Ni-Cu Alloys, Euro PM. (2007) 2 405-410.

11. N. K. Çalışkan, Ş Bor, B. Öğel, Yüksek Yoğunluklu W(Ağ.%90)-Ni-Cu Alaşımlarının Sinterlenmesi, 13.Uluslararası Metalurji ve Malzeme Kongresi. (2006).

HOBBIES

Computer Games, Tennis, Model Sports, Swimming